Fall 2020

Search for Selection: Genomic, Transcriptomic, and Phenotypic Investigations of Spotted Seatrout (Cynoscion nebulosus)

Jingwei Song
Virginia Institute of Marine Science, jsong@vims.edu

Search for Selection: Genomic, Transcriptomic, and Phenotypic Investigations of Spotted Seatrout (*Cynoscion nebulosus*)

A Dissertation

Presented to

The Faculty of the School of Marine Science

The College of William & Mary

In Partial Fulfillment

of the Requirements for the Degree of

Doctor of Philosophy

by

Jingwei Song

August 2020

APPROVAL PAGE

This dissertation is submitted in partial fulfillment of

the requirements for the degree of

Doctor of Philosophy

Jingwei Song

Approved by the Committee, August 2020

Jan R. McDowell, Ph.D.
Committee Chair / Advisor

Richard W. Brill, Ph.D

Kimberly S. Reece, Ph.D.

Eric J. Hilton, Ph.D.

Christine N. Meynard, Ph.D
French National Institute for Agriculture, Food, and Environment (INRAE)
Montpellier, France

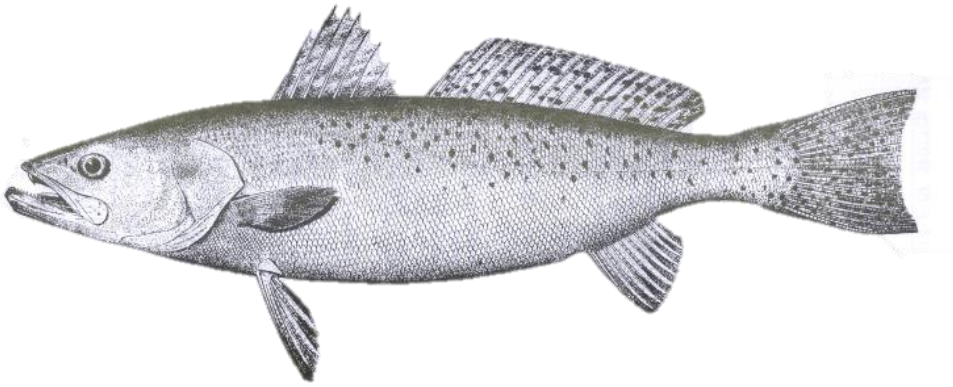

Spotted seatrout, *Cynoscion nebulosus* (Cuvier, 1830), illustrated by Goode (1884)

TABLE OF CONTENTS

ACKNOWLEDGEMENTS

First and foremost, I would like to thank my advisor, Jan, for the opportunity to undertake this work. Your intolerance for unclear thinking and mediocrity have led me to excel at VIMS. Your mentorship from the past five years will have lasting impacts on my future life and career.

Next, I would like to thank my committee members: Rich, Kim, Eric and Christine for their continued interests and time invested in my dissertation. Your suggestions and comments have greatly improved this manuscript.

For sampling and field assistance, I would like to thank Pat McGrath, Susanna Musick, Tim Ellis, Sheldon Arey, John Archambault, Nancy Brown-Peterson, Jenny Goodell and other recreational fishers who contributed samples to this study but I have not met.

For lab assistance, discussions and listening to many of my practice presentations, I would like to thank the past and current members of the Fisheries Genetics Lab at VIMS (Heidi, Ellen, Hamish, Nadya, Ann, Lindsey, Sam and Jackson).

Finally, I would like to thank my parents for their unwavering support, wisdom, and sacrifices over the years.

LIST OF TABLES

LIST OF FIGURES

ABSTRACT

Climate change has resulted in both increased mean water temperature and higher frequencies of extreme water temperatures in coastal areas. These new thermal regimes exert strong selective pressure on the thermal physiology of coastal aquatic species. Phenotypic plasticity (the ability of one genotype to display multiple phenotypes) and local adaptation (increased fitness to local environment due to natural selection) dictate both short-term (from hours to days to weeks) and long-term (from years to decades) resilience of a species. To better predict how a species will respond to the negative impacts of climate change, one first needs to know the current levels of variation in plasticity and local adaptation. Marginal populations are especially critical for the persistence of a species, as those populations can harbor unique genetic variation and the interaction between plasticity and local adaptation determines the boundaries of future distributional ranges. This dissertation focuses on the northern marginal population of spotted seatrout (*Cynoscion nebulosus*), an estuarine-dependent fish, and compares them with those from the core region of the distribution to elucidate the physiological, transcriptomic and genetic mechanisms of plasticity and adaptation. I discovered significant differences between fish from different areas at all three levels of biological organization: Chapter 1 shows different whole-organism metabolic physiology of fish sampled from distinct populations and the northern population is consistent with cold-adaptation, given the pressure of natural selection from more severe and frequent winter kills in the region. Chapter 2 presents functional genetic evidence that the cold-adapted northern spotted seatrout are more vulnerable to heat stress than the warm-adapted southern spotted seatrout, suggesting that differential gene expression is contributing to observed differences in thermal tolerance. A liver transcriptome is *de novo* assembled and serves as a valuable resource for future genetic studies of spotted seatrout. Chapter 3 discovers signatures of selection based on over 15,000 genome-wide single nucleotide polymorphism (SNP) markers. The pattern of genetic variation is consistent with thermal adaptation along the US east coast. Genes involved in metabolic pathways and transcriptional regulation are the main targets of natural selection. In summary, spotted seatrout are relatively resilient to the thermal effects of climate change due to a wide range of metabolic plasticity and adaptive potential in climate-related genetic variation. Range expansion at the leading edge, however, is largely constrained by the species' cold tolerance limit. The northern and southern population will likely respond to climate change differently and this should be taken into consideration in future conservation management of this species.

Search for Selection: Genomic, Transcriptomic, and Phenotypic Investigations of Spotted Seatrout (*Cynoscion nebulosus*)

GENERAL INTRODUCTION

The importance of variation in phenotypic plasticity and local adaptation in aquatic ecosystems is increasingly recognized (Sanford and Kelly 2011; Evans and Logan 2020). Phenotypic plasticity can be defined as the ability of a genotype to be expressed as different phenotypes in response to varying biotic or abiotic conditions (Bradshaw 1965), whereas local adaptation is the result of evolutionary change which confers higher fitness to individual organisms in their native habitat (Kawecki and Ebert 2004). Phenotypic plasticity can buffer individual organisms from the adverse effects of extreme climatic conditions in the short term (from hours to days to weeks), whereas existing adaptive genetic variation among populations that live in heterogeneous environments, some of which mimic conditions under climate change, determine the resilience and adaptive potential in the long term (from years to decades) (Savolainen et al. 2013). An understanding of how populations differ in phenotypic plasticity and how adaptive genetic variation is distributed among populations is thus a prerequisite for making predictions about how species will respond to climate change (Fitzpatrick and Keller 2015; Razgour et al. 2019).

Discovering ecologically relevant genetic variation requires the integration of multiple approaches focusing on different levels of biological organizations (e.g., whole-organism, transcriptome, genome; Dalziel et al. 2009). A first step usually involves the determination of the phenotypic variation underlying fitness because natural selection directly acts on phenotypic variation. Next, populations in question are investigated with genetic methods to discover whether the frequencies of any alleles correlate with the observed phenotypic differences, thus providing evidence they are related to fitness

(Bernatchez et al. 2016). More recently, it has become clear that differential gene expression also plays an important part in phenotypic variation (Todd et al. 2016; Connon et al. 2018). An integrated perspective is desirable because evidence of selection at different levels of biological organization can complement each other by generating testable hypotheses, differentiate the relative importance of adaptation and plasticity, and ultimately provide mechanistic links from cells to populations to inform conservation management (Dalziel et al. 2009; Horodysky et al. 2015). The rapid advances in DNA sequencing technology and associated molecular methods (e.g., RNA-sequencing, restriction site-associated DNA sequencing) have enabled studies that integrate across multiple biological levels for evolutionary biologists studying traditionally non-model organisms (Wang et al. 2009; Elshire et al. 2011).

Across the entire distribution of a species, the population dynamics at the current range margins are especially critical for species resilience and future distributions under climate change (Hampe and Petit 2005). Populations at the coolest parts of the current range (leading edge) lead the expansion into new habitats, where temperature regimes become more similar to those once at the core range as the warming continues (Donelson et al. 2019). Those populations at the warmest parts of the current range (trailing edge) face stronger selective pressure on their thermal physiology. When the rate of warming exceeds a species' tolerance limits and both phenotypic plasticity and evolutionary adaptation fail to cope, population size will decline and range contractions are predicted. In addition, marginal populations usually display local adaptation to more severe and frequent climatic events as compared to core populations (Rehm et al. 2015). The unique standing genetic variation of these marginal populations is critical for the potential of

evolutionary adaptation and the extent of future species distribution, as more extreme climatic events are also predicted by climate models (Hewitt 2004). Understanding the interaction between plasticity and local adaptation in marginal populations is important for accurate prediction of a species response to climate change.

Estuaries are one of the most vulnerable ecosystems to the effects of climate change (Ding and Elmore 2015). These shallow systems are warming faster than the open ocean (Scanes et al. 2020), and their proximity to human activities poses additional threats (e.g., hypoxia, lower pH and sea-level rise) to the organisms found in them (Scavia et al. 2002). Aside from the mummichog (*Fundulus heteroclitus*, Linnaeus, 1776), no other strictly estuarine fish species has been studied collectively at the whole-organism, transcriptomic, and genomic level. The mummichog is a small teleostean species inhabiting marshes and coastal bays of the Atlantic Coast of North America (Mundy and Musick 2013) with two recognized subspecies of *F. heteroclitus* exist: *F.h.macrolepidotus* (northern) and *F.h.heteroclitus* (southern), and both have been intensively studied in a comparative framework to understand mechanisms of evolution and adaptation (Fangue, 2006). Decades of research have shed light on a range of differences between the two subspecies in phenotypic traits including swimming performance, metabolic rate, and larval hatching time (DiMichele and Powers 1982, 1984; Healy and Schulte 2012), as well as gene expression (Schulte et al. 1997; Whitehead and Crawford 2006; Healy et al. 2017), and genetic variation (Duvernell et al. 2008; Strand et al. 2012). Together these studies show that variation is pervasive and a large number of genes are involved in adaptive divergence within killifish. The genetic basis of adaptation in aquatic species is, however, still far from clear. Without a good understanding of the

standing phenotypic and genetic variation, it is difficult to monitor or predict the future response to climate change of estuarine species.

Cynoscion nebulosus (Cuvier, 1830), commonly known as spotted seatrout or speckled trout, is a member of the family Sciaenidae. It is commonly found in the western Atlantic Ocean from Chesapeake Bay to Florida and throughout the northern Gulf of Mexico (Iversen and Tabb 1962). Spotted seatrout is a year-round resident of the estuarine environment, often found in areas with submerged aquatic vegetation (Powers 2012). Spotted seatrout is one of the most popular saltwater sport fisheries within northern Gulf of Mexico and Southeastern United States. (NOAA Fisheries 2020). In addition, limited commercial fisheries also exist in Florida and North Carolina (ASMFC 2011).

Due to its economic importance, the biology and life history of spotted seatrout have been intensively studied (Ramsey and Wakeman 1987; Ihde 2000; Bortone 2002; Ellis 2014). Unlike most other sciaenids, which reproduce offshore and utilize estuarine habitats primarily as nursery areas, spotted seatrout spawn inshore and tend to spend their entire lives in estuaries (Moffett 1961). Spotted seatrout are relatively short-lived, with a maximum life span of 10 years (Ihde and Chittenden 2002). They grow and mature quickly, as nearly all fish are mature by age 1 (Brown-Peterson 2003; Jensen 2009). A protracted spawning season is found across the entire distribution, with the longest spawning season occurring in Tampa Bay, Florida (early April to later October; McMichael and Peters 1989) and the shortest spawning season in Chesapeake Bay (from April to August; Ihde 2000). Estimates of fecundity range from 3 to 20 million eggs per year depending on age, length, and water temperature (Nieland et al. 2002; Roumillat and

Brouwer 2004). Fecundity of females increase with age and size (Lowerre-Barbieri et al. 2009).

Along the U.S. East Coast, variation has been documented for spotted seatrout from distinct regions. A recent tagging study conducted in Virginia and North Carolina found 25% of the northern spotted seatrout migrated over 100 km from the point of release (Ellis, 2014); this is in contrast to almost 100% recaptures within 13 km from the point of release in South Carolina (Davy, 1994) and within 50 km in Florida (Moffett, 1961; Iversen & Tabb, 1962a). This discrepancy suggests that fish in the northern part of the range are more migratory than their southern counterparts. In addition to the differences in migratory behavior, spotted seatrout sampled from the northern range limit have been found to mature at a larger size than those in the south; the smallest size at maturity was 290 mm for females and 250 mm for males in Chesapeake Bay as compared to 225 mm for females and 197 mm for males in South Carolina (Brown, 1981; Wenner *et al.*, 1990). Growth rates of spotted seatrout also differ among areas. In Chesapeake Bay, juvenile spotted seatrout growth rates were estimated to be two to three times higher than those reported for Florida fish (Smith *et al.*, 2008). Both the larger size at maturity and faster growth rate have been attributed to a shorter growing season and natural selection due to high winter mortality (Ellis et al. 2017b).

In addition to the observed differences in migration distance and growth rate, there are genetic differences among spotted seatrout sampled from different locations. Based on protein electrophoresis, one early study by Weinstein and Yerger (1976) concluded that spotted seatrout sampled in seven estuaries along the Gulf Coast of Florida were comprised of discrete populations. Sequencing of the mitochondrial DNA

(mtDNA) control region of spotted seatrout sampled along the Texas shoreline revealed a pattern of isolation by distance (Anderson and Karel 2009), and further analysis using both mtDNA control region sequences and six microsatellite loci found evidence of multiple subpopulations (Anderson and Karel 2010). On the Atlantic Coast, a study using two microsatellites to study population structure found that spotted seatrout in Chesapeake Bay were significantly different from samples collected in South Carolina, Georgia, and Florida (Wiley and Chapman 2003). More recently, O'Donnell et al. (2014) used 13 microsatellite loci and discovered a genetic break at the border between North Carolina and South Carolina. They hypothesized that New River, NC is an important mixing zone between the two populations. The most recent genetic study along the U.S. East Coast using 22 microsatellite loci also uncovered a similar genetic break between northern (Virginia, North Carolina) and southern (South Carolina, Georgia, Florida) populations (Ellis et al. 2019). Results of tagging studies have corroborated these patterns; less than 1% of North Carolina-tagged fish have been recovered in SC (Ellis 2014), and vice versa (John Archambault, South Carolina Department of Natural Resources, pers. comm). From 2008-2018, 93% of the spotted seatrout tagged in Virginia were recaptured in Virginia. During this time period, only three fish were recaptured south of North Carolina (Susanna Musick, Virginia Game Fish Tagging Program, pers. comm).

Natural selection due to abiotic conditions (e.g., temperature) is generally the strongest at a species' range limit (Hurst 2007; Donaldson et al. 2008). Cold stun, also referred to as winter kill, takes place when the water temperature drops rapidly below the species' lethal limit or remains sub-lethal for an extended period of time (Hurst 2007). Both situations can cause significant mortality of spotted seatrout in shallow water areas,

where they tend to overwinter (McGrath and Hilton 2017; Ellis et al. 2017a). Cold stuns have been documented in spotted seatrout population throughout the species' range (Gunter 1952; Tabb 1958; Moore 1976; Adkins et al. 1979; Jensen 2009), but these events are generally observed at lower water temperatures (0 to 5°C) that occur more frequently in Virginia and North Carolina than in locations further south (5 to 10°C). The genetic differentiation between northern and southern populations may be driven by natural selection favoring different phenotypes in different thermal regimes (local adaptation), in addition to just genetic drift (random changes in allele frequencies) due to a lack of gene flow. Thus, if genetic drift is the only determinant of the observed genetic differentiation, significant differences between spotted seatrout sampled from the two populations in putatively adaptive genetic loci (coding regions of the genome) should be relatively rare. If natural selection is also playing a role in shaping the observed genetic differentiation, significant differences in putatively adaptive genetic loci should be relatively common. To date, no study has directly tested for natural selection in spotted seatrout along the U.S. East Coast and thus it is unknown whether natural selection facilitates genetic differentiation.

Multiple lines of evidence (including differences in migratory behavior, population subdivision, and reproductive biology) indicate that spotted seatrout along the U.S. East Coast might be adapted to water temperatures in local estuaries. The overarching goal of my dissertation was to search for signatures of selection using an integrated approach, with a focus on the leading edge of expansion for spotted seatrout under climate change. Chapter 1 compares metabolic plasticity between spotted seatrout sampled from two genetically distinct populations across a large, ecologically relevant

temperature gradient. Chapter 2 compares the changes in transcriptomic signatures in spotted seatrout after being exposed to acute temperature stresses. Chapter 3 investigates the genomic signatures of selection in fish collected across a large latitudinal gradient using a population genomics approach. Understanding whether spotted seatrout along the U.S. Atlantic Coast are locally adapted to different temperature regimes, including insight into how the observed genetic break is maintained, can ultimately inform conservation of this important fishery resource.

References

Adkins, G., J. Tarver, P. Bowman, and B. Savoie. 1979. A Study of the Commercial Finfish in Coastal Louisiana. LA. Dep. Wildl. Fish. Tech. Bull.

Anderson, J. D., and W. J. Karel. 2009. A Genetic Assessment of Current Management Strategies for Spotted Seatrout in Texas. Marine and Coastal Fisheries 1(1):121–132.

Anderson, J. D., and W. J. Karel. 2010. Population Genetics and Dynamics of Spotted Seatrout in the Estuarine Waters of Texas. Fisheries and Aquaculture Journal 01(06):1–19.

ASMFC. 2011. Omnibus amendment to the Interstate Fishery Management Plans for Spanish Mackerel, Spot, and Spotted Seatrout (August 2011):143.

Bernatchez, S., M. Laporte, C. Perrier, P. Sirois, and L. Bernatchez. 2016. Investigating genomic and phenotypic parallelism between piscivorous and planktivorous lake trout (*Salvelinus namaycush*) ecotypes by means of RADseq and morphometrics analyses. Molecular Ecology 25(19):4773–4792.

Bortone, S. A. 2002. Biology of the spotted seatrout. Biology of the Spotted Seatrout, 1st edition. CRC Press.

Bradshaw, A. D. 1965. Evolutionary Significance of Phenotypic Plasticity in Plants. Pages 115–155 *in* E. W. Caspari and J. M. Thoday, editors. Advances in Genetics. Academic Press.

Brown-Peterson, N. 2003. The Reproductive Biology of Spotted Seatrout. Pages 99–133 *in* S. A. Bortone, editor. Biology of the spotted seatrout. CRC Press.

Connon, R. E., K. M. Jeffries, L. M. Komoroske, A. E. Todgham, and N. A. Fangue. 2018. The utility of transcriptomics in fish conservation. Journal of Experimental Biology 221(2):UNSP jeb148833.

Dalziel, A. C., S. M. Rogers, and P. M. Schulte. 2009. Linking genotypes to phenotypes and fitness: how mechanistic biology can inform molecular ecology. Molecular Ecology 18(24):4997–5017.

DiMichele, L., and D. A. Powers. 1982. Physiological basis for swimming endurance differences between LDH-B genotypes of *Fundulus heteroclitus*. Science (New York, N.Y.) 216(4549):1014–1016.

DiMichele, L., and D. A. Powers. 1984. Developmental and Oxygen Consumption Rate Differences between Lactate Dehydrogenase-B Genotypes of *Fundulus heteroclitus* and Their Effect on Hatching Time. Physiological Zoology 57(1):52–56.

Ding, H., and A. J. Elmore. 2015. Spatio-temporal patterns in water surface temperature from Landsat time series data in the Chesapeake Bay, U.S.A. Remote Sensing of Environment 168:335–348. Elsevier Inc.

Donaldson, M. R., S. J. Cooke, D. A. Patterson, and J. S. Macdonald. 2008. Cold shock and fish. Journal of Fish Biology 73(7):1491–1530.

Donelson, J. M., J. M. Sunday, W. F. Figueira, J. D. Gaitán-Espitia, A. J. Hobday, C. R. Johnson, J. M. Leis, S. D. Ling, D. Marshall, J. M. Pandolfi, G. Pecl, G. G. Rodgers, D. J. Booth, and P. L. Munday. 2019. Understanding interactions between plasticity, adaptation and range shifts in response to marine environmental change. Philosophical Transactions of the Royal Society B: Biological Sciences 374(1768).

Duvernell, D. D., J. B. Lindmeier, K. E. Faust, and A. Whitehead. 2008. Relative influences of historical and contemporary forces shaping the distribution of genetic variation in the Atlantic killifish, *Fundulus heteroclitus*. Molecular Ecology 17(5):1344–1360.

Ellis, T. A. 2014. Mortality and Movement of Spotted Seatrout at Its Northern Latitudinal Limits. North Carolina State University.

Ellis, T. A., J. A. Buckel, and J. E. Hightower. 2017a. Winter severity influences spotted seatrout mortality in a southeast US estuarine system. Marine Ecology Progress Series 564:145–161.

Ellis, T. A., J. A. Buckel, J. E. Hightower, and S. J. Poland. 2017b. Relating cold tolerance to winterkill for spotted seatrout at its northern latitudinal limits. Journal of Experimental Marine Biology and Ecology 490:42–51.

Ellis, T. A., J. R. McDowell, and J. A. Buckel. 2019. Stock structure of spotted seatrout: assessing genetic connectivity at northern latitudinal limits. North Carolina Coastal Recreational Fishing License Fund Final Report.

Elshire, R. J., J. C. Glaubitz, Q. Sun, J. A. Poland, K. Kawamoto, E. S. Buckler, and S. E. Mitchell. 2011. A robust, simple genotyping-by-sequencing (GBS) approach for high diversity species. PLoS ONE 6(5):1–10.

Evans, T. G., and C. A. Logan. 2020. Mechanisms of biological sensitivity and resistance to a rapidly changing ocean. Comparative Biochemistry and Physiology -Part A : Molecular and Integrative Physiology 241(November 2019).

Fitzpatrick, M. C., and S. R. Keller. 2015. Ecological genomics meets community-level

modelling of biodiversity: Mapping the genomic landscape of current and future environmental adaptation. Ecology Letters 18(1):1–16.

Goode, G. 1884. The fisheries and fishery industries of the United States. United States. Bureau of Fisheries., Washington.

Gunter, G. 1952. The Import of Catastrophic Mortalities for Marine Fisheries along the Texas Coast. The Journal of Wildlife Management 16(1):63.

Hampe, A., and R. J. Petit. 2005. Conserving biodiversity under climate change: The rear edge matters. Ecology Letters 8(5):461–467.

Healy, T. M., H. J. Bryant, and P. M. Schulte. 2017. Mitochondrial genotype and phenotypic plasticity of gene expression in response to cold acclimation in killifish. Molecular Ecology 26(3):814–830.

Healy, T. M., and P. M. Schulte. 2012. Thermal Acclimation Is Not Necessary to Maintain a Wide Thermal Breadth of Aerobic Scope in the Common Killifish (*Fundulus heteroclitus*). Physiological and Biochemical Zoology 85(2):107–119.

Hewitt, G. M. 2004. Genetic consequences of climatic oscillations in the Quaternary. Philosophical Transactions of the Royal Society B: Biological Sciences 359(1442):183–195.

Horodysky, A. Z., S. J. Cooke, and R. W. Brill. 2015. Physiology in the service of fisheries science: Why thinking mechanistically matters. Reviews in Fish Biology and Fisheries 25(3):425–447. Springer International Publishing.

Hurst, T. P. 2007. Causes and consequences of winter mortality in fishes. Journal of Fish Biology 71(2):315–345.

Ihde, T. 2000. Biology of the spotted seatrout, *Cynoscion nebulosus*, in the Chesapeake Bay region. College of William and Mary.

Ihde, T. F., and M. E. Chittenden. 2002. Comparison of Calcified Structures for Aging Spotted Seatrout. Transactions of the American Fisheries Society 131(4):634–642.

Iversen, E., and D. C. Tabb. 1962. Subpopulations based on growth and tagging studies of spotted seatrout, *Cynoscion nebulosus*, in Florida. Copeia 3:544–548.

Jensen, C. C. 2009. Stock Status of Spotted Seatrout , *Cynoscion nebulosus* , in North Carolina, 1991-2008. Morehead City, NC.

Kawecki, T. J., and D. Ebert. 2004. Conceptual issues in local adaptation. Ecology Letters 7(12):1225–1241.

Lowerre-Barbieri, S. K., N. Henderson, J. Llopiz, S. Walters, J. Bickford, and R. Muller. 2009. Defining a spawning population (spotted seatrout *Cynoscion nebulosus*) over temporal, spatial, and demographic scales. Marine Ecology Progress Series 394:231–245.

McGrath, P. E., and E. J. Hilton. 2017. Temperature selectivity and movement patterns of speckled trout Temperature selectivity and movement patterns of speckled trout Patrick E . McGrath and Eric J . Hilton Virginia Institute of Marine Science College of William and Mary Gloucester Point , VA (March).

McMichael, R. H., and K. M. Peters. 1989. Early Life History of Spotted Seatrout, *Cynoscion nebulosus* (Pisces: Sciaenidae), in Tampa Bay, Florida. Estuaries 12(2):98. Springer-Verlag.

Moffett, A. 1961. Movements and growth of spotted seatrout, *Cynoscion nebulosus*

(Cuvier), in west Florida. Tallahassee, Florida, USA.

Moore, R. H. 1976. Observations on fishes killed by cold at Port Aransas, Texas, January 1973 (20):461–466.

Mundy, E. O., and J. A. Musick. 2013. Field Guide to Fishes of the Chesapeake Bay. Johns Hopkins University Press.

Nieland, D. L., R. G. Thomas, and C. A. Wilson. 2002. Age, Growth, and Reproduction of Spotted Seatrout in Barataria Bay, Louisiana. Transactions of the American Fisheries Society 131(2):245–259.

NOAA Fisheries. 2020, January. South Atlantic Saltwater Recreational Fisheries Snapshot. NOAA Fisheries.

O'Donnell, T. P., M. R. Denson, and T. L. Darden. 2014. Genetic population structure of spotted seatrout *Cynoscion nebulosus* along the south-eastern U.S.A. Journal of Fish Biology 85(2):374–393.

Powers, J. P. 2012. Distribution Patterns of Juvenile Spotted Seatrout (*Cynoscion nebulosus*) and Red Drum (Sciaenops ocellatus) Along Shallow Beach Habitats in Pamlico River, North Carolina.

Ramsey, P., and J. N. Wakeman. 1987. Population Structure of Sciaenops ocellatus and *Cynoscion nebulosus* (Pisces : Sciaenidae): Biochemical Variation , Genetic Subdivision and Dispersal. Copeia 1987(3):682–695.

Razgour, O., B. Forester, J. B. Taggart, M. Bekaert, J. Juste, C. Ibáñez, S. J. Puechmaille, R. Novella-Fernandez, A. Alberdi, and S. Manel. 2019. Considering adaptive genetic variation in climate change vulnerability assessment reduces species range

loss projections. Proceedings of the National Academy of Sciences 116(21):10418–10423.

Rehm, E. M., P. Olivas, J. Stroud, and K. J. Feeley. 2015. Losing your edge: Climate change and the conservation value of range-edge populations. Ecology and Evolution 5(19):4315–4326.

Roumillat, W. A., and M. C. Brouwer. 2004. Reproductive dynamics of female spotted seatrout (*Cynoscion nebulosus*) in South Carolina. Fishery Bulletin 102(3):473–487.

Sanford, E., and M. W. Kelly. 2011. Local Adaptation in Marine Invertebrates. Annual Review of Marine Science 3(1):509–535.

Savolainen, O., M. Lascoux, and J. Merilä. 2013. Ecological genomics of local adaptation. Nature Reviews Genetics 14(11):807–820.

Scanes, E., P. R. Scanes, and P. M. Ross. 2020. Climate change rapidly warms and acidifies Australian estuaries. Nature Communications 11(1):1803.

Scavia, D., J. C. Field, D. F. Boesch, R. W. Buddemeier, V. Burkett, D. R. Cayan, M. Fogarty, M. A. Harwell, R. W. Howarth, C. Mason, D. J. Reed, T. C. Royer, A. H. Sallenger, and J. G. Titus. 2002. Climate change impacts on U.S. Coastal and Marine Ecosystems. Estuaries 25(2):149–164.

Schulte, P. M., M. Gómez-Chiarri, and D. A. Powers. 1997. Structural and Functional Differences in the Promoter and 5′ Flanking Region of Ldh-B Within and Between Populations of the Teleost *Fundulus heteroclitus*. Genetics 145(3):759–769.

Strand, A. E., L. M. Williams, M. F. Oleksiak, and E. E. Sotka. 2012. Can Diversifying Selection Be Distinguished from History in Geographic Clines? A Population

Genomic Study of Killifish (*Fundulus heteroclitus*). PLoS ONE 7(9).

Tabb, D. C. 1958. Differences in the estuarine ecology of Florida waters and their effect on populations of the spotted weakfish, *Cynoscion nebulosus*. Pages 392–401 Transactions of the 23rd North American Wildlife Conference.

Todd, E. V., M. A. Black, and N. J. Gemmell. 2016. The power and promise of RNA-seq in ecology and evolution. Molecular Ecology 25(6):1224–1241.

Wang, Z., M. Gerstein, and M. Snyder. 2009. RNA-Seq: a revolutionary tool for transcriptomics. Nature Reviews Genetics 10(1):57–63.

Whitehead, A., and D. L. Crawford. 2006. Variation within and among species in gene expression: raw material for evolution. Molecular Ecology 15(5):1197–1211.

Wiley, B., and R. Chapman. 2003. Population Structure of Spotted Seatrout, *Cynoscion nebulosus*, along the Atlantic Coast of the U.S. Pages 31–40 *in* S. Borton, editor. Biology of the spotted seatrout. CRC Press, Boca Raton, FL.

1 Chapter 1. Plasticity in Standard and Maximum Aerobic Metabolic Rates in Two Populations of an Estuarine Dependent Teleost, Spotted Seatrout (*Cynoscion nebulosus*)*

1.1 Abstract

We studied the effects of metabolic cold adaptation (MCA) in two populations of a eurythermal species, spotted seatrout (*Cynoscion nebulosus*) along the U.S. East Coast. Fish were captured from their natural environment and acclimated at control temperatures 15 °C or 20 °C. Their oxygen consumption rates, a proxy for metabolic rates, were measured using intermittent flow respirometry during acute temperature decrease or increase (2.5 °C per hour). Mass-specific standard metabolic rates (SMR) were higher in fish from the northern population across an ecologically relevant temperature gradient (5 °C to 30 °C). SMR were up to 37% higher in the northern population at 25 °C and maximum metabolic rates (MMR) were up to 20% higher at 20 °C. We found evidence of active metabolic compensation in the southern population from 5 °C to 15 °C ($Q_{10} < 2$), but not in the northern population. Taken together, our results indicate differences in metabolic plasticity between the northern and southern populations of spotted seatrout and provide a mechanistic basis for predicting population-specific responses to climate change.

1.2 Introduction

Temperature has long been known to have a profound influence on the physiology and metabolic rates of fishes (Fry and Hart 1948; Fry 1967). It dictates the rate of biochemical reactions at the cellular level and leads to increased metabolic rates in warm water (Hochachka and Somero 1973; Angilletta et al. 2010). The metabolic cold adaptation hypothesis (MCA) was first proposed over 100 years ago and has since been a controversial topic in fish physiology (Krogh 1916; Wohlschlag 1960; Steffensen 2002; Holeton 2016). MCA predicts that species from colder environments (higher latitudes or altitudes) will have elevated standard metabolic rates (SMR, minimum metabolic rates needed to sustain life) compared to those from warmer climates when measurements are made at a common temperature. The basis for MCA hypothesis is that low temperature decreases metabolic rates, and the negative relationship between the temperature and metabolic rates acts to compensate for such effect. A meta-analysis approach found support for MCA in that fishes with ranges extending to higher latitudes have higher SMR, higher rates of mitochondrial respiration, and higher enzyme activity than counterparts living at lower latitudes (White et al. 2012). Other studies, including those by Holeton (1974) and Steffensen (2002), argued that MCA is an experimental artifact and there was no evidence of elevated SMR in Arctic or Antarctic fishes when comparisons were made to similar species from temperate regions (Steffensen 2002; Holeton 2016) and metabolic rate data are extrapolated to a common temperature. Within the *Fundulus notatus* species group (*F. notatus*, *F. olivaceus*, and *F. euryzonus*), evidence of MCA was found at the intraspecific level, but not at the interspecific level (Schaefer and Walters 2010).

Climate change is predicted to bring disproportionately large impacts to coastal estuaries due to their shallow depths and proximity to human activities (Scavia et al. 2002). The metabolic physiology of eurythermal species living in these environments is much less studied compared to other economically important fishes such as cod and salmon. Anthropogenic climate change is causing increasing average water temperatures and larger temperature variation, which warrants a better understanding of the metabolic capacities and limits of estuarine fishes (IPCC 2014). In addition, most studies of metabolic adaptation of fishes have treated species as a single homogeneous unit and ignored intraspecific variation in phenotypic plasticity (Costa et al. 2013; Lefevre et al. 2017; Rangel and Johnson 2018). This hinders our ability to predict population-specific response to acute thermal change (Conover 1998; Roessig et al. 2004; Somero 2010).

Spotted seatrout, *Cynoscion nebulosus* (Cuvier), is a coastal species distributed from the Chesapeake Bay to the Gulf of Mexico (Robins 1991). With such a wide coastal distribution, it is likely that spotted seatrout populations inhabiting heterogeneous thermal environments have developed metabolic plasticity. At the northern range limit, spotted seatrout encounter comparatively low winter water temperatures, while the maximum water temperatures in summer are like those encountered in more southern regions (Figure 1). Periodic winter mortalities are most severe at high latitudes for these fishes and act as a strong selective pressure on cold tolerance (Hurst 2007). Tagging studies have shown dispersal distances of spotted seatrout are generally less than 50 km in the Gulf of Mexico and the southeastern coast of the U.S. (Moffett 1961; Iversen and Tabb 1962; Overstreet 1983; Music Jr. and Pafford 1984; Baker et al. 1986). Near the northern latitudinal limit of spotted seatrout in Virginia and North Carolina (hereafter the

"northern population") at least 25% of tagged fish were found to migrate over 100 km, presumably in response to changing water temperature (Ellis 2014). Studies have also found differences in life history characteristics as compared to fish sampled farther south. Spotted seatrout sampled from Chesapeake Bay grow faster and mature at a larger size than their counterparts from South Carolina and Florida (Wenner et al. 1990; Brown-Peterson 2003; Smith et al. 2008). In addition, genetic studies indicate that the northern population is genetically distinct from spotted seatrout from regions south of the New River, North Carolina on the U.S. Atlantic coast (hereafter the "southern population") (Wiley and Chapman 2003; O'Donnell et al. 2014; McDowell et al. 2015). This north-south differentiation provides an opportunity for intraspecific comparison of metabolic plasticity within a widely distributed estuarine species.

A better understanding in the mechanistic basis of the observed differences between the two spotted seatrout populations is critical for predicting future response under climate change. For example, if the northern spotted seatrout are cold-adapted (e.g., higher SMR), then they will likely be less heat-tolerant and thus more vulnerable to the warming effects of climate change. We were interested in whether plasticity in metabolic phenotypes has arisen in populations of spotted seatrout, and whether the pattern is consistent with MCA. Our null hypotheses were:

(1) there are no significant differences in metabolic phenotypes across a range of ecologically relevant temperatures between the two populations as measured by SMR, MMR, factorial aerobic scope (FAS) or absolute aerobic scope (AAS) (defined as MMR/SMR and MMR-SMR, respectively);

(2) there is no significant difference in thermal sensitivity of SMR (quantified as Q_{10} values) between the two populations across a range of ecologically relevant temperatures.

1.3 Materials and Methods

1.3.1 Animal Collection and Husbandry

All animal care and use protocols were approved by The College of William and Mary's Institutional Animal Care and Use Committee (IACUC-2017-09-25-12356-jrmcdo). Spotted seatrout (*Cynoscion nebulosus*) were captured by hook and line from two locations approximately 800 km apart: (1) Corrotoman River, Virginia (n = 20, VA, latitude 37.732985, longitude -76.408968) and (2) areas near Charleston, South Carolina (n=11, SC, latitude 32.753055, longitude -79.896670). Both populations were sampled in November 2017, however, some SC died after transportation from SC to VA. The southern population (SC) was sampled again (n=6) in April 2018. Sampling dates for each fish in each site, weight, time spent in acclimation, and the test it was used are included in Table S 1 . Fish from each sampling location were acclimated in separate flow-through 10,000L circular aquaria. Water temperature was maintained at 15 ± 1°C and 20 ± 1°C using heat exchangers (subsequently referred to as cold-stress experiments and heat-stress experiments, respectively). Salinity from the York River ranged from 15-22 ppt over the acclimation periods. Water quality including pH, ammonia, nitrate, and nitrite levels was checked daily using a commercial kit (API Master Test Kits). The cold-stress experiments were conducted between January and May 2018 and the heat-stress experiments were conducted between July and August 2018. All fish were fed frozen and

thawed bay anchovies (*Anchoa mitchilli*) every two days to satiation. Prior to an experiment, food was withheld for 48 h to ensure complete gastric evacuation (Jobling 1981).

1.3.2 Experimental Procedures

We used automated intermittent-flow respirometry to determine oxygen consumption rates (MO_2, mg O_2 kg^{-1} h^{-1}) as described elsewhere (Horodysky et al. 2011; Lapointe et al. 2014). This procedure is considered the best practice for measuring MO_2 in fishes as it records MO_2 with high temporal resolution, without the constant presence of a researcher (Steffensen et al. 1984; Svendsen et al. 2016b).

At the start of each trial, fish were gently netted from the holding tanks and placed into either a 4 L or 7 L cylindrical respirometer (Loligo System, Viborg, Denmark) depending on the total length of the fish. The partial pressure of oxygen (PO_2, mm Hg) in the respirometers was continuously measured with a fiber-optic oxygen meter (model FSO2-4, PyroScience, Aachen, Germany). The sensors were calibrated using two-point methods according to the manufacturer's handbook prior to experiments and mounted in the recirculation loop of the respirometer. Each $\dot{M}O_2$ measurement was executed using a 180 s flush, 60 s wait and 180–1200 s measurement period (5 °C, 1200 s; 10 °C, 600 s; 15 °C, 300 s; 20 °C, 240 s; 25 °C, 240 s; 30 °C, 180 s). This is because fish metabolic rate correlates positively with water temperature. Longer measurement periods were needed at lower temperatures for fish to consume a similar amount of oxygen to what was consumed at higher temperatures. The operation of the system and data recording was done via the AquaResp software (available at: www.aquaresp.com).

Individual fish in the cold-stress group were exposed to three water temperatures: 15 °C (20 h), 10 °C (5 h) and 5 °C (18 h) in each experiment (the same fish used at all three temperatures, same below). Experiments on individuals from the heat-stress group were also exposed to three water temperatures: 20 °C (20 h), 25 °C (5 h) and 30 °C (18 h). The acute decreases or increases between temperature steps were completed within 2 h. The range of temperatures is representative of the temperature limits of the estuarine environment spotted seatrout occupy. Because of the limited availability of specimens from SC, the last six fish were returned to the holding tank after the cold-stress experiment and re-acclimated for at least 30 days at 20 °C before the heat-stress experiments (all fish survived the acute temperature changes, except for a single fish from SC, which died during a heat stress experiment due to equipment failure). Between trials, respirometers and connecting tubing were thoroughly cleaned with bleach and rinsed with a large amount of fresh water. Bacterial background respiration was measured after fish were removed at the end of cold-stress or heat-stress experiments (5 °C, 30 °C, respectively). Background respiration values were negligible (< 1% of the rate of oxygen decline recorded when fish were present) during both the cold-stress and heat-stress experiments and were subsequently ignored.

MO_2 for a given measurement period was calculated from the time course of oxygen partial pressure (PO_2) change: $MO_2=V\Delta PO_2\Delta t^{-1}\beta$, where V is the respirometer volume (L) corrected for fish volume (assuming 1 kg=1 L), $\Delta PO_2\Delta t^{-1}$ is the slope of the linear regression (mm Hg h^{-1}), and β is the oxygen solubility coefficient (mg O_2 mm Hg^{-1} L^{-1}) (Garcia and Gordon 1992). Slopes with $r^2 < 0.95$ were excluded from analyses.

1.3.3 Correcting for Body Weight

To compare the metabolic rates between different fish, all values were normalized to a standard body weight (the mean body weight of all fish used in the experiments, which equaled 0.34 kg). The following formula was used:

$$\boldsymbol{MO_{2,std} = MO_{2,obs}(\frac{BW}{0.34})^{(1-b)}}$$

Where $\boldsymbol{MO_{2,std}}$ is the mass-specific oxygen consumption rate (mg O_2 kg^{-1} h^{-1}), $\boldsymbol{MO_{2,obs}}$ is the observed oxygen consumption rate (mg O_2 kg^{-1} h^{-1}), BW is the actual weight (kg) of the fish. The range of body weight of experimental animals was too small (less than an order of magnitude) to determine the mass exponent *b* (White and Seymour 2011). Therefore, we used $b = 0.948$, which is the average value using all available data on teleost to correct for SMR (Killen et al. 2016). MMR was corrected using the same formula but with $b = 0.937$ (Killen et al. 2016).

1.3.4 Data Analysis and Statistical Procedures

We defined SMR as the minimum metabolic rate of a post-absorptive fish at a given temperature. At the starting temperatures, 15°C and 20°C, MO_2 was initially elevated because of handling stress and gradually declined to SMR (Figure 2). We used the mclust package (Fraley and Raftery 2002) implemented in R (R Core Team 2018) which fits a mixture of normal distributions to the data (Fraley and Raftery 2002). For each fish, the mean of the lowest normal distribution was taken as the SMR (Svendsen et al. 2016a).

MMR was defined as the single highest MO_2 value at 15°C and 20°C for individual fish. We calculated two measures of aerobic scope: absolute aerobic scope (AAS) and factorial aerobic scope (FAS). The former is the difference between MMR and SMR, and the latter calculated as the ratio MMR/SMR (Halsey et al. 2018). We quantified thermal sensitivity by Q_{10} values (i.e., the factor by which the rate of a biochemical process changes over a 10 °C change in temperature) using the following formula (Schurmann and Steffensen 1997):

$$\boldsymbol{Q_{10}} = \left(\frac{\boldsymbol{R_2}}{\boldsymbol{R_1}}\right)^{\left(\frac{\mathbf{10}}{\boldsymbol{t_2}-\boldsymbol{t_1}}\right)}$$

where R_1 and R_2 are the SMR at temperature t_1 and t_2 (t_1 + 10°C), respectively.

We used the nlme package (Pinheiro et al. 2018) implemented in R (R Core Team 2018) to perform a linear mixed effects analysis of the relationship between SMR and origin of the fish. As fixed effects, we entered fish origin, temperature and their interaction term into the model. We used individual fish as a random effect. *p*-values were obtained by likelihood ratio tests of the full model with the effect in question against the model without the effect in question. Two-tailed Student's *t*-test was used to compare means between groups. A significance level of $\alpha = 0.05$ was used for all statistical tests.

1.4 Results

1.4.1 SMR

SMR in both VA and SC spotted seatrout increased exponentially from 5 °C to 30 °C. SMR in SC ranged from 24 to 233 mg O_2 kg^{-1} h^{-1}; VA ranged from 28 to 349 mg O_2 kg^{-1} h^{-1}. Mean SMR between the northern and southern populations differed significantly at 5 °C (t_{19} = 2.1), 10 °C (t_{19} = 4.25), 15 °C (t_{19} = 4.53), 25 °C (t_{13} = 2.42) but not at 20 °C (t_{13} = 1.41) or 30 °C (t_{13} = 1.90) (Figure 3). Developmental plasticity and seasonality could cause SMR to differ between batches of fishes sampled at different times. To test if this effect was detectable in SC fish sampled at different time periods, SMR was plotted separately for SC fish sampled from the second time period. No significant differences were detected (not shown), therefore data from the two groups of SC were pooled in subsequent analyses.

In cold stress experiments, the origin of fish had a significant effect on SMR (χ^2 (1) = 8.97, p =0.0027), as did temperature (χ^2 (2) = 104.06, $p < 0.0001$). The fish–temperature interaction was also significant (χ^2 (2) = 20.14, $p < 0.001$). Contrasts revealed that: (1) the effect of temperature on SMR was significantly larger in individuals from the northern population versus individuals from the southern population (5 °C to 10 °C: b = -6.65, t_{38} = -4.121, $p < 0.001$; 10 °C to 15 °C: b = -6.59, t_{38} = -4.17, $p < 0.001$).

In heat stress experiments, the origin of fish had no significant effect on SMR (χ^2 (1) = 2.48, p =0.12), perhaps due to a small sample size in the SC group. Temperature had a significant effect on SMR (χ^2 (2) = 69, $p < 0.0001$). Origin–temperature interaction did not significantly improve the fit of the model (χ^2 (2) = 3.54, p =0.17). Predicted SMR in spotted seatrout originating from the northern population was up to 37% higher than

SMR in spotted seatrout from the southern population at 25 °C (185.6 vs. 135.1 mg O_2 kg^{-1} h^{-1}, respectively). The smallest difference was at 5 °C, with fish from the northern population showing an approximately 19% higher SMR than fish from the southern population (34 vs. 28.6 mg O_2 kg^{-1} h^{-1}, respectively) (Table 2).

1.4.2 Maximum Metabolic Rates

Mean MMR between northern and southern spotted seatrout was not significantly different at 15 °C ($t_{19} = 1.38$, $p = 0.18$), but was significantly different at 20 °C ($t_{14} = 3.07$, $p = 0.008$) (Figure 4).

1.4.3 Aerobic Scope

Mean AAS of fish from the northern population was significantly higher at 20 °C ($t_{14} = 2.62$, $p = 0.01$) but not at 15 °C ($t_{19} = 0.93$, $p = 0.366$). For FAS, the differences were reversed. Mean FAS of fish from the southern population was significantly higher at 15 °C ($t_{19} = 3.93$, $p < 0.001$) than mean FAS of fish from the northern population, but not at 20 °C ($t_{14} = 0.87$, $p = 0.4$) (Figure 5).

1.4.4 Q_{10}

The Q_{10} values ranged between 1.4 and 3.4 among SC fish and 1.9 to 2.4 among VA fish. There were no significant differences in Q_{10} values between the two populations at temperatures between 5 °C and 15 °C, ($t_{18} = 1.2$, $p = 0.32$). There was, however, a

significant difference in Q_{10} values between the two populations between 20 °C and 30 °C ($t_{13} = 3.77$, $p = 0.0025$) (Figure 6).

1.5 Discussion

Estuaries are characterized by large daily and seasonal temperature fluctuations (Baumann and Smith 2018) and we argue that spotted seatrout have evolved metabolic plasticity to cope with these challenges occurring in these dynamic environments. The degree of physiological plasticity can, however, also vary among populations inhabiting heterogeneous environments (Dhillon and Schulte 2011; Larsen et al. 2011). Using cold- and heat-stress experiments, we showed that spotted seatrout can maintain a broad range of metabolic rates from 5°C to 30°C. In addition, we found that the reaction norms of metabolic responses to acute temperature changes are population-specific, with northern fish having higher SMR than southern fish, consistent with the predictions of MCA (Schulte 2015). Similar patterns have been observed in another estuarine dependent species, the mummichog (*Fundulus heteroclitus*); fish sampled from a northern population (New Hampshire, USA) were found to have a higher metabolic rate than fish sampled from a southern population (Georgia, USA) (Fangue et al. 2009). Our sampling locations were in closer proximity to each other as compared to the killifish study (800 km vs 1800 km). Thus, the observed differences in SMR between spotted seatrout sampled from different thermal regimes provide evidence that intraspecific metabolic plasticity can take place at a spatial scale of a few hundred kilometers and suggest that temperature may play an important role in the maintenance of genetic breaks. It should be noted that our sample size in the SC heat stress group is relatively low (n=5) due to

difficulty in obtaining live specimens. This might have an effect on our ability to detect statistical significance in SMR at 20 and 30°C (Figure 3). Nevertheless, MMR, AAS and Q_{10} values all show significant differences between the SC and VA groups during heat stress despite a small sample size of the former, supporting that there are true differences in metabolic phenotypes between the northern and southern spotted seatrout.

SMR appears to approach a threshold at the lowest experimental temperature (5°C) in both spotted seatrout populations and this threshold likely limits overwinter survival of this species at its northern distributional limit. This finding is consistent with the results of both telemetry studies and previous cold tolerance experiments. In North Carolina, all winter mortality events of telemetered spotted seatrout in their natural environment occurred in water temperatures below 7°C, and a precipitous increase in natural mortality occurred at water temperatures below ~4°C (Ellis et al. 2018). Cold tolerance experiments using fish from both North Carolina and South Carolina show that when fish are exposed to water temperatures below ~4°C, survival is short-term and physiological impairments due to acute cold stress are largely irreversible (Anweiler et al. 2014; Ellis et al. 2017).

AS has been linked to fitness related traits in fishes such as growth, reproduction and locomotion (Clark et al. 2013; Schulte 2015). Individuals with a larger AS at a given temperature are considered to be more capable of performing energetically demanding tasks. AS is most commonly represented as AAS in fishes, but FAS is also used (albeit less frequently) (Clark et al. 2013; Farrell 2016; Halsey et al. 2018). AAS provides an exact value for metabolic rates above SMR while FAS accounts for the fact that different individuals require proportionally different rates of oxygen delivery to the tissues to

perform a given physiological task (Halsey et al. 2018). Here we report both measures of AS but base our interpretation on AAS. Our reason is that the latter has been found to be more robust when the variability in SMR is larger than that of MMR (Halsey et al. 2018). Our data show that the standard deviation in percentage of the mean value is lower for MMR than SMR (Table S 2, Table S 3). Our experiments obtained MMR at 15 °C and 20 °C and therefore AAS at these two temperatures. Both temperatures are well below the maximum temperature (> 35°C) spotted seatrout tolerate (McDonald et al. 2013). AAS is significantly larger in VA than SC fish at 20 °C. Previous studies found juvenile spotted seatrout in Chesapeake Bay grow faster than fish from South Carolina, despite a shorter growing season for a month (Brown-Peterson 2003; Roumillat and Brouwer 2004; Smith et al. 2008). The size of AS plays an important role in growth rates, such that large pelagic fishes with exceptionally high MMR have extremely high growth rates (Brill and Bushnell 1991; Brill 1996; Korsmeyer and Dewar 2001). Thus, the faster growth of juvenile spotted seatrout in Chesapeake Bay is likely achieved when water temperatures are ~20°C. It is unclear if AAS is also larger in temperatures over 20 °C or between 15°C and 20°C.

The temperature sensitivity (i.e., Q_{10} values) of metabolic rates differ among species and even populations and reflects physiological adaptations (Somero 2002). Q_{10} values in this study ranged from 1.4 to 3.4. This is in general agreement with those commonly reported in teleost fishes (2-3) across a broad range of temperatures (Schurmann and Steffensen 1997; Tirsgaard et al. 2015). The finding that northern spotted seatrout have higher Q_{10} values at low temperatures suggest the northern population can suppress their metabolic costs more than southern fish, possibly as a

means of conserving energy during cold winter months. A previous study comparing seasonal metabolic rates of spotted seatrout with its congener sand seatrout (*Cynoscion arenarius*), found that the former shows a greater degree of metabolic compensation (i.e., lower Q_{10} values) from 15 °C to 30 °C (Vetter 1982). Spotted seatrout are resident year-round in estuaries, whereas sand seatrout migrate offshore in the winter months (Shlossman and Chittenden 1981). A lower Q_{10} value indicates that water temperatures have a smaller effect on the metabolic rates of spotted seatrout than sand seatrout, allowing the former to remain active in the estuarine environment during the warmest months (Vetter 1982). Analogous to the congenic comparison, Q_{10} is lower in VA than SC spotted seatrout between 20 °C and 30 °C. We conclude that this possibly allows VA fish to survive similar maximum water temperature in the summer, despite a higher SMR that could be detrimental at higher temperatures.

Whether the observed differences in metabolic phenotypes have a genetic basis in spotted seatrout is unknown. Future studies should use a common garden experimental design in which metabolic rates are measured over multiple generations to rule out effects from ontogeny or an individual's thermal history (Kawecki and Ebert 2004; Rooke et al. 2017). Although spotted seatrout can reach sexual maturity relatively quickly compared to other sciaenid fishes (age 1), such experiments would still require multiple years to complete. Alternatively, genome scan approaches can be used to look for functional loci that show unusually large differentiation between populations, which can serve as indirect evidence for the genetic basis of whole-organism physiological differences (Helyar et al. 2011; Hemmer-Hansen et al. 2014). For example, a study combined physiological tests and genomic analyses to examine thermal adaptation between

conspecific populations of redband trout (a subspecies of rainbow trout *Oncorhynchus mykiss*; Chen et al. 2018). Populations from a desert climate (hot) showed improved cardiorespiratory capacity at high test temperatures compared to a population from montane climate (cool). In addition, genomic and transcriptomic analyses revealed candidate genes that show differential expressions between populations, providing additional evidence that the observed physiological differences have a heritable component.

Our results support the MCA hypothesis at the intraspecific level between spotted seatrout populations via metabolic plasticity. Organisms with greater plasticity will likely be more resilient to accelerated rate of environmental changes, especially temperatures (Auer et al. 2015; Norin and Metcalfe 2019). There is increasing efforts to predict future range shifts in fishes based on physiological abilities and tolerances (Cooke et al. 2013; Sokolova 2013). Failure to account for physiological plasticity among local populations could over- or underestimate the potential for migration and compromise the utility of these species distribution models. We contend, therefore, that our results should be explicitly incorporated into projects aiming at predicting range shifts of spotted seatrout in response to climate change.

1.6 References

Angilletta, M., B. S. Cooper, M. S. Schuler, and J. G. Boyles. 2010. The evolution of thermal physiology in endotherms. Frontiers in bioscience (Elite edition) 2:861–81.

Anweiler, K. V., S. A. Arnott, and M. R. Denson. 2014. Low-Temperature Tolerance of Juvenile Spotted Seatrout in South Carolina. Transactions of the American Fisheries Society 143(4):999–1010.

Auer, S. K., K. Salin, A. M. Rudolf, G. J. Anderson, and N. B. Metcalfe. 2015. Flexibility in metabolic rate confers a growth advantage under changing food availability. Journal of Animal Ecology 84(5):1405–1411. John Wiley & Sons, Ltd (10.1111).

Baker, W., G. Matlock, L. McEachron, A. Green, and H. Hegen. 1986. Movement, growth and survival of spotted seatrout tagged in Bastrop Bayou, Texas. Contributions in Marine Science 29:91–101.

Baumann, H., and E. M. Smith. 2018. Quantifying Metabolically Driven pH and Oxygen Fluctuations in US Nearshore Habitats at Diel to Interannual Time Scales. Estuaries and Coasts 41(4):1102–1117.

Brill, R. 1996. Selective Advantages Conferred by the High Performance Physiology of Tunas, Billfishes, and Dolphin Fish. Comp Biochem Physiol 113A(1):3–15.

Brill, R. W., and P. G. Bushnell. 1991. Metabolic and cardiac scope of high energy demand teleosts, the tunas. Canadian Journal of Zoology 69(7):2002–2009.

Brown-Peterson, N. 2003. The Reproductive Biology of Spotted Seatrout. Pages 99–133 *in* S. A. Bortone, editor. Biology of the spotted seatrout. CRC Press.

Chen, Z., A. P. Farrell, A. Matala, and S. R. Narum. 2018. Mechanisms of thermal adaptation and evolutionary potential of conspecific populations to changing environments. Molecular Ecology 27(3):659–674.

Clark, T. D., E. Sandblom, and F. Jutfelt. 2013. Aerobic scope measurements of fishes in an era of climate change: respirometry, relevance and recommendations. Journal of Experimental Biology 216(15):2771–2782.

Conover, D. O. 1998. Local Adaptation in Marine Fishes: Evidence and Implications for Stock Enhancement. Bulletin Of Marine Science 62(2):17.

Cooke, S. J., L. Sack, C. E. Franklin, A. P. Farrell, J. Beardall, M. Wikelski, and S. L. Chown. 2013. What is conservation physiology? Perspectives on an increasingly integrated and essential science. Conservation Physiology 1(1):cot001–cot001. Narnia.

Costa, I. A. S. F., W. R. Driedzic, and A. K. Gamperl. 2013. Metabolic and Cardiac Responses of Cunner Tautogolabrus adspersus to Seasonal and Acute Changes in Temperature. Physiological and Biochemical Zoology 86(2):233–244. The University of Chicago PressDivision of Comparative Physiology and Biochemistry, Society for Integrative and Comparative Biology.

Dhillon, R. S., and P. M. Schulte. 2011. Intraspecific variation in the thermal plasticity of mitochondria in killifish. Journal of Experimental Biology 214(21):3639–3648.

Ellis, T. A. 2014. Mortality and Movement of Spotted Seatrout at Its Northern Latitudinal Limits. North Carolina State University.

Ellis, T. A., J. A. Buckel, J. E. Hightower, and S. J. Poland. 2017. Relating cold tolerance to winterkill for spotted seatrout at its northern latitudinal limits. Journal of Experimental Marine Biology and Ecology 490:42–51. Elsevier B.V.

Ellis, T. A., J. E. Hightower, and J. A. Buckel. 2018. Relative importance of fishing and natural mortality for spotted seatrout (*Cynoscion nebulosus*) estimated from a tag-return model and corroborated with survey data. Fisheries Research 199:81–93. Elsevier B.V.

Fangue, N. A., J. G. Richards, and P. M. Schulte. 2009. Do mitochondrial properties explain intraspecific variation in thermal tolerance? Journal of Experimental Biology 212(4):514–522.

Farrell, A. P. 2016. Pragmatic perspective on aerobic scope: Peaking, plummeting, pejus and apportioning. Journal of Fish Biology 88(1):322–343.

Fraley, C., and A. E. Raftery. 2002. Model-Based Clustering, Discriminant Analysis, and Density Estimation. Journal of the American Statistical Association 97(458):611–631.

Fry, F. 1967. Responses of vertebrate poikilotherms to temperature. Thermobiology. Academic Press, New York.

Fry, F. E. J., and J. S. Hart. 1948. The relation of temperature to oxygen consumption in the goldfish. The Biological Bulletin 94(1):66–77.

Garcia, H., and L. Gordon. 1992. Oxygen solubility in seawater: Better fitting equations. limnol.Oceanogr 37(6):1307–1312.

Halsey, L. G., S. S. Killen, T. D. Clark, and T. Norin. 2018. Exploring key issues of aerobic scope interpretation in ectotherms: absolute versus factorial. Reviews in Fish Biology and Fisheries 28(2):405–415.

Helyar, S. J., J. Hemmer-Hansen, D. Bekkevold, M. I. Taylor, R. Ogden, M. T. Limborg, A. Cariani, G. E. Maes, E. Diopere, G. R. Carvalho, and E. E. Nielsen. 2011. Application of SNPs for population genetics of nonmodel organisms: New opportunities and challenges. Molecular Ecology Resources 11(SUPPL. 1):123–136.

Hemmer-Hansen, J., N. O. Therkildsen, and J. M. Pujolar. 2014. Population genomics of marine fishes: next-generation prospects and challenges. The Biological Bulletin 227(2):117–132.

Hochachka, P., and G. Somero. 1973. Strategies of biochemical adaptation. W.B. Saunders, Philadelphia, Pennsylvania, USA.

Holeton, G. F. 2016. Metabolic Cold Adaptation of Polar Fish: Fact or Artefact? Physiological Zoology 47(3):137–152.

Horodysky, A. Z., R. W. Brill, P. G. Bushnell, J. A. Musick, and R. J. Latour. 2011. Comparative metabolic rates of common western North Atlantic Ocean sciaenid fishes. Journal of Fish Biology 79(1):235–255.

Hurst, T. P. 2007. Causes and consequences of winter mortality in fishes. Journal of Fish Biology 71(2):315–345.

IPCC. 2014. IPCC, 2014: Climate Change 2014: Synthesis Report. Contribution of Working Groups I, II and III to the Fifth Assessment Report of the

Intergovernmental Panel on Climate Change [Core Writing Team, R.K. Pachauri and L.A. Meyer (eds.)]. IPCC, Geneva, Switzer.

Iversen, E., and D. C. Tabb. 1962. Subpopulations based on growth and tagging studies of spotted seatrout, *Cynoscion nebulosus*, in Florida. Copeia 3:544–548.

Jobling, M. 1981. The influences of feeding on the metabolic rate of fishes: a short review. Journal of Fish Biology 18(4):385–400.

Kawecki, T. J., and D. Ebert. 2004. Conceptual issues in local adaptation. Ecology Letters 7(12):1225–1241.

Killen, S. S., D. S. Glazier, E. L. Rezende, T. D. Clark, D. Atkinson, A. S. T. Willener, and L. G. Halsey. 2016. Ecological Influences and Morphological Correlates of Resting and Maximal Metabolic Rates across Teleost Fish Species. The American Naturalist 187(5):592–606.

Korsmeyer, K. E., and H. Dewar. 2001. Tuna metabolism and energetics. Pages 35–78 Fish Physiology. Academic Press.

Krogh, A. 1916. The respiratory exchange of animals and man. Longmans, London.

Lapointe, D., W. K. Vogelbein, M. C. Fabrizio, D. T. Gauthier, and R. W. Brill. 2014. Temperature, hypoxia, and mycobacteriosis: Effects on adult striped bass *Morone saxatilis* metabolic performance. Diseases of Aquatic Organisms 108(2):113–127.

Larsen, P. F., P. M. Schulte, and E. E. Nielsen. 2011. Gene expression analysis for the identification of selection and local adaptation in fishes. Journal of Fish Biology 78(1):1–22.

Lefevre, S., D. J. McKenzie, and G. E. Nilsson. 2017. Models projecting the fate of fish populations under climate change need to be based on valid physiological mechanisms. Global Change Biology 23(9):3449–3459.

McDonald, D. L., P. D. Cason, B. W. Bumguardner, and S. Bonnot. 2013. Critical Thermal Maximum of Juvenile Spotted Seatrout (*Cynoscion nebulosus*) Reared for Summer Stocking in Texas. Journal of Applied Aquaculture 25(4):308–319.

McDowell, J. R., S. Musick, and J. Graves. 2015. Speckled trout, *Cynoscion nebulosus*, in Virginia: are these fish genetically distinct? Virginia Recreational Fishing Development Fund Final Report Project.

Moffett, A. 1961. Movements and growth of spotted seatrout, *Cynoscion nebulosus* (Cuvier), in west Florida. Tallahassee, Florida, USA.

Music Jr., J. L., and J. M. Pafford. 1984. Population Dynamics and Life History Aspects of Major Marine Sportfishes in Geogia's Coastal Waters. Georgia Department of Natural Resources, No. 38, Brunswick, GA, USA.

Norin, T., and N. B. Metcalfe. 2019. Ecological and evolutionary consequences of metabolic rate plasticity in response to environmental change. Philosophical Transactions of the Royal Society B: Biological Sciences 374(1768):20180180.

O'Donnell, T. P., M. R. Denson, and T. L. Darden. 2014. Genetic population structure of spotted seatrout *Cynoscion nebulosus* along the south-eastern U.S.A. Journal of Fish Biology 85(2):374–393.

Overstreet. 1983. Aspects of the biology of the spotted seatrout, *Cynoscion nebulosus*, in Mississippi. Gulf Research Reports 1:1–43.

Pinheiro, J., D. Bates, S. DebRoy, D. Sarkar, and R. C. Team. 2018. nlme: Linear and Nonlinear Mixed Effects Models.

R Core Team. 2018. R: A Language and Environment for Statistical Computing. R Foundation for Statistical Computing, Vienna, Austria.

Rangel, R. E., and D. W. Johnson. 2018. Metabolic responses to temperature in a sedentary reef fish, the bluebanded goby (*Lythrypnus dalli* , Gilbert). Journal of Experimental Marine Biology and Ecology 501:83–89.

Robins, C. R. 1991. Common and scientific names of fishes from the United States and Canada. American Fisheries Society, Bethesda, Md.

Roessig, J. M., C. M. Woodley, J. J. Cech, and L. J. Hansen. 2004, June. Effects of global climate change on marine and estuarine fishes and fisheries.

Rooke, A. C., G. Burness, and M. G. Fox. 2017. Thermal physiology of native cool-climate, and non-native warm-climate Pumpkinseed sunfish raised in a common environment. Journal of Thermal Biology 64(December 2016):48–57. Elsevier.

Roumillat, W. A., and M. C. Brouwer. 2004. Reproductive dynamics of female spotted seatrout (*Cynoscion nebulosus*) in South Carolina. Fishery Bulletin 102(3):473–487.

Scavia, D., J. C. Field, D. F. Boesch, R. W. Buddemeier, V. Burkett, D. R. Cayan, M. Fogarty, M. A. Harwell, R. W. Howarth, C. Mason, D. J. Reed, T. C. Royer, A. H. Sallenger, and J. G. Titus. 2002. Climate change impacts on U.S. Coastal and Marine Ecosystems. Estuaries 25(2):149–164.

Schaefer, J., and A. Walters. 2010. Metabolic cold adaptation and developmental plasticity in metabolic rates among species in the *Fundulus notatus* species complex. Functional Ecology 24(5):1087–1094.

Schulte, P. M. 2015. The effects of temperature on aerobic metabolism: towards a mechanistic understanding of the responses of ectotherms to a changing environment. Journal of Experimental Biology 218(12):1856–1866.

Schurmann, H., and J. F. Steffensen. 1997. Effects of temperature, hypoxia and activity on the metabolism of juvenile Atlantic cod. Journal of Fish Biology 50(6):1166–1180.

Shlossman, P. A., and J. M. E. Chittenden. 1981. Reproduction, movements, and population dynamics of the sand seatrout, *Cynoscion arenarius*. Fishery Bulletin 79(4):649–669.

Smith, N. G., C. M. Jones, and J. Van Montfrans. 2008. Spatial and temporal variability of juvenile spotted seatrout *Cynoscion nebulosus* growth in Chesapeake Bay. Journal of Fish Biology 73(3):597–607.

Sokolova, I. M. 2013. Energy-Limited Tolerance to Stress as a Conceptual Framework to Integrate the Effects of Multiple Stressors. Integrative and Comparative Biology 53(4):597–608. Narnia.

Somero, G. N. 2002. Thermal physiology and vertical zonation of intertidal animals: Optima, limits, and costs of living. Pages 780–789 Integrative and Comparative Biology.

Somero, G. N. 2010. The physiology of climate change: how potentials for acclimatization and genetic adaptation will determine “winners” and “losers.” Journal of Experimental Biology 213(6):912–920.

Steffensen, J. ., K. Johansen, and P. . Bushnell. 1984. An automated swimming respirometer. Comparative Biochemistry and Physiology Part A: Physiology 79(3):437–440.

Steffensen, J. F. 2002. Metabolic cold adaptation of polar fish based on measurements of aerobic oxygen consumption: Fact or artefact? Artefact! Comparative Biochemistry and Physiology - A Molecular and Integrative Physiology 132(4):789–795.

Svendsen, M. B. S., P. G. Bushnell, E. A. F. Christensen, and J. F. Steffensen. 2016a. Sources of variation in oxygen consumption of aquatic animals demonstrated by simulated constant oxygen consumption and respirometers of different sizes. Journal of Fish Biology 88(1):51–64.

Svendsen, M. B. S., P. G. Bushnell, and J. F. Steffensen. 2016b. Design and setup of intermittent-flow respirometry system for aquatic organisms. Journal of Fish Biology 88(1):26–50.

Tirsgaard, B., J. W. Behrens, and J. F. Steffensen. 2015. The effect of temperature and body size on metabolic scope of activity in juvenile Atlantic cod *Gadus morhua* L. Comparative Biochemistry and Physiology Part A: Molecular & Integrative Physiology 179:89–94. Elsevier Inc.

Vetter, R. D. 1982. Seasonal metabolic compensation in sympatric seatrout: Adaptation to the estuary. Trans.Am.Fish.Soc. 111(2):193–198.

Wenner, C. A., W. A. Roumillat, J. E. Moran, M. B. Maddox, L. B. Daniel, and J. W. Smith. 1990. Investigations on the life history and population dynamics of marine recreational fishes in South Carolina: Part 1. : Marine Resources Research Institute, South Carolina Wildlife and Marine Resources Dept., [1990], Charleston, S.C.

White, C. R., L. A. Alton, and P. B. Frappell. 2012. Metabolic cold adaptation in fishes occurs at the level of whole animal, mitochondria and enzyme. Proceedings of the Royal Society of London B: Biological Sciences 279(1734):1740–1747.

White, C. R., and R. S. Seymour. 2011. Physiological Functions that Scale to Body Mass in Fish. Pages 1573–1582 Encyclopedia of Fish Physiology. Elsevier Inc.

Wiley, B., and R. Chapman. 2003. Population Structure of Spotted Seatrout, *Cynoscion nebulosus*, along the Atlantic Coast of the U.S. Pages 31–40 *in* S. Borton, editor. Biology of the spotted seatrout. CRC Press, Boca Raton, FL.

Wohlschlag, D. E. 1960. Metabolism of an Antarctic Fish and the Phenomenon of Cold Adaptation. Ecology 41(2):287–292.

1.7 Tables

Table 1. Number and weight of spotted seatrout used in respirometry experiments. M = mean (and range) body mass in grams.

	Cold Stress	**Heat Stress**
Corrotoman River, Virginia	*n* = 10 M = 192 g (140–252 g)	*n* = 10 M = 238 g (122–439 g)
Charleston, South Carolina	*n* = 11 M = 467 g (235–838)	*n* = 5 M = 454 g (368–508)

Table 2. Predicted SMR from linear mixed effect model. SC = southern population, VA = northern population. Fit = predicted SMR, sd = standard deviation, se = standard error, ci = 95% confidence interval.

Origin	Temp. (°C)	N	fit	sd	se	ci
SC	5	11	28.6	5.7	1.7	3.8
SC	10	11	33.1	4.5	1.4	3.1
SC	15	11	53.8	7.1	2.1	4.8
VA	5	10	34.0	5.7	1.8	4.1
VA	10	10	45.2	7.8	2.5	5.6
VA	15	10	72.5	10.0	3.2	7.2
SC	20	5	86.6	13.4	6.0	16.6
SC	25	5	135.1	24.3	10.9	30.1
SC	30	5	231.7	29.4	13.1	36.5
VA	20	10	100.2	10.7	3.4	7.7
VA	25	10	185.6	38.3	12.1	27.4
VA	30	10	291.7	59.4	18.8	42.5

Table S 1. Details on the spotted seatrout specimens used in respirometry experiments.

ID	Sampling dates	location	coordinates	test group	Acclimation start	Acclimation temp	experiment date	weight (g)	days in acclimation
1	11/6/2017	VA	37.732985, -76.408968	cold stress	11/6/2017	15	1/23/2018	252	78
2	11/6/2017	VA	37.732985, -76.408968	cold stress	11/6/2017	15	2/15/2018	187	101
3	11/6/2017	VA	37.732985, -76.408968	cold stress	11/6/2017	15	2/19/2018	213	105
4	11/6/2017	VA	37.732985, -76.408968	cold stress	11/6/2017	15	2/19/2018	217	105
5	11/6/2017	VA	37.732985, -76.408968	cold stress	11/6/2017	15	2/23/2018	157	109
6	11/6/2017	VA	37.732985, -76.408968	cold stress	11/6/2017	15	2/23/2018	180	109
7	11/6/2017	VA	37.732985, -76.408968	cold stress	11/6/2017	15	2/23/2018	140	109
8	11/6/2017	VA	37.732985, -76.408968	cold stress	11/6/2017	15	2/26/2018	174	112
9	11/6/2017	VA	37.732985, -76.408968	cold stress	11/6/2017	15	2/26/2018	185	112
10	11/6/2017	VA	37.732985, -76.408968	cold stress	11/6/2017	15	2/26/2018	211	112
11	11/6/2017	VA	37.732985, -76.408968	heat stress	6/6/2018	20	7/3/2018	224	27
12	11/6/2017	VA	37.732985, -76.408968	heat stress	6/6/2018	20	7/6/2018	231	30
13	11/6/2017	VA	37.732985, -76.408968	heat stress	6/6/2018	20	7/11/2018	179	35
14	11/6/2017	VA	37.732985, -76.408968	heat stress	6/6/2018	20	7/11/2018	210	35
15	11/6/2017	VA	37.732985, -76.408968	heat stress	6/6/2018	20	7/13/2018	155	37
16	11/6/2017	VA	37.732985, -76.408968	heat stress	6/6/2018	20	7/18/2018	122	42
17	11/6/2017	VA	37.732985, -76.408968	heat stress	6/6/2018	20	7/22/2018	240	46
18	11/6/2017	VA	37.732985, -76.408968	heat stress	6/6/2018	20	8/7/2018	439	62
19	11/6/2017	VA	37.732985, -76.408968	heat stress	6/6/2018	20	8/10/2018	323	65
20	11/6/2017	VA	37.732985, -76.408968	heat stress	6/6/2018	20	8/20/2018	258	75
21	11/23/2017	SC	32.753055, -79.896670	cold stress	11/23/2017	15	1/23/2018	235	61
22	11/23/2017	SC	32.753055, -79.896670	cold stress	11/23/2017	15	2/15/2018	393	84
23	11/23/2017	SC	32.753055, -79.896670	cold stress	11/23/2017	15	2/19/2018	394	88
24	11/23/2017	SC	32.753055, -79.896670	cold stress	11/23/2017	15	2/23/2018	548	92
25	11/23/2017	SC	32.753055, -79.896670	cold stress	11/23/2017	15	2/26/2018	458	95
26	3/4/2018	SC	32.753055, -79.896670	cold stress	3/4/2018	15	5/4/2018	368	61
27	3/4/2018	SC	32.753055, -79.896670	cold stress	3/4/2018	15	5/8/2018	838	65
28	3/4/2018	SC	32.753055, -79.896670	cold stress	3/4/2018	15	5/10/2018	508	67

29	3/4/2018	SC	32.753055, -79.896670	cold stress	3/4/2018	15	5/29/2018	447	86
30	3/4/2018	SC	32.753055, -79.896670	cold stress	3/4/2018	15	6/1/2018	452	89
31	3/4/2018	SC	32.753055, -79.896670	cold stress	3/4/2018	15	6/6/2018	473	94
32	3/4/2018	SC	32.753055, -79.896670	heat stress	6/6/2018	20	7/6/2018	368	30
33	3/4/2018	SC	32.753055, -79.896670	heat stress	6/6/2018	20	7/11/2018	838	35
34	3/4/2018	SC	32.753055, -79.896670	heat stress	6/6/2018	20	7/13/2018	508	37
35	3/4/2018	SC	32.753055, -79.896670	heat stress	6/6/2018	20	7/18/2018	447	42
36	3/4/2018	SC	32.753055, -79.896670	heat stress	6/6/2018	20	7/22/2018	452	46
37	3/4/2018	SC	32.753055, -79.896670	heat stress	6/6/2018	20	7/26/2018	473	50

Table S 2. Summary of mass-specific SMR and MMR for both SC and VA spotted seatrout populations in cold stress experiments.

		15°C		10°C	5°C
Fish	Weight(g)	SMR	MMR	SMR	SMR
SC	235	63.9	189.3	37.9	30.9
SC	393	50.8	187.7	25.5	14.8
SC	394	51.2	162.0	32.0	27.0
SC	548	66.7	175.6	37.7	28.1
SC	458	44.3	208.7	30.7	30.7
SC	833	48.8	176.3	34.4	32.9
SC	436	46.1	183.9	26.0	26.8
SC	554	59.5	215.5	29.7	26.6
SC	540	44.4	187.8	33.8	27.8
SC	410	60.8	217.8	38.6	41.3
SC	500	55.5	187.2	37.2	27.3
VA	252	95.9	243.5	60.9	47.7
VA	187	63.2	183.0	38.0	31.3
VA	213	67.2	167.8	47.1	29.0
VA	217	85.0	205.3	55.9	39.4
VA	157	71.7	206.2	39.2	31.7
VA	180	67.9	225.1	48.1	32.6
VA	140	64.3	194.4	38.4	30.3
VA	174	69.1	208.3	36.8	33.1
VA	185	62.3	187.2	41.6	31.7
VA	211	78.3	197.9	45.9	33.3
mean		62.7	195.7	38.8	31.2
std. dev		12.9	19.4	8.7	6.3
sd/mean		0.2	0.1		

Table S 3. Summary of mass-specific SMR and MMR for both SC and VA spotted seatrout populations in heat stress experiments.

		20°C		25°C	30°C	
Fish	Weight (g)	SMR	MMR	SMR	SMR	
VA	224.0	112.8	360.9	200.8	283.1	
VA	231.0	91.1	267.1	162.2	243.4	
VA	179.0	112.2	331.7	151.1	317.0	
VA	210.0	107.8	341.0	232.0	338.9	
VA	155.0	110.8	345.7	192.0	402.8	
VA	122.0	96.3	294.4	264.6	302.5	
VA	240.0	86.8	343.0	172.5	366.8	
VA	439.0	105.4	347.9	208.6	221.5	
VA	323.0	83.8	304.4	142.4	201.7	
VA	258.0	95.5	337.2	129.9	239.3	
SC	368.0	72.0	254.1	113.4	248.0	
SC	838.0	105.6	239.7	n/a	n/a	fish died due to equipment failure
SC	508.0	104.9	349.8	168.2	244.5	
SC	447.0	85.9	286.7	124.5	199.8	
SC	452.0	74.3	261.0	111.3	196.3	
SC	473.0	95.7	252.7	158.1	270.1	
mean		96.3	307.3	168.8	271.7	
std. dev		12.7	40.6	42.7	60.7	
sd/mean		0.1	0.1			

1.8 Figures

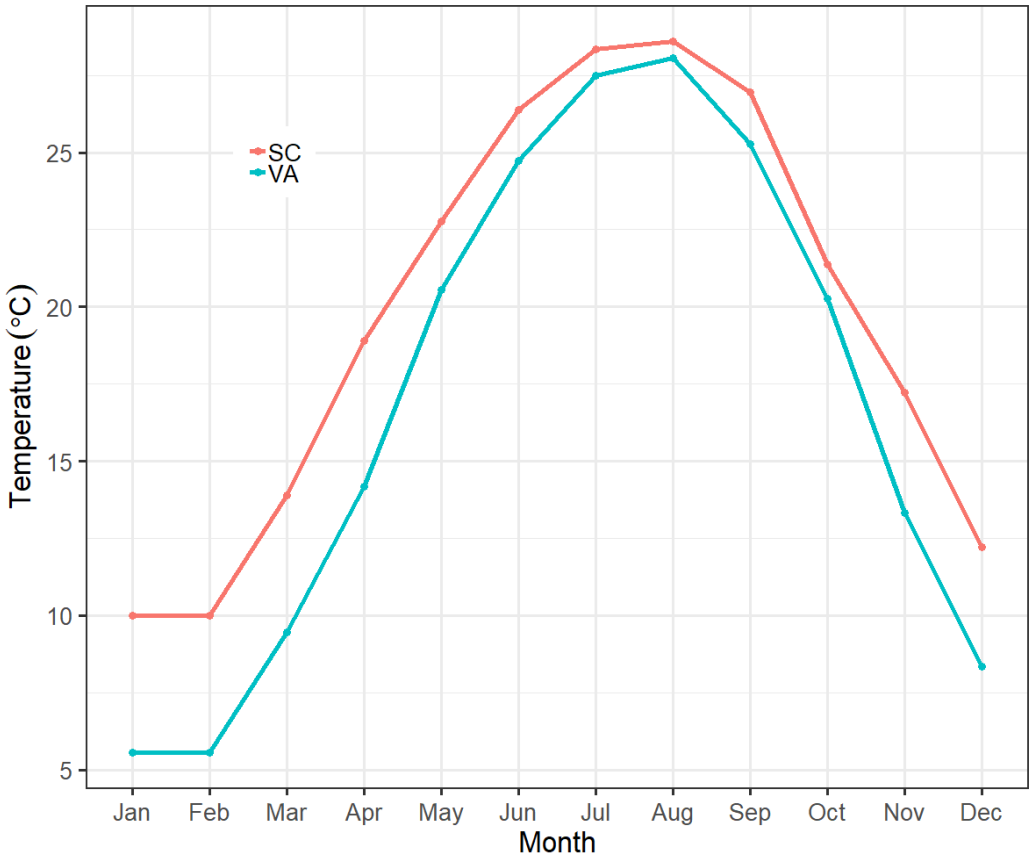

Figure 1. Monthly mean water temperature at two sampling locations. VA = Corrotoman River, Virginia, SC = Charleston, South Carolina.

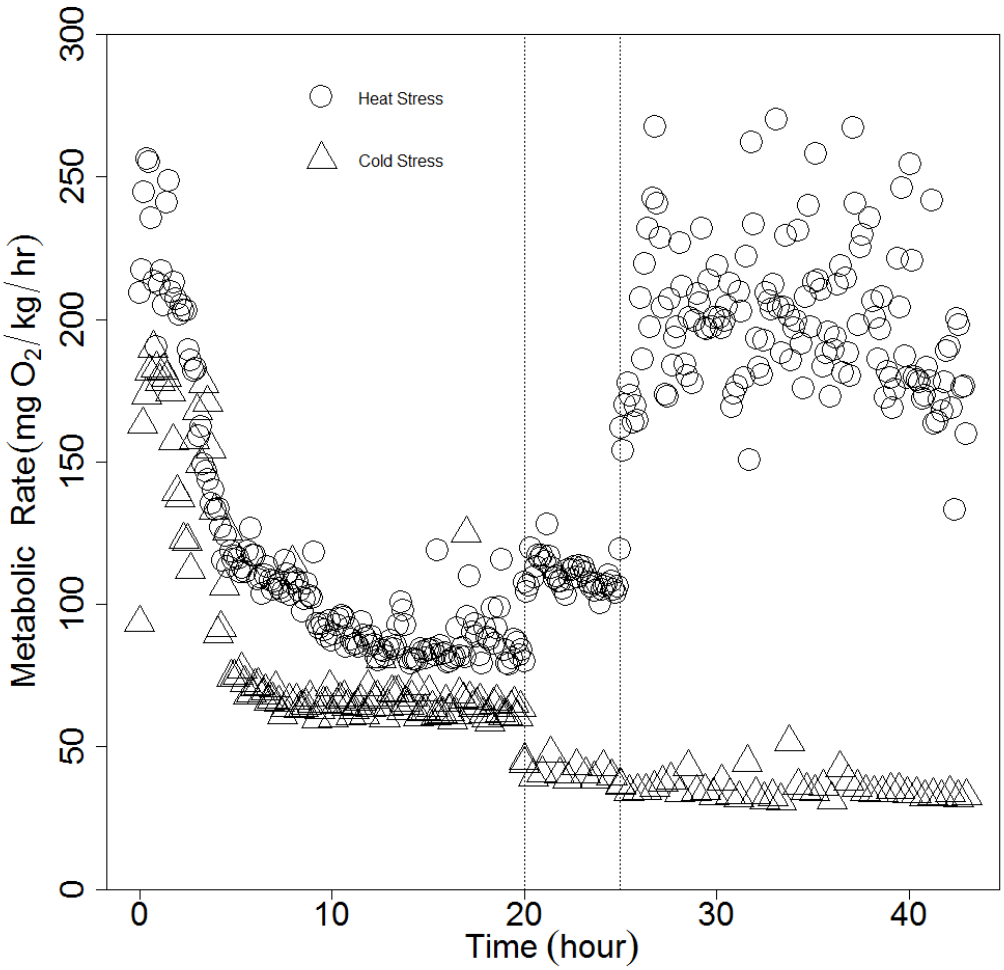

Figure 2. Time course of metabolic rate change in spotted seatrout under two sets of experimental conditions. Empty circles: heat stress; empty triangles: cold stress. Each dot represents the oxygen consumption rate from one respirometry cycle. Vertical dotted lines separate different temperatures. Within each treatment, from left to right: 20 °C, 25 °C, 30 °C (heat stress); 15 °C, 10 °C, 5 °C (cold stress).

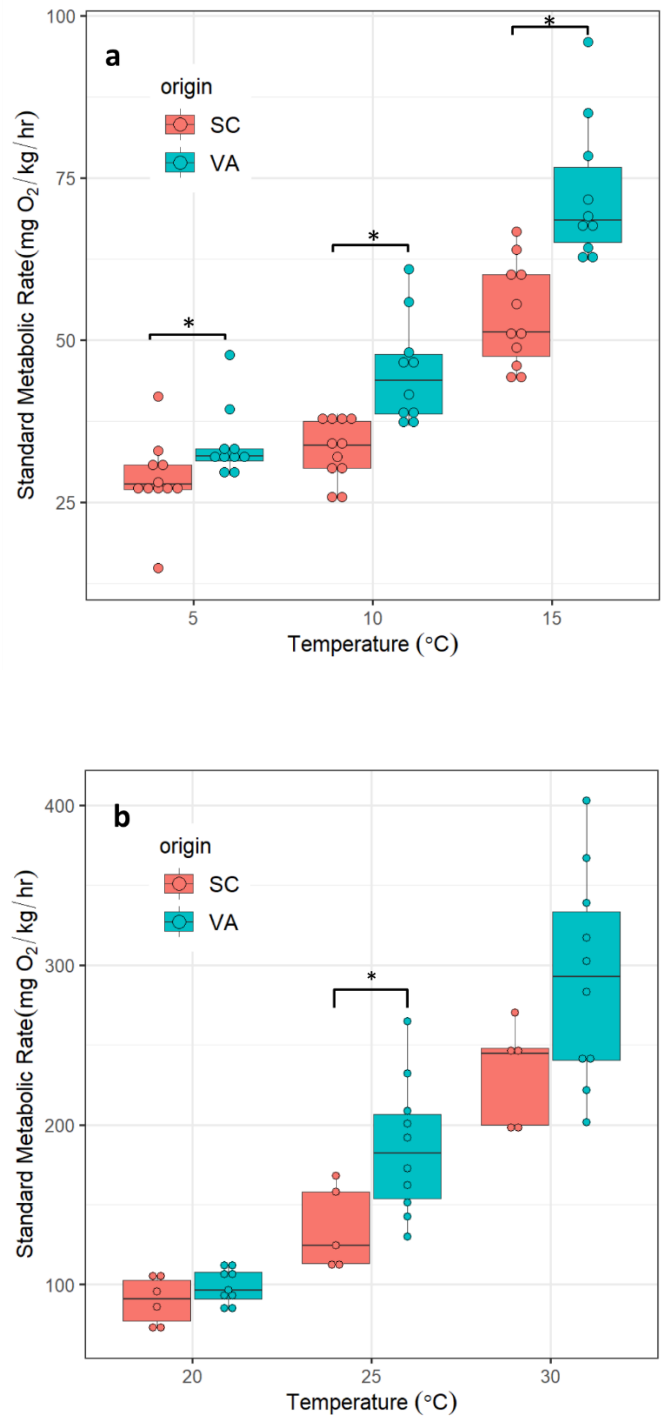

Figure 3. SMR of spotted seatrout from two genetically distinct populations measured at six discrete temperatures. SC = southern population, VA = northern population. (a) cold stress; (b) heat stress. Asterisks indicate significant differences between groups ($p \leq 0.05$, two tailed Student's t-test).

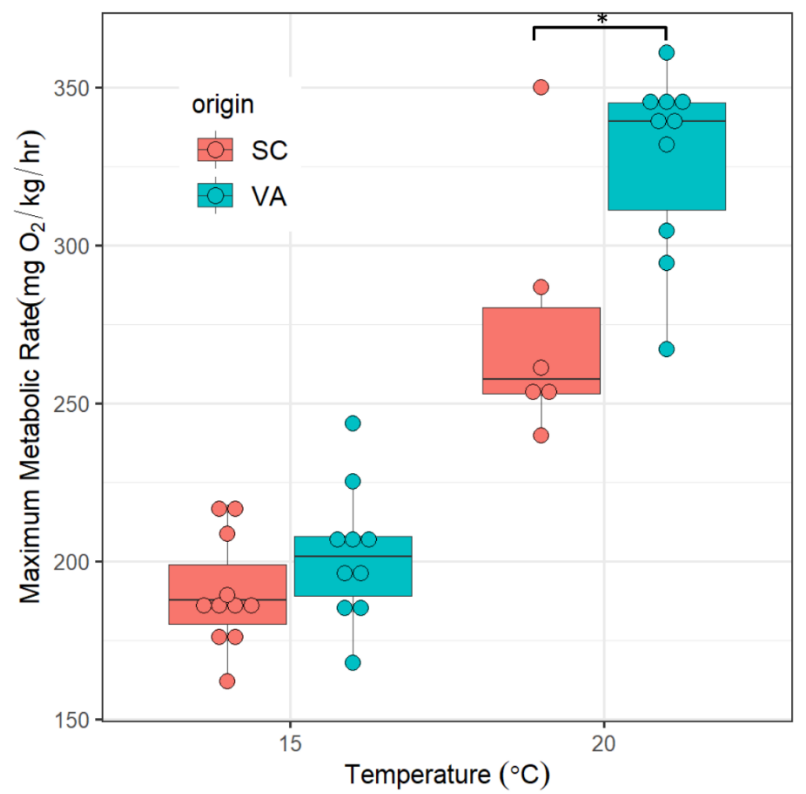

Figure 4. MMR of spotted seatrout from two genetically distinct populations measured at 15 °C and 20 °C. SC = southern population, VA = northern population. Asterisks indicate significant differences between groups ($p \leqslant 0.05$, two tailed Student' t-test).

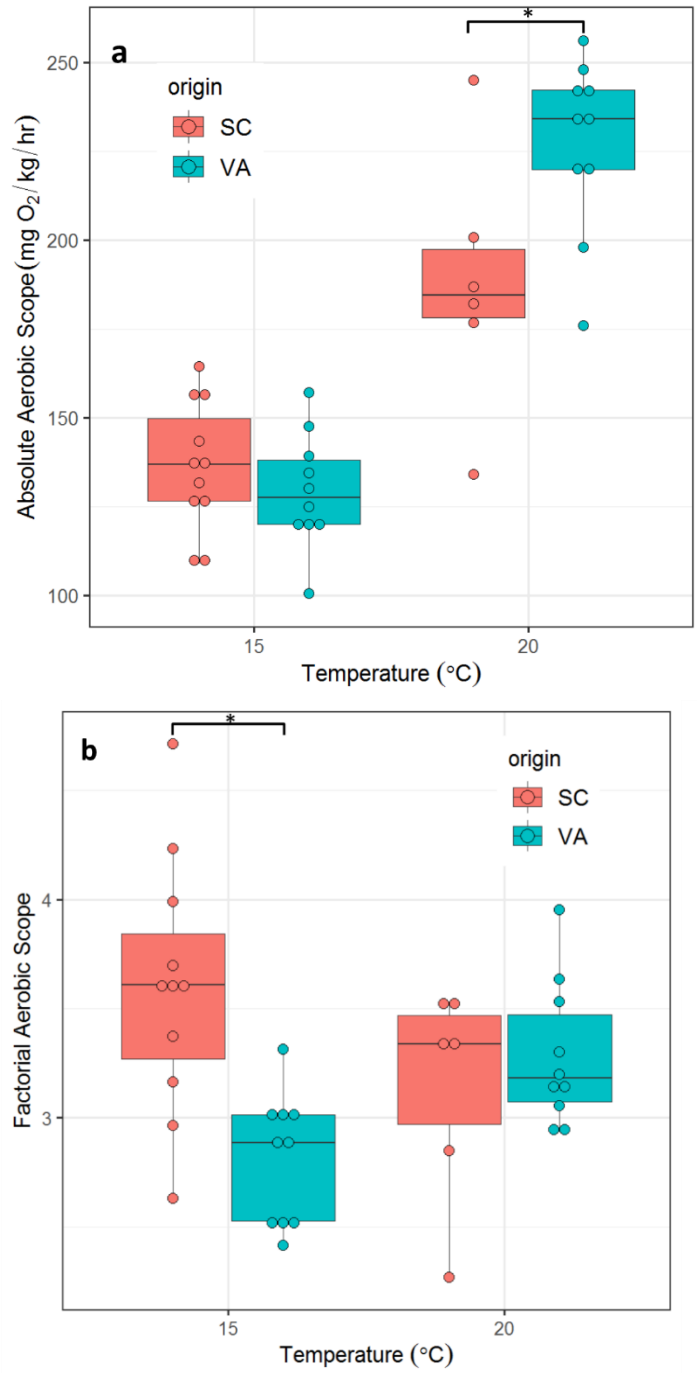

Figure 5. Absolute aerobic scope (AAS, a) and factorial aerobic scope (FAS, b) between two northern and southern spotted seatrout populations, at 15 °C and 20 °C. SC = southern population, VA = northern population. Asterisks indicate significant differences between groups ($p \leq 0.05$, two tailed Student's t-test).

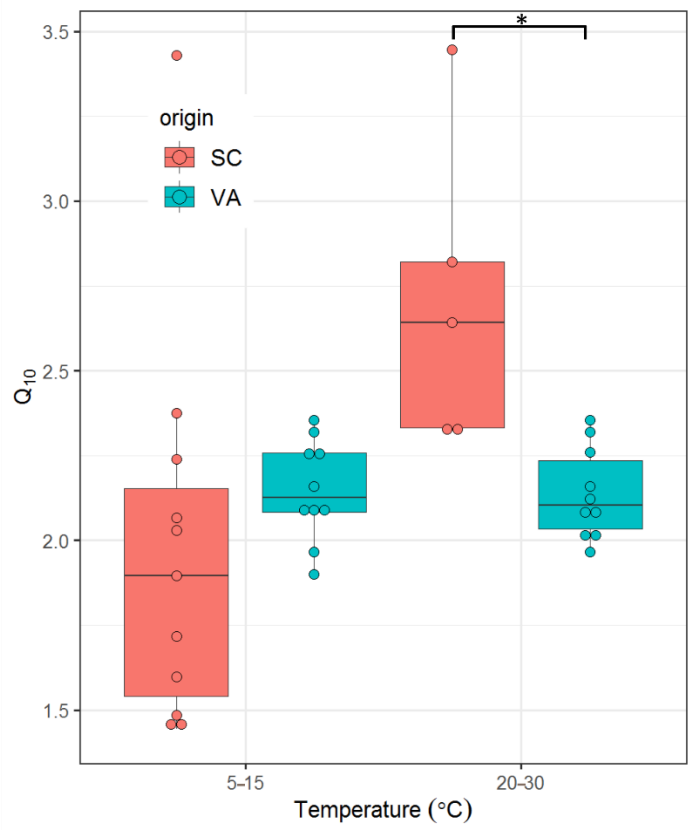

Figure 6. Temperature coefficient (Q10) of spotted seatrout between northern and southern spotted seatrout populations subjected to cold stress (5 to 15 °C) and heat stress (20 to 30 °C). SC = southern population, VA = northern population. Asterisks indicate significant differences between groups ($p \leq 0.05$, two tailed Student's t-test).

2 Chapter 2. Comparative Transcriptomics of Spotted Seatrout (*Cynoscion nebulosus*) Populations to Cold and Heat Stress

2.1 Abstract

Resilience to climate change depends on a species' adaptive potential and phenotypic plasticity. The latter can enhance survival of individual organisms during short periods of extreme environmental perturbations, allowing genetic adaptation to take place over generations. Along the U.S. East Coast, estuarine-dependent spotted seatrout (*Cynoscion nebulosus*) populations span a steep temperature gradient that provides an ideal opportunity to explore the molecular basis of phenotypic plasticity. Spotted seatrout sampled from a northern and a southern population were exposed to acute cold and heat stress (n = 5 in each treatment and control group) and their transcriptomic responses were compared. The southern population showed a larger transcriptomic response to acute cold stress, whereas the northern population showed a larger transcriptomic response to acute heat stress compared to controls based on differential expression analyses. The results corroborate previous findings of differences in metabolic plasticity between the two populations. Transcripts showing significant differences in expression levels were predominantly enriched in a few pathways including the metabolic, mitogen-activated protein kinase (MAPK) signaling, and forkhead box O (FoxO) signaling pathways. Genes showing population-specific patterns of expression, including *hpt, acot, hspa5, hsc70* are candidates for future studies aiming to monitor intraspecific differences in temperature stress responses in spotted seatrout. Our findings contribute to the current understanding of phenotypic plasticity and provide a basis for predicting the response of a eurythermal species under various climate change scenarios.

2.2 Introduction

Phenotypic plasticity can be defined as the ability of a genotype to be expressed as different phenotypes in response to varying biotic or abiotic conditions (Bradshaw 1965). Historically, the genetic basis of phenotypic plasticity has been either neglected or considered a factor that hinders evolutionary adaptation (Sarkar 2004; Kelly et al. 2012). The importance of this less-studied aspect of evolution is being increasingly recognized, due in part to the prediction that individual organisms with greater plasticity in ecologically relevant traits will have higher fitness in the face of climate change (Munday et al. 2013; Crozier and Hutchings 2014; King et al. 2017). Studies of phenotypic plasticity are incredibly diverse and encompass a wide range of morphological (e.g., gill raker number in freshwater fishes; Lindsey 1981), behavioral (e.g., boldness in foraging behavior; Stamps, 2007) and physiological (e.g., temperature sensitivity of cardiac excitability; Badr et al. 2016) traits. An improved understanding of the mechanisms underlying phenotypic plasticity will not only broaden the current understanding of evolution, but will also lead to better informed conservation management under future climate change scenarios (Forsman 2015; Connon et al. 2018).

Temperature has a direct and pervasive effect on fish physiology (Fry 1947; Angilletta et al. 2010) because it governs the rate of biochemical reactions (Allen et al. 2002), metabolic rates (Chabot et al. 2016), and the distribution of species (Pinsky et al. 2013). There is ample evidence that fish populations from different thermal regimes show divergent physiological responses to the same water temperatures. For example, sockeye salmon (*Oncorhynchus nerka*) populations differ in their cardiovascular physiology, which was found to be correlated with the historical river temperatures each population

encountered during upriver migration (Eliason et al. 2011). Mummichogs (*Fundulus heteroclitus*) collected from their northern and southern range limit along the western Atlantic coast show different thermal tolerance; the critical thermal maximum was significantly higher in the southern population (~1.5°C; Fangue 2006). The underlying molecular mechanisms for the thermal reaction norms, however, are complex and are only starting to be studied for fishes (Oomen and Hutchings 2017).

Molecular studies of phenotypic plasticity have benefited tremendously from the advancement in DNA sequencing technologies (Alvarez et al. 2015; Todd et al. 2016). A transcriptome refers to the whole set of the messenger RNA molecules in a cell and is dependent on the developmental stage and health state of an organism and on physiological conditions. Comparative transcriptomics can effectively determine the functional importance of specific genes under known environmental stressors and disease states (DeBiasse and Kelly 2016; Byron et al. 2016). Previously, the expression profiles of only a small number (~1 to 10) of pre-selected genes were measured in a single study, especially in non-model organisms (Airaksinen et al. 2003; Fangue 2006). Hybridization-based microarray technology improved the capacity for gene expression analyses, allowing comparison of differential expression in hundreds of genes, but was reliant on prior genomic information and required extensive array customization (Gracey 2007; Logan and Somero 2011). RNA-sequencing (RNA-seq) leverages the power of high-throughput sequencing and bioinformatics and allows the entire transcriptome to be surveyed simultaneously (Wang et al. 2009). This method is especially useful for studies involving species without any existing genetic resources (Alvarez et al. 2015).

Most studies of phenotypic plasticity in fishes have examined long-term transcriptomic responses, with temperature stress lasting weeks to months (Guo et al. 2013; Newton et al. 2013; Narum and Campbell 2015; Healy et al. 2017; Veilleux et al. 2018). Few studies have focused on the effects of acute thermal stress, which is more pertinent to the immediate survival of individual organisms. An example of long-term stress is a study in which redband trout (*Oncorhynchus mykiss gairdneri*) populations from the desert (hot) and montane (cool) habitats were collected and the offspring of each pure strain and their F1 crosses maintained in common garden experiments (Narum and Campbell 2015). When subjected to the diel water temperatures normally experienced by the desert population for six weeks, RNA-seq of the gill transcriptome of the desert strain offspring showed the strongest transcriptional response, followed by the F1 crosses and the montane strain offspring. In a follow-up study using acute warming stress, the same pattern was observed between the desert and montane populations, except the most cold-adapted population showed the largest transcriptional response (Chen et al. 2018). Transcriptomic studies focusing on the impacts of acute temperature stress of a wide taxonomic range of fishes will complement our current understanding of chronic temperature stress and allow better prediction of how fish in general will respond to climate change.

Spotted seatrout (*Cynoscion nebulosus*) is a teleostean fish distributed from the Atlantic coast of southeastern US to the Gulf of Mexico (Bortone 2002). Spotted seatrout inhabits estuaries for its entire life cycle and can be found in waters ranging from near freezing to 39.9°C (Jensen 2009; McDonald et al. 2013). Distinct populations of spotted seatrout exist throughout its range (Weinstein and Yerger 1976; Anderson and Karel

2010; Seyoum et al. 2018). Along the U.S. South Atlantic, spotted seatrout in Chesapeake Bay (hereafter called the northern population, or VA) are genetically distinct from those in South Carolina and farther south (hereafter called the southern population, or SC; Wiley and Chapman 2003; McDowell et al. 2015) with a changeover near New River, North Carolina (O'Donnell et al. 2014). Studies of spotted seatrout have found a range of physiological and life history differences such as growth rate (Smith et al. 2008), size at maturity (Ihde 2000; Brown-Peterson 2003), and metabolic rates (Song et al. 2019) between the two populations, while the molecular mechanisms underlying these differences have never been explored. A recent study by O'Donnell et al. (2014) suggests that a lack of suitable habitat may be driving the observed genetic separation and hence differences are mainly due to genetic drift. Population structure in aquatic systems can, however, also be maintained by natural selection (Conover et al. 2006; DeFaveri et al. 2013). Species generally experience the most stressful abiotic conditions, such as limiting temperatures, at their distributional margins (Parsons 1991; Hurst 2007). The northern population lives at the species' northern range limit, and experiences mean water temperatures that are on average 5 °C lower than the southern population in winter. During the summer, the northern population experiences average water temperatures comparable to those in the south (Song et al. 2019). A recent tagging study conducted in Virginia and North Carolina found 25% of the northern population migrated over 100 km from the point of release (Ellis 2014); in contrast to almost 100% recaptures occurring within 13 km in the portion of southern population residing in South Carolina (Davy 1994) and 50 km in Florida and Mississippi (Moffett 1961; Iversen and Tabb 1962; Overstreet 1983; Hendon et al. 2002). Large-scale winterkills of spotted seatrout are

common in Virginia and North Carolina, but rare farther south. The differences in movement patterns and the frequency to winter mortality events suggest that the two populations are under different selective pressure and this may contribute to the observed population structure.

The purpose of my study was to compare transcriptomic response in two genetically distinct and physiologically divergent spotted seatrout populations subjected to acute temperature stress. The objectives were threefold:

1. To construct a high-quality transcriptome for spotted seatrout;
2. To discover and quantify shared transcriptomic responses to cold and heat stress in both populations;
3. To discover and quantify unique transcriptomic response to cold and heat stress in each population.

2.3 Materials and Methods

All animal care and use protocols were approved by William & Mary's Institutional Animal Care and Use Committee (protocol: IACUC-2017-09-25-12356-jrmcdo).

2.3.1 Sample Collection and Experimental Design

Spotted seatrout (*Cynoscion nebulosus*) were captured by hook and line in 2017 and 2018 from the Corrotoman River, Virginia (VA, 37°43'58.8"N, 76°24'32.3"W) and near James Island, South Carolina (SC, 32°45'11.0"N, 79°53'48.0"W). Acclimation and experiments were carried out at the Seawater Research Lab at Virginia Institute of

Marine Science (Table 3, Figure 7). Details on the date of capture and the duration of acclimations are in Table S 4. Fish from each sampling location were acclimated in separate flow-through 10,000 L circular tanks. Water temperature was maintained at 15°C prior to cold-stress experiments and 20°C prior to heat-stress experiments. Fish were held in a cylindrical respirometer immersed in experimental tanks for a separate study measuring metabolic rates at various temperatures (Song et al. 2019). Briefly, fish from both VA and SC in the cold-stress group were consecutively exposed to decreasing temperatures: 15°C (20 h), 10°C (5 h) and 5°C (18 h). Fish in the heat-stress group were similarly exposed to increasing water temperatures: 20°C (20 h), 25°C (5 h) and 30°C (18 h). The acute decreases or increases between temperature steps were completed within 2 hours. At the end of each respirometry experiment, fish were euthanized by cranial concussion followed by pithing. This two-step protocol follows the American Veterinary Medical Association Guideline for the Euthanasia of Animals (Leary and Johnson 2020). This protocol is faster than other euthanasia methods, such as immersing fish in icy slurry or anesthesia via immersion in tricaine methanesulfonate (MS-222) solution, and therefore minimized the impact of euthanasia on gene expression. A small piece of liver tissue from each fish was collected after euthanasia using sterilized scissors. Liver tissue was used in this study because it is a key regulator for metabolic processes, and produces many stress-responsive proteins (Currie and Schulte 2013). The tissues were stored in cryovials and flash frozen in liquid nitrogen until RNA extraction. Spotted seatrout in the control groups were held at 15°C in the same flow-through tanks for at least 30 days. Control fish were directly netted out of the tanks without going through the respirometry

experiments or temperature stresses; control fish were processed and livers were preserved as described above.

2.3.2 RNA Extraction and RNA-seq

A subsample of liver (20 mg) from each sample was weighed and pulverized in liquid nitrogen using a mortar and pestle. The mortar and pestle were thoroughly cleaned by rinsing under deionized water and wiped with RNase AWAY solution (Thermo Scientific, Waltham, MA, USA) between samples to ensure no RNA contamination occurred. Total RNA was extracted from the pulverized tissues using the RNeasy Mini Kit (Qiagen, Valencia, CA, USA) according to the manufacturer's protocol including the on-column DNase digestion step to eliminate genomic DNA. RNA concentration was determined using a Qubit 2.0 fluorometer (BR RNA Assay, Invitrogen, Carlsbad, CA, USA). RNA quality was assessed in two ways. First, the ratio of absorbance at 260nm and 280nm (260/280) was evaluated using a NanoDrop ND-1000 spectrophotometer (NanoDrop Technologies, Wilmington, DE, USA). Samples with a 260/280 ratio of approximately of two indicate high purity of RNA. Second, an aliquot of each sample (5 ul) was run on a 1% agarose gel mixed with GelRed (Biotium, Fremont, CA, USA) and immersed in 1X Tris/Borate/EDTA (TBE) buffer at 100 V for 35 minutes. The RNA was then visualized under UV transillumination. The presence of two bright bands representing the 28S and 18S rRNA was used to evaluate intactness of the RNA. All samples met the criteria above. Samples of extracted RNA were then shipped on dry ice to the Biocomplexity Institute (BI) at Virginia Polytechnic Institute and State University. The quality and quantity of the RNA samples were again assessed using a TapeStation

(Agilent Technologies, Santa Clara, USA). RNA samples were standardized to 50 ng/ul and a fresh 25 ul aliquot of each RNA sample was sent in a second shipment to BI for construction of cDNA libraries using an Illumina TruSeq Stranded mRNA HT Sample Prep Kit (Illumina, San Diego, CA, USA). The resulting libraries were multiplexed and paired-end sequenced using a NextSeq 500/550 High Output kit V2 (2 x 75 cycles, 400 million clusters). The Illumina NextSeq Control Software v2.1.0.32 with Real Time Analysis RTA v2.4.11.0 was used to provide the management and execution of the NextSeq 500 sequencing run and to generate binary base call (BCL) files. The BCL files were converted to FASTQ files, adapters were trimmed, and reads were demultiplexed using bcl2fastq Conversion Software v2.20 (Illumina, San Diego, CA, USA). Raw data were submitted to NCBI's short read archive (accession PRJNA649515, release date 2021-08-07).

2.3.3 Bioinformatic Analyses

FASTQ files were downloaded to Carbonate (https://kb.iu.edu/d/aopq), Indiana University's large-memory computer cluster. For each sample, there was a FASTQ file containing all the forward sequencing reads and a FASTQ file containing all the reverse sequencing reads. To reduce the quantity of the input reads for *de novo* assembly and to improve assembly efficiency (Brown et al. 2012; Fletcher et al. 2013), forward and reverse reads from each sample were first concatenated and *in silico* normalization was performed using the default setting in Trinity (Haas et al. 2013). Different assembly algorithms can complement each other in discovering genes that might be missed using a single method (MacManes 2018), therefore *de novo* transcriptome assembly was

performed on the *in silico* normalized data using four different programs with varying k-mer sizes (subsequences with length k within a longer sequence): Trinity v2.8.4 (k-mer = 25; Haas et al. 2013), Velvet-Oases v1.2.10 (k-mer = 35, 45, 55; Schulz et al. 2012), SOAPdenovo v1.03 (k-mer = 35, 45, 55; Xie et al. 2014) and TransAbyss v1.5.5 (k-mer = 35, 45, 55; Robertson et al. 2010). All assemblies were concatenated into a single transcriptome and further processed with the EvidentialGene tr2aacds pipeline to select high-quality sequences based on length and gene-coding potential and to reduce redundancy (Evigene, http://eugenes.org/EvidentialGene; Gilbert 2013). This resulted in a final version of the spotted seatrout liver transcriptome (supplemental information S1).

To assess the quality of the newly generated spotted seatrout transcriptome, QUAST (Gurevich et al. 2013) was used to calculate common genomic metrics, including contig length summary, N50 (length of at least half of all the contigs) and GC content. BUSCO (Benchmarking Universal Single Copy Orthologs) was used to assess the completeness of the assembled transcriptome in terms of expected gene content (Simão et al. 2015). Specifically, the spotted seatrout liver transcriptome was searched against the database actinopterygii_odb9, which contains 4584 evolutionarily conserved genes expected to be found as single-copy orthologs in at least 90% of Actinopterygii (ray-finned fishes).

To assess gene expression levels for each transcript in the transcriptome for all 30 fish, original sequences were mapped back to the new transcriptome using kallisto (Bray et al. 2016). Kallisto uses a novel “pseudoalignment” approach to eliminate the need for perfectly aligning individual bases, thereby reducing the computing time by two orders of magnitude compared to alternative programs while achieving similar mapping accuracy

(Bray et al. 2016). Transcript abundances were normalized and reported in transcripts per million (TPM).

To assess differential expression among transcripts between the treatment groups (SC cold, VA cold, SC heat, VA heat) and the control groups (SC control, VA control), two programs with different statistical frameworks were used: DESeq2 (Love et al. 2014) and limma+voom (Law et al. 2014; Ritchie et al. 2015). Currently, there is no clear consensus on which differential expression algorithm achieves the best balance between Type I and Type II errors (Soneson and Delorenzi 2013; Costa-Silva et al. 2017). Similar to our use of different *de novo* assemblers, we used more than one approach to detect consensus transcripts because a false positive is less likely to be identified twice. DESeq2 uses a negative binomial distribution and a shrinkage estimator for dispersion and fold change. Limma+voom uses normal distribution and fits a linear model with all genes and samples combined. Both methods have been shown to achieve a good balance between accuracy and sensitivity when the number of biological replicates is at least three (five in this study; Costa-Silva et al. 2017). Differential expression (DE) was defined as those transcripts with a log2 fold change $\geq$ two and a multi-test adjusted p-value ≤ 0.05 (Benjamini and Hochberg 1995). Consensus transcripts that showed significant DE levels by both methods were retained and used in downstream analyses.

The new transcriptome was annotated using Trinotate (Bryant et al. 2017). It conducts BLASTx and BLASTp searches against the Swissprot database to identify matches to known proteins using default E-value cutoffs (Altschul et al. 1990; The Uniprot Consortium 2019). Transmembrane protein domains were searched on TMHMM (Krogh et al. 2001). Based on the matches from both BLASTx and BLASTp searches,

Trinotate extracts Gene Ontology (GO) (The Gene Ontology Consortium 2019) terms and K numbers from Kyoto Encyclopedia of Genes and Genomes (KEGG) Orthology Database (Kanehisa et al. 2016). The results from Trinotate were stored in a tab-delimited file (supplemental information S2). Higher-level molecular pathways were discovered based on the K numbers associated with differentially expressed transcripts for both cold and heat stress in each population (Kanehisa and Sato 2019). The search mode was set to spotted seatrout's closest relative available in the database: large yellow croaker, *Larimichthys crocea* (lco).

2.3.4 Validation using RT-qPCR

To validate the accuracy of RNA-seq results, real-time quantitative polymerase chain reaction (RT-qPCR) was used to calculate $\log_2$ fold change of a subset of the transcripts (n=6). Primers were designed based on contigs assembled in the *de novo* transcriptome using Primer-BLAST (Ye et al. 2012), with primer length set to 20 bp and melting temperature set to 60°C (Table S 5). 18S ribosomal RNA was used as an internal control using primers from Brewton et al. 2013, and VA and SC control group samples were used as reference samples. Total RNA (1 ug) was reverse transcribed using the SuperScript IV First-Strand Synthesis System (Invitrogen, Carlsbad, CA, USA) with both the random hexamers (50 ng/ul) and oligo$(dT)_{20}$ (50 uM). The synthesized cDNA template was diluted 1:100. Each 20 ul reaction consisted of 10 ul of PowerUp™ SYBR™ Green Master Mix (2X), 1ul for each of the forward and reverse primers (10 uM), 1ul of cDNA template, 7ul of PCR-grade water. All reactions were run on a QuantStudio 3 Real-Time PCR System (Thermo Fisher Scientific, Waltham, MA, USA).

Thermocycling conditions were: 50°C (2 min), 95°C (10 min), 40 cycles of 95°C (15 sec) and 60°C (1 min). Melt curve analyses were conducted immediately following thermal cycling with 95°C (15 sec), 60°C (1 min), 95°C (15 sec). Each reaction was performed in triplicate and the mean threshold cycle (C_T) was used for subsequent analyses. The comparative C_T method was used to present $\log_2$ fold change in order to make results directly comparable to RNA-seq results. To assess the validity of using the comparative C_T method, PCR efficiencies of all primers were calculated by running a standard curve with five 1:10 serial dilutions points (Schmittgen and Livak 2008).

2.4 Results

2.4.1 Transcriptome Assembly

All 30 samples had an RNA Integration Number (RIN) value > 8, indicating high quality RNA. Sequencing reads per sample ranged from 13.6 million to 18.6 million (mean ± SD = 15.7 ± 1.2). After *in silico* normalization, 6.6 million paired end reads were retained for *de novo* transcriptome assembly. Four different assemblers produced the following numbers of contigs: Trinity, 185,556; SOAPdenovo, 403,848; TransAbyss, 209,799; Velvet, 416,310. The final draft spotted seatrout liver transcriptome consisted of 37,398 contigs.

The quality of the *de novo* assembled spotted seatrout liver transcriptome was assessed using QUAST and BUSCO. QUAST indicated that this transcriptome contained 21,316 transcript contigs longer than 500 bp, an N50 of 3,121 bp and a GC content of 48.98% (Table S 6). BUSCO analysis discovered 81.3% complete genes and 6.1%

fragmented genes in the transcriptome when compared to expectation (lineage dataset: actinopterygii_odb9, 20 species, 4,584 total BUSCO groups searched).

2.4.2 Gene Expression Plasticity between and within Populations

Overall gene expression levels showed good correlation among biological replicates within treatment and control groups (Pearson's r = 0.89, Figure 8). A total of 1,653 unique transcripts showed DE in VA and SC samples combined in response to both cold and heat stress treatments. Of these, 1,281 transcripts showed DE in the cold treatment groups, and 570 transcripts showed DE in the heat treatment groups as compared to controls. A set of 20 transcripts showed DE in response to both heat and cold stress in both populations (supplemental information S3). A total of 655 transcripts were upregulated vs. 626 downregulated in the cold groups and 324 transcripts were upregulated vs. 246 downregulated in the heat groups.

Comparing the number of transcripts that showed DE by population, 40% more transcripts showed DE were found in SC (941) as compared to VA (669) in response to cold stress. In response to heat stress, 14% more transcripts showed DE were found in VA (351) as compared to SC (309) (Figure 9 a, b). Upregulation of gene expression was more common than downregulation, regardless of the population (Figure 10): in cold stress treatments, VA spotted seatrout had 376 upregulated vs. 293 downregulated transcripts. SC spotted seatrout had 498 upregulated transcripts vs. 443 downregulated transcripts. In the heat stress treatment, VA spotted seatrout had 198 upregulated transcripts vs. 153 downregulated transcripts. SC spotted seatrout had 177 upregulated transcripts vs. 132 downregulated transcripts. A complete list of all the significant DE

transcripts and the matrix of contig quantification can be found in the supplemental information (S4, S5).

2.4.3 Functional Analysis

Among the 37,398 contigs in the transcriptome, Trinotate found 12,778 unique BLASTx hits and 12,594 unique BLASTp matches. Within the BLASTp hits, 7,715 contigs were matched across at least 80% to the target protein's length. Trinotate retrieved 7,027 unique K numbers from the KEGG Orthology Database and 13,649 GO terms.

Based on the K numbers associated with significant DE transcripts, four lists of higher-level molecular pathways were obtained (2 populations x 2 temperature stresses). In the VA cold stress group, a total of 104 pathways was discovered based on 117 K numbers. Top pathways included metabolic (lco01100), apoptosis (lco04210), insulin signaling (lco04910), forkhead box O (FoxO) signaling (lco04068), and protein processing in endoplasmic reticulum (lco04141) pathways (Table 4). A total of 120 pathways was discovered based on 213 K numbers in SC spotted seatrout subjected to cold stress. Top pathways included metabolic (lco01100), mitogen-activated protein kinase (MAPK) signaling (lco04010), apelin signaling (lco04371), FoxO signaling (lco04068), and steroid biosynthesis (lco00100) pathways. There were 91 common cold stress pathways with 13 unique in VA spotted seatrout and 29 unique in SC spotted seatrout.

In the heat stress group, a total of 82 KEGG pathways was discovered based on 102 K numbers in the VA spotted seatrout. Top pathways included metabolic (lco01100),

protein processing in endoplasmic reticulum (lco04141), N-Glycan biosynthesis (lco00510), MAPK signaling (lco04010), and purine metabolism (lco00230) pathways (Table 4). A total of 71 KEGG pathways were discovered based on 79 K numbers in the SC heat stress group. Top pathways included metabolic (lco01100), MAPK signaling (lco04010), adipocytokine signaling (lco04920), PPAR signaling (lco03320), and cellular senescence (lco04218) pathways. There were 53 common pathways with 29 unique in VA and 18 unique in SC. A list of all the molecular pathways can be found in the supplemental information (S6).

Amplification efficiencies of the target genes and the internal control (18S rRNA) ranged from 1.80 to 2.13. Log_2 fold changes obtained from RT-qPCR showed strong correlation with RNA-seq results (Pearson's $r = 0.995$, $p < 0.05$, Figure S 1).

2.5 Discussion

We conducted RNA-seq on spotted seatrout exposed to acute temperature stress and *de novo* assembled the first liver transcriptome for this species. Based on this transcriptome, we compared the molecular mechanisms underlying two genetically distinct and physiologically divergent spotted seatrout populations. The putatively cold-adapted northern population showed lower transcriptional response to cold stress, while the putatively warm-adapted southern population showed lower transcriptional response to heat stress. KEGG pathway analyses of the significant DE transcripts revealed both common and unique pathways in both populations in response to temperature stress. When exposed to cold stress, a higher number of unique pathways were observed in the southern population while a higher number of unique pathways in response to heat stress

were seen in the northern population. Log_2 fold change of a subset of genes between RT-qPCR and RNA-seq were highly consistent, validating the accuracy of the RNA-seq results.

A high-quality transcriptome is essential for differential expression analyses and functional annotation (Grabherr et al. 2011). In general, a longer N50 indicates a better assembly. The N50 for our liver transcriptome was 3,121 bp, much longer than similar *de novo* assembled transcriptomes for other fishes, including yellow perch *Perca falvescens* (1,066 bp; Li et al. 2017), spotted rainbowfish *Melanotaenia duboulayi* (1,856 bp; Smith et al. 2013), and Patagonian toothfish *Dissostichus eleginoides* (1,434 bp; Touma et al. 2019). The percentage of the BUSCO gene content present in the assembled transcriptome (87.4%) was higher compared to that of the European sardine *Sardina pilchardus* (82.1%; Machado et al. 2018), Patagonian toothfish *Dissostichus eleginoides* (78.92%; Touma et al. 2019), and clown anemonefish *Amphiprion percula* (85.4%; Maytin et al. 2018). The high-quality transcriptome can be attributed to the use of high-quality samples, a combination of assemblers, a range of k-mers as well as the subsequent redundancy-reducing step. Future transcriptomic studies of spotted seatrout that include more tissue types may discover genes that are not expressed in the liver and result in a more comprehensive transcriptome for spotted seatrout.

In comparative studies of populations or closely related species, a larger transcriptomic response can either indicate a general stress response or physiological adaptation (Narum and Campbell 2015; Veilleux et al. 2018). Thus, transcriptomic studies should always be viewed within an ecological and physiological context (DeBiasse and Kelly 2016). For spotted seatrout, whole-organism standard metabolic rate

(SMR), as measured by oxygen consumption rate, is 19% higher in the northern population than the southern population at 5°C (Song et al. 2019). The difference is consistent with the metabolic cold adaptation (MCA) hypothesis, which states that cold-adapted species having higher SMR than warm-adapted species when compared at the same temperatures (White et al. 2012). Thus, the larger transcriptional response observed in the southern population at 5°C as compared to the northern population can be interpreted as greater stress. Similarly, a larger transcriptional response by the northern population at 30°C indicates that this population experienced greater physiological stress than the southern population when temperatures were elevated, likely due to a mismatch between oxygen demand (high SMR) and oxygen supply (low dissolved oxygen) (Pörtner and Knust 2007). SMR was found to be 26% higher in the VA than the SC spotted seatrout at 30°C, compared to a 37% difference at 25°C. This result suggests that VA spotted seatrout show reduced capacity of oxygen supply above 25°C (Song et al. 2019).

Cold stress resulted in a substantially larger number of transcripts that show DE than heat stress, a pattern that has been reported in several other RNA-seq studies. A recent study focusing on gene expression plasticity in the livers of two goby species compared DE between cold treatment (5°C) and heat treatment (25°C) relative to the control group (18°C). In round goby (*Neogobius melanostomus*), cold treatment led to 5,863 transcripts showing DE and heat treatment led to 642. In tubenose goby (*Proterorhinus semilunaris*) cold treatment led to 5,070 transcripts showing DE while heat treatment led to 424 (Wellband and Heath 2017). The authors associated the more successful invasion history of the round goby in the Great Lakes with its greater transcriptomic plasticity. Another study compared the effects of cold (5°C) and heat

acclimation (25°C) on the muscle transcriptome of adult three-spined stickleback (*Gasterosteus aculeatus*). Relative to fish held at the control temperature (18°C), cold acclimation resulted in 7,940 DE transcripts and heat acclimation resulted in 7,015 DE transcripts (Metzger and Schulte 2018). Whether this represents a general pattern in fishes requires additional studies that examine cold and heat stress simultaneously in the same study.

Another explanation for the large number of significant DE transcripts under acute cold stress could be an artifact of the endpoint temperature I chose. Ellis et al. (2017) conducted cold tolerance experiments on adult spotted seatrout in North Carolina and found they could tolerate water temperature at 5°C for up to five days, after which mortality increased rapidly. McDonald et al. (2013) reported the critical thermal maximum (temperature at which 50% of the fish die) of juvenile spotted seatrout in Texas was around 39°C. These data suggests that 5°C is closer to spotted seatrout's lower thermal tolerance threshold than 30°C is to its upper tolerance threshold. Future studies aiming to elicit an even stronger physiological stress response in spotted seatrout should choose an endpoint temperature above 30°C.

A higher number of upregulated transcripts compared to downregulated transcripts was discovered in all treatments for both groups. This finding agrees with a study using zebrafish larvae that found severe cold stress (12°C) induced 1,431 upregulated genes compared to 399 downregulated genes (Long et al. 2013). In mummichogs, cold acclimation at 5°C induced 5,460 upregulated genes compared to 1,746 downregulated gene in muscle transcriptomes (Healy et al. 2017). This trend is predicted because low temperature depresses the rate of biochemical processes, and

increased expression can compensate for this kinetic restraint (Currie and Schulte 2013). There are exceptions however. In orange-spotted grouper (*Epinephelus coioides*), there were 2,093 upregulated genes and 3,812 downregulated genes under cold stress (Sun et al. 2019). This might reflect different adaptative strategies among species in coping with low temperatures. Spotted seatrout, zebrafish, and killifish all live in shallow systems where water temperatures undergo large daily and seasonal fluctuations. Coupled with a limited ability to migrate, these species have to turn up their transcriptional machinery to survive periods of low water temperature. In contrast, orange-spotted grouper experience more stable ambient temperature in the open ocean and therefore may have evolved an opposite strategy by turning down gene expression to conserve energy during cold periods. Transcriptomic studies of strictly marine teleostean species are limited and more research is needed to understand the impact of acute temperature stress (Logan and Buckley 2015; Oomen and Hutchings 2017).

We found 20 genes with significant DE in both cold and heat stress in both populations. These genes most likely play important roles in the cellular stress response (CSR). Seven out of the 20 genes were annotated and associations included the heat shock protein 90-alpha (*hs90A*), apolipoprotein (*apom*) and haptoglobin (*hpt*). Heat shock proteins are a group of well-studied gene families which act as generic molecular chaperons to help maintain protein integrity under a range of stressors such as temperature, salinity and disease (Iwama et al. 2001). Apolipoproteins bind to lipids and play a major role in lipid transport and have been shown to play a role in the innate immunity in fishes (Concha et al. 2004; Pereiro et al. 2012; Causey et al. 2018). Haptoglobin is one of the acute-phase stress proteins synthesized by the liver (Windisch

et al. 2014; Cordero et al. 2017) and can bind to hemoglobin in the plasma and reduce oxidative stress (Alayash 2011). Haptoglobin shows the largest $\log_2$ fold change (~10) among all DE transcripts in this study and there are substantial differences between the two populations. It thus may be a good candidate genetic marker for estimating population-level temperature stress in spotted seatrout. Unfortunately, 13 out of the 20 generic stress genes did not return a BLAST hit, highlighting the problem with poor functional annotation in non-model organisms (Pavey et al. 2012).

2.5.1 Shared KEGG Pathways

A few shared molecular pathways between the northern and southern populations accounted for a disproportionately large number of DE transcripts. Metabolic pathways accounted for the most DE transcripts. The MAPK signaling pathway is one of the top pathways observed in response to heat stress and is one of the hallmarks of CSR (Kültz 2004). MAPKs are kinases which are involved in protein phosphorylation cascades in order to regulate the expression of many downstream targets (Cowan and Storey 2003; Huang et al. 2017). This pathway has been shown to be particularly important in modulating gene expression in gill epithelial cells in mummichogs during hyper- and hyposmotic stress and in the swim bladders of channel catfish (*Ictalurus punctatus*) in response to low dissolved oxygen (Kültz and Avila 2001; Yang et al. 2018). Under cold stress, the forkhead box O (FoxO) signaling pathway (lco04068) is a top pathway in both populations. Similar to the MAPK pathway, the FoxO signaling pathway can effect global transcriptomic change via a group of transcription factors that target genes

involved in apoptosis, oxidative-stress resistance and cell-cycle control (Ronnebaum and Patterson 2010; Puig and Mattila 2011).

2.5.2 Population-specific Genes and KEGG Pathways

In response to cold stress, the northern population downregulated acyl-coenzyme A thioesterase (*acot*) in the fatty acid elongation (lco00062) and biosynthesis of unsaturated fatty acids (lco01040) pathways. *Acot* plays a critical role in fatty acids metabolism and ATP generation (Tillander et al. 2017). This suggests that fat metabolism is suppressed, at least in the short term, in response to cold stress. In addition, genes involved in protein synthesis and transport are upregulated in pathways such as ribosome biogenesis in eukaryotes (lco03008) and protein export (lco03060). These genes include ribonuclease P protein subunit (*pop4*), U4/U6 small nuclear ribonucleoprotein (*snu13*) and transport protein subunit alpha (*sec61a*). 26S proteasome regulatory subunit T3 (*psmc4*) in the proteasome (lco03050) pathway is also upregulated. Proteasome is a large molecular complex where protein degradation and turnover occurs (Glickman and Ciechanover 2002). The upregulation of *psmc4* could suggest that the northern spotted seatrout were more efficient at protein turnover under cold stress condition. Protein synthesis, export and degradation are all energetically expensive processes requiring ATP. The upregulation of genes in these pathways suggest the northern population is capable of producing sufficient ATP to meet the energy requirement at low temperature.

Under acute cold stress, the southern population was found to upregulate uniquely long-chain acyl-CoA synthetase (*acsl*) and long-chain-fatty-acid-CoA ligase (*acsbg*) in the fatty acid biosynthesis (lco00061) and fatty acid metabolism (lco01212) pathways.

Both genes play critical roles in the fatty acids oxidation (Cheng et al. 2017). Large subunit ribosomal protein L23Ae (*rp-l23ae*) in the ribosome (lco03010) pathway is upregulated, suggesting enhanced protein production. However, genes in the protein degradation pathway, lysosome (lco04142), are downregulated: deoxyribonuclease II (*dnase2*), lysosomal alpha-glucosidase (*gaa*), and acid ceramidase (*asah1*). Lysosomes are organelles in eukaryotic cells containing hydrolytic enzymes that degrade biomolecules (Levine and Klionsky 2004). A mismatch between protein synthesis and protein degradation suggests the increased accumulation of misfolded proteins in the cell can lead to apoptosis (Fribley et al. 2009).

When subjected to heat stress, the northern population uniquely upregulated heat shock 70kDa protein (*hspa5*), a member of the heat shock protein 70 family (Roberts et al. 2010). Acetyl-CoA synthetase (*acss1*) is upregulated in the pyruvate metabolism (lco00620) and carbonhydrate metabolism (lco01200) pathways. *Acss1* catalyzes the reaction that produces the raw material, acetyl-CoA, for the citric acid cycle (aka. tricarboxylic acid cycle) in order to produce ATP. This pathway is only activated, however, when cells have depleted their normal carbon source (pyruvate) (Wolfe 2005). Isocitrate dehydrogenase (*idh1*) involved in the citric acid cycle was also uniquely upregulated. Relating to the physiological data, high SMR may have exhausted the pyruvate in the northern population and the upregulation of *acss1* serves as a short-term solution to supply acetyl-CoA. In addition, genes in the N-glycan biosynthesis (lco00510) pathways were upregulated: alpha-1,2-mannosyltransferase (*alg9*) and mannosyl-oligosaccharide glucosidase (*mogs*). These enzymes are involved in N-linked

glycosylation (addition of oligosaccharides to proteins) and play important roles in protein stability and cell signaling (Sinclair and Elliott 2005).

In heat stress, the southern population uniquely upregulated heat shock cognate 71 kDa protein (*hsc70*). *Hsc70* belongs to the same protein family as *hspa5* above and performs similar functions, however, *hsc70* is known to be constitutively expressed in unstressed cells and *hspa5* is only upregulated during stress (Goldfarb et al. 2006; Roberts et al. 2010). In European flounder (*Platichthys flesus)*, *hsc70* has been proposed to be involved in local adaptation to minimum seawater temperature (Hemmer-Hansen et al. 2007). RAC serine/threonine-protein kinase (*akt*) is downregulated in the following pathways: mTOR signaling pathway (lco04150), insulin signaling pathway (lco04910), and apelin signaling pathway (lco04371). G1/S-specific cyclin-D2 (*ccnd2*) was downregulated in the hedgehog signaling pathway (lco04340). Both *akt* and *ccnd2* play a role in cell proliferation and cell cycle (Manning and Cantley 2007; Katoh and Katoh 2009), thus their downregulation may indicate heat stress also induces cell growth arrest in the southern population.

My study provides a basis for predicting how spotted seatrout will cope with climate change. Despite the documented range shifts seen in many other fish species in the western Atlantic (Nye et al. 2009), there is no reported northward range expansion for spotted seatrout. Being extremely eurythermal may allow the species to withstand ongoing climate change *in situ*. We predict the center of species abundance will expand northward of Chesapeake Bay in the future for two reasons: i) mean winter water temperature is increasing and more suitable overwintering habitats will become available in more northern states such as Maryland, Delaware and New Jersey and, ii) Chesapeake

Bay water temperature is warming faster than air temperature (Ding and Elmore 2015). The high metabolic demand of the northern spotted seatrout at high temperature and will gradually force a portion of the current northern population to seek cooler water at higher latitudes. Occasional winterkills may still occur at the northern range limit, but the population at the leading edge of range expansion may be resilient to such events given the species' early maturation and fast growth.

In summary, differences in thermal tolerance, as reflected by differential gene expression is contributing to the population-level divergence observed in spotted seatrout from the U.S. South Atlantic and provides mechanistic insights into physiological responses to acute temperature stress. The northern population shows transcriptional signatures consistent with cold adaptation, yet they may be more vulnerable to elevated water temperature than the southern population. The liver transcriptome represents a valuable resource for future genetic monitoring studies. Candidate genes (*hpt, acot, hsc70, hspa5, etc.)* identified in this study should be functionally validated or screened more broadly across the species' range to verify their ecological importance. Furthermore, genomic-level and cross-generational investigations would also complement this study by discovering genes under selection and improve our understanding of adaptive evolution in general.

2.6 References

Airaksinen, S., T. Jokilehto, C. M. I. Råbergh, and M. Nikinmaa. 2003. Heat- and cold-inducible regulation of HSP70 expression in zebrafish ZF4 cells. Comparative Biochemistry and Physiology Part B: Biochemistry and Molecular Biology 136(2):275–282.

Alayash, A. I. 2011. Haptoglobin: Old protein with new functions. Clinica Chimica Acta 412(7–8):493–498.

Allen, A. P., J. H. Brown, and J. F. Gillooly. 2002. Global biodiversity, biochemical kinetics, and the energetic-equivalence rule. Science 297(5586):1545–1548.

Altschul, S. F., W. Gish, W. Miller, E. W. Myers, and D. J. Lipman. 1990. Basic local alignment search tool. Journal of Molecular Biology 215(3):403–410.

Alvarez, M., A. W. Schrey, and C. L. Richards. 2015. Ten years of transcriptomics in wild populations: what have we learned about their ecology and evolution? Molecular Ecology 24(4):710–725.

Anderson, J. D., and W. J. Karel. 2010. Population Genetics and Dynamics of Spotted Seatrout in the Estuarine Waters of Texas. Fisheries and Aquaculture Journal 01(06).

Angilletta, M., B. S. Cooper, M. S. Schuler, and J. G. Boyles. 2010. The evolution of thermal physiology in endotherms. Frontiers in bioscience (Elite edition) 2:861–81.

Badr, A., M. F. El-Sayed, and M. Vornanen. 2016. Effects of seasonal acclimatization on temperature-dependence of cardiac excitability in the roach, *Rutilus rutilus*. The Journal of experimental biology (March):1495–1504.

Benjamini, Y., and Y. Hochberg. 1995. Controlling the false discovery rate: a practical and powerful approach to multiple testing.

Bortone, S. A. 2002. Biology of the spotted seatrout. Biology of the Spotted Seatrout, 1st edition. CRC Press.

Bradshaw, A. D. 1965. Evolutionary Significance of Phenotypic Plasticity in Plants. Pages 115–155 *in* E. W. Caspari and J. M. Thoday, editors. Advances in Genetics. Academic Press.

Bray, N. L., H. Pimentel, P. Melsted, and L. Pachter. 2016. Near-optimal probabilistic RNA-seq quantification. Nature Biotechnology 34(5):525–527.

Brewton, R. A., R. Fulford, and R. J. Griffitt. 2013. Gene expression and growth as indicators of effects of the bp deepwater horizon oil spill on spotted seatrout (*Cynoscion nebulosus*). Journal of Toxicology and Environmental Health - Part A: Current Issues 76(21):1198–1209.

Brown-Peterson, N. 2003. The Reproductive Biology of Spotted Seatrout. Pages 99–133 *in* S. A. Bortone, editor. Biology of the spotted seatrout. CRC Press.

Brown, C. T., A. Howe, Q. Zhang, A. B. Pyrkosz, and T. H. Brom. 2012. A Reference-Free Algorithm for Computational Normalization of Shotgun Sequencing Data.

Bryant, D. M., K. Johnson, T. DiTommaso, T. Tickle, M. B. Couger, D. Payzin-Dogru, T. J. Lee, N. D. Leigh, T. H. Kuo, F. G. Davis, J. Bateman, S. Bryant, A. R. Guzikowski, S. L. Tsai, S. Coyne, W. W. Ye, R. M. Freeman, L. Peshkin, C. J. Tabin, A. Regev, B. J. Haas, and J. L. Whited. 2017. A Tissue-Mapped Axolotl De Novo Transcriptome Enables Identification of Limb Regeneration Factors. Cell Reports 18(3):762–776. ElsevierCompany.

Byron, S. A., K. R. Van Keuren-Jensen, D. M. Engelthaler, J. D. Carpten, and D. W. Craig. 2016. Translating RNA sequencing into clinical diagnostics: opportunities and challenges. Nature Reviews. Genetics 17(5):257–271.

Causey, D. R., M. A. N. Pohl, D. A. Stead, S. A. M. Martin, C. J. Secombes, and D. J. Macqueen. 2018. High-throughput proteomic profiling of the fish liver following bacterial infection. BMC Genomics 19:719.

Chabot, D., D. J. McKenzie, and J. F. Craig. 2016. Metabolic rate in fishes: definitions, methods and significance for conservation physiology. Journal of Fish Biology 88(1):1–9.

Chen, Z., A. P. Farrell, A. Matala, and S. R. Narum. 2018. Mechanisms of thermal adaptation and evolutionary potential of conspecific populations to changing environments. Molecular Ecology 27(3):659–674.

Cheng, H.-L., S. Chen, J.-H. Xu, L.-F. Yi, Y.-X. Peng, Q. Pan, X. Shen, Z.-G. Dong, X.-Q. Zhang, and W.-X. Wang. 2017. Molecular cloning and nutrient regulation analysis of long chain acyl-CoA synthetase 1 gene in grass carp, *Ctenopharyngodon idella* L. Comparative Biochemistry and Physiology. Part B, Biochemistry & Molecular Biology 204:61–68.

Concha, M. I., V. J. Smith, K. Castro, A. Bastías, A. Romero, and R. J. Amthauer. 2004. Apolipoproteins A-I and A-II are potentially important effectors of innate immunity in the teleost fish *Cyprinus carpio*. European Journal of Biochemistry 271(14):2984–2990.

Connon, R. E., K. M. Jeffries, L. M. Komoroske, A. E. Todgham, and N. A. Fangue. 2018. The utility of transcriptomics in fish conservation. The Journal of Experimental Biology 221(2):jeb148833.

Conover, D. O., L. M. Clarke, S. B. Munch, and G. N. Wagner. 2006. Spatial and temporal scales of adaptive divergence in marine fishes and the implications for conservation. Journal of Fish Biology 69:21–47.

Cordero, H., C. H. Li, E. Chaves-Pozo, M. Angeles Esteban, and A. Cuesta. 2017. Molecular identification and characterization of haptoglobin in teleosts revealed an important role on fish viral infections. Developmental and Comparative Immunology 76:189–199.

Costa-Silva, J., D. Domingues, and F. M. Lopes. 2017. RNA-Seq differential expression analysis: An extended review and a software tool. PLoS ONE 12(12):1–18.

Cowan, K. J., and K. B. Storey. 2003. Mitogen-activated protein kinases: new signaling pathways functioning in cellular responses to environmental stress. Journal of Experimental Biology 206(7):1107–1115.

Crozier, L. G., and J. A. Hutchings. 2014. Plastic and evolutionary responses to climate change in fish. Evolutionary Applications 7(1):68–87.

Currie, S., and P. M. Schulte. 2013. Thermal Stress. Pages 257–279 Physiology of Fishes, 4th edition. CRC Press.

Davy, K. B. 1994. South Carolina Marine Game Fish Tagging Program 1974-1992.

DeBiasse, M. B., and M. W. Kelly. 2016. Plastic and evolved responses to global change: What can we learn from comparative transcriptomics? Journal of Heredity 107(1):71–81.

DeFaveri, J., T. Shikano, Y. Shimada, and J. Merila. 2013. High degree of genetic differentiation in marine three-spined sticklebacks (*Gasterosteus aculeatus*). Molecular Ecology 22(18):4811–4828.

Ding, H., and A. J. Elmore. 2015. Spatio-temporal patterns in water surface temperature from Landsat time series data in the Chesapeake Bay, U.S.A. Remote Sensing of Environment 168:335–348. Elsevier Inc.

Eliason, E. J., T. D. Clark, M. J. Hague, L. M. Hanson, Z. S. Gallagher, K. M. Jeffries, M. K. Gale, D. A. Patterson, S. G. Hinch, and A. P. Farrell. 2011. Differences in Thermal Tolerance Among Sockeye Salmon Populations. Science 332(6025):109–112.

Ellis, T. 2014. Mortality and Movement of Spotted Seatrout at Its Northern Latitudinal Limits. North Carolina State University.

Ellis, T. A., J. A. Buckel, J. E. Hightower, and S. J. Poland. 2017. Relating cold tolerance to winterkill for spotted seatrout at its northern latitudinal limits. Journal of Experimental Marine Biology and Ecology 490:42–51.

Fangue, N. A. 2006. Intraspecific variation in thermal tolerance and heat shock protein gene expression in common killifish, *Fundulus heteroclitus*. Journal of Experimental Biology 209(15):2859–2872.

Fletcher, M. C., S. J. Silverman, W. Abbott, L. J. Girard, D. Guber, and E. Tomlinson. 2013. De novo transcript sequence reconstruction from RNA-Seq: reference generation and analysis with Trinity. Nature protocols 19(8):31–39.

Forsman, A. 2015. Rethinking phenotypic plasticity and its consequences for individuals, populations and species. Heredity 115(4):276–284.

Fribley, A., K. Zhang, and R. J. Kaufman. 2009. Regulation of Apoptosis by the Unfolded Protein Response. Methods in molecular biology (Clifton, N.J.) 559:191–204.

Fry, F. E. J. 1947. Effects of the environment on animal activity. Publications of the Ontario Fisheries Research Laboratory 55(55):1–62.

Gilbert, D. 2013. Gene-omes built from mRNA seq not genome DNA. 7th annual arthropod genomics symposium. Notre Dame.

Glickman, M. H., and A. Ciechanover. 2002. The ubiquitin-proteasome proteolytic pathway: Destruction for the sake of construction. Physiological Reviews 82(2):373–428.

Goldfarb, S. B., O. B. Kashlan, J. N. Watkins, L. Suaud, W. Yan, T. R. Kleyman, and R. C. Rubenstein. 2006. Differential effects of Hsc70 and Hsp70 on the intracellular trafficking and functional expression of epithelial sodium channels. Proceedings of the National Academy of Sciences of the United States of America 103(15):5817–5822.

Grabherr, M. G., B. J. Haas, M. Yassour, J. Z. Levin, D. A. Thompson, I. Amit, X. Adiconis, L. Fan, R. Raychowdhury, Q. Zeng, Z. Chen, E. Mauceli, N. Hacohen, A. Gnirke, N. Rhind, F. di Palma, B. W. Birren, C. Nusbaum, K. Lindblad-Toh, N. Friedman, and A. Regev. 2011. Full-length transcriptome assembly from RNA-Seq data without a reference genome. Nature Biotechnology 29(7):644–652.

Gracey, A. Y. 2007. Interpreting physiological responses to environmental change through gene expression profiling. Journal of Experimental Biology 210(9):1584–1592.

Guo, H., C. X. Ye, A. L. Wang, J. A. Xian, S. A. Liao, Y. T. Miao, and S. P. Zhang. 2013. Trascriptome analysis of the Pacific white shrimp *Litopenaeus vannamei* exposed to nitrite by RNA-seq. Fish and Shellfish Immunology 35(6):2008–2016. Elsevier Ltd.

Gurevich, A., V. Saveliev, N. Vyahhi, and G. Tesler. 2013. QUAST: Quality assessment tool for genome assemblies. Bioinformatics 29(8):1072–1075.

Haas, B. J., A. Papanicolaou, M. Yassour, M. Grabherr, P. D. Blood, J. Bowden, M. B. Couger, D. Eccles, B. Li, M. Lieber, M. D. MacManes, M. Ott, J. Orvis, N. Pochet, F. Strozzi, N. Weeks, R. Westerman, T. William, C. N. Dewey, R. Henschel, R. D. LeDuc, N. Friedman, and A. Regev. 2013. *De novo* transcript sequence reconstruction from RNA-seq using the Trinity platform for reference generation and analysis. Nature Protocols 8(8):1494–1512.

Healy, T. M., D. J. Chung, K. G. Crowther, and P. M. Schulte. 2017. Metabolic and regulatory responses involved in cold acclimation in Atlantic killifish, *Fundulus heteroclitus*. Journal of Comparative Physiology B: Biochemical, Systemic, and Environmental Physiology 187(3):463–475. Springer Berlin Heidelberg.

Hemmer-Hansen, J., E. E. Nielsen, J. Frydenberg, and V. Loeschcke. 2007. Adaptive divergence in a high gene flow environment: Hsc70 variation in the European flounder (*Platichthys flesus L.*). Heredity 99(6):592–600.

Hendon, J., J. Warren, J. Franks, and M. Buchanan. 2002. Movements of spotted seatrout (*Cynoscion nebulosus*) in mississippi coastal waters based on tag-recapture. Gulf of Mexico Science 2:91–97.

Huang, W., C. Ren, H. Li, D. Huo, Y. Wang, X. Jiang, Y. Tian, P. Luo, T. Chen, and C. Hu. 2017. Transcriptomic analyses on muscle tissues of *Litopenaeus vannamei* provide the first profile insight into the response to low temperature stress. PLOS ONE 12(6):e0178604.

Hurst, T. 2007. Causes and consequences of winter mortality in fishes 71:315–345.

Ihde, T. 2000. Biology of the spotted seatrout, *Cynoscion nebulosus*, in the Chesapeake Bay region. College of William and Mary.

Iversen, E. S., and D. C. Tabb. 1962. Subpopulations Based on Growth and Tagging Studies of Spotted Seatrout, *Cynoscion nebulosus*, in Florida. Copeia 1962(3):544.

Iwama, G. K., M. Mathilakath, M. M. Vijayan, R. B. Forsyth, and P. A. AcKerman. 2001. Heat shock proteins and physiological stress in fish. American Zoology 39:901–909.

Jensen, C. 2009. Stock Status of Spotted Seatrout, *Cynoscion nebulosus*, in North Carolina, 1991-2008.

Kanehisa, M., and Y. Sato. 2019. KEGG Mapper for inferring cellular functions from protein sequences. Protein Science: A Publication of the Protein Society.

Kanehisa, M., Y. Sato, M. Kawashima, M. Furumichi, and M. Tanabe. 2016. KEGG as a reference resource for gene and protein annotation. Nucleic Acids Research 44(D1):D457–D462.

Katoh, Y., and M. Katoh. 2009. Hedgehog Target Genes: Mechanisms of Carcinogenesis Induced by Aberrant Hedgehog Signaling Activation. Current Molecular Medicine 9(7):873–886.

Kelly, S. A., T. M. Panhuis, and A. M. Stoehr. 2012. Phenotypic plasticity: Molecular mechanisms and adaptive significance. Comprehensive Physiology 2(2):1417–1439.

King, N. G., N. J. McKeown, D. A. Smale, and P. J. Moore. 2017. The importance of phenotypic plasticity and local adaptation in driving intraspecific variability in thermal niches of marine macrophytes. Ecography 41(9):1469–1484.

Krogh, A., B. Larsson, G. von Heijne, and E. L. Sonnhammer. 2001. Predicting transmembrane protein topology with a hidden Markov model: application to complete genomes. Journal of Molecular Biology 305(3):567–580.

Kültz, D. 2004. Molecular and evolutionary basis of the cellular stress response. Annual Review of Physiology 67(1):225–257.

Kültz, D., and K. Avila. 2001. Mitogen-activated protein kinases are in vivo transducers of osmosensory signals in fish gill cells. Comparative Biochemistry and Physiology Part B: Biochemistry and Molecular Biology 129(4):821–829.

Law, C. W., Y. Chen, W. Shi, and G. K. Smyth. 2014. voom: Precision weights unlock linear model analysis tools for RNA-seq read counts. Genome biology 15(2):R29.

Leary, S., and C. L. Johnson. 2020. AVMA Guidelines for the Euthanasia of Animals: 2020 Edition* Members of the Panel on Euthanasia AVMA Staff Consultants.

Levine, B., and D. J. Klionsky. 2004. Development by self-digestion: Molecular mechanisms and biological functions of autophagy. Developmental Cell 6(4):463–477.

Li, Y. H., H. P. Wang, H. Yao, P. O'Bryant, D. Rapp, L. Guo, and E. A. Waly. 2017. De novo transcriptome sequencing and analysis of male, pseudo-male and female yellow perch, *Perca flavescens*. PLoS ONE 12(2):1–20.

Lindsey, C. C. 1981. Stocks are Chameleons: Plasticity in Gill Rakers of Coregonid Fishes. Canadian Journal of Fisheries and Aquatic Sciences 38(12):1497–1506. Canadian Science Publishing.

Logan, C. A., and B. A. Buckley. 2015. Transcriptomic responses to environmental temperature in eurythermal and stenothermal fishes. Journal of Experimental Biology 218(12):1915–1924.

Logan, C. A., and G. N. Somero. 2011. Effects of thermal acclimation on transcriptional responses to acute heat stress in the eurythermal fish *Gillichthys mirabilis* (Cooper). AJP: Regulatory, Integrative and Comparative Physiology 300(6):R1373–R1383.

Long, Y., G. Song, J. Yan, X. He, Q. Li, and Z. Cui. 2013. Transcriptomic characterization of cold acclimation in larval zebrafish. BMC Genomics 14(1).

Love, M. I., W. Huber, and S. Anders. 2014. Moderated estimation of fold change and dispersion for RNA-seq data with DESeq2. Genome Biology 15(12):550.

Machado, A. M., O. K. Tørresen, N. Kabeya, A. Couto, B. Petersen, M. Felício, P. F. Campos, E. Fonseca, N. Bandarra, M. Lopes-Marques, R. Ferraz, R. Ruivo, M. M. Fonseca, S. Jentoft, Ó. Monroig, R. R. Da Fonseca, and L. F. C. Castro. 2018. "Out of the Can": A Draft Genome Assembly, Liver Transcriptome, and Nutrigenomics of the European Sardine, *Sardina pilchardus*. Genes 9(10):485.

MacManes, M. D. 2018. The Oyster River Protocol: a multi-assembler and kmer approach for de novo transcriptome assembly. PeerJ 6:e5428.

Manning, B. D., and L. C. Cantley. 2007. AKT/PKB Signaling: Navigating Downstream. Cell 129(7):1261–1274.

Maytin, A. K., S. W. Davies, G. E. Smith, S. P. Mullen, and P. M. Buston. 2018. De novo transcriptome assembly of the clown anemonefish (*Amphiprion percula*): A new resource to study the evolution of fish color. Frontiers in Marine Science 5:284.

McDonald, D. L., P. D. Cason, B. W. Bumguardner, and S. Bonnot. 2013. Critical Thermal Maximum of Juvenile Spotted Seatrout (*Cynoscion nebulosus*) Reared for Summer Stocking in Texas. Journal of Applied Aquaculture 25(4):308–319.

McDowell, J. R., S. Musick, and J. Graves. 2015. Speckled trout, *Cynoscion nebulosus*, in Virginia: are these fish genetically distinct? Virginia Recreational Fishing Development Fund Final Report Project.

Metzger, D. C. H., and P. M. Schulte. 2018. Similarities in temperature-dependent gene expression plasticity across timescales in threespine stickleback (*Gasterosteus aculeatus*). Molecular Ecology 27(10):2381–2396.

Moffett, A. 1961. Movements and growth of spotted seatrout, *Cynoscion nebulosus* (Cuvier), in west Florida. Tallahassee, Florida, USA.

Munday, P. L., R. R. Warner, K. Monro, J. M. Pandolfi, and D. J. Marshall. 2013. Predicting evolutionary responses to climate change in the sea. Ecology Letters 16(12):1488–1500.

Narum, S. R., and N. R. Campbell. 2015. Transcriptomic response to heat stress among ecologically divergent populations of redband trout. BMC Genomics 16(1):103.

Newton, J. R., K. R. Zenger, and D. R. Jerry. 2013. Next-generation transcriptome profiling reveals insights into genetic factors contributing to growth differences and temperature adaptation in Australian populations of barramundi (*Lates calcarifer*). Marine Genomics 11:45–52.

Nye, J. A., J. S. Link, J. A. Hare, and W. J. Overholtz. 2009. Changing spatial distribution of fish stocks in relation to climate and population size on the Northeast United States continental shelf. Marine Ecology Progress Series 393:111–129.

O'Donnell, T. P., M. R. Denson, and T. L. Darden. 2014. Genetic population structure of spotted seatrout *Cynoscion nebulosus* along the south-eastern U.S.A. Journal of Fish Biology 85(2):374–393.

Oomen, R. A., and J. A. Hutchings. 2017. Transcriptomic responses to environmental change in fishes: Insights from RNA sequencing. Facets 2(2):610–641.

Overstreet. 1983. Aspects of the biology of the spotted seatrout, *Cynoscion nebulosus*, in Mississippi. Gulf Research Reports 1:1–43.

Parsons, P. 1991. Evolutionary Rates - Stress and Species Boundaries. Annual Review of Ecology and Systematics 22:1–18.

Pavey, S. A., L. Bernatchez, N. Aubin-Horth, and C. R. Landry. 2012. What is needed for next-generation ecological and evolutionary genomics? Trends in Ecology & Evolution 27(12):673–678.

Pereiro, P., P. Balseiro, A. Romero, S. Dios, G. Forn-Cuni, B. Fuste, J. V Planas, S. Beltran, B. Novoa, and A. Figueras. 2012. High-Throughput Sequence Analysis

of Turbot (*Scophthalmus maximus*) Transcriptome Using 454-Pyrosequencing for the Discovery of Antiviral Immune Genes. Plos One 7(5):e35369.

Pinsky, M. L., B. Worm, M. J. Fogarty, J. L. Sarmiento, and S. A. Levin. 2013. Marine Taxa Track Local Climate Velocities. Science 341(6151):1239–1242.

Pörtner, H. O., and R. Knust. 2007. Climate change affects marine fishes through the oxygen limitation of thermal tolerance. Science 315(5808):95–97.

Puig, O., and J. Mattila. 2011. Understanding Forkhead Box Class O Function: Lessons from *Drosophila melanogaster*. Antioxidants & Redox Signaling 14(4):635–647.

Ritchie, M. E., B. Phipson, D. Wu, Y. Hu, C. W. Law, W. Shi, and G. K. Smyth. 2015. limma powers differential expression analyses for RNA-sequencing and microarray studies. Nucleic Acids Research 43(7):e47--e47.

Roberts, R. J., C. Agius, C. Saliba, P. Bossier, and Y. Y. Sung. 2010. Heat shock proteins (chaperones) in fish and shellfish and their potential role in relation to fish health: A review. Journal of Fish Diseases 33(10):789–801.

Robertson, G., J. Schein, R. Chiu, R. Corbett, M. Field, S. D. Jackman, K. Mungall, S. Lee, H. M. Okada, J. Q. Qian, M. Griffith, A. Raymond, N. Thiessen, T. Cezard, Y. S. Butterfield, R. Newsome, S. K. Chan, R. She, R. Varhol, B. Kamoh, A. L. Prabhu, A. Tam, Y. Zhao, R. A. Moore, M. Hirst, M. A. Marra, S. J. M. Jones, P. A. Hoodless, and I. Birol. 2010. De novo assembly and analysis of RNA-seq data. Nature Methods 7(11):909–912.

Ronnebaum, S. M., and C. Patterson. 2010. The FoxO Family in Cardiac Function and Dysfunction. Annual Review of Physiology 72:81–94.

Sarkar, S. 2004. From the Reakionsnorm to the evolution of adaptive plasticity. *in* T. DeWitt and S. Schiener, editors. Phenotypic Plasticity: Runctional and Conceptual Approaches. Oxford University Press, New York.

Schmittgen, T. D., and K. J. Livak. 2008. Analyzing real-time PCR data by the comparative CT method. Nature Protocols 3(6):1101–1108.

Seyoum, S., R. S. McBride, M. D. Tringali, V. L. Villanova, C. Puchutulegui, S. Gray, and N. Van Bibber. 2018. Genetic population structure of the spotted seatrout (*Cynoscion nebulosus*): simultaneous examination of the mtDNA control region and microsatellite marker results. Bulletin of Marine Science 94(1):47–71.

Simão, F. A., R. M. Waterhouse, P. Ioannidis, E. V. Kriventseva, and E. M. Zdobnov. 2015. BUSCO: Assessing genome assembly and annotation completeness with single-copy orthologs. Bioinformatics 31(19):3210–3212.

Sinclair, A. M., and S. Elliott. 2005. Glycoengineering: The effect of glycosylation on the properties of therapeutic proteins. Journal of Pharmaceutical Sciences 94(8):1626–1635.

Smith, N. G., C. M. Jones, and J. Van Montfrans. 2008. Spatial and temporal variability of juvenile spotted seatrout *Cynoscion nebulosus* growth in Chesapeake Bay. Journal of Fish Biology 73(3):597–607.

Smith, S., L. Bernatchez, and L. B. Beheregaray. 2013. RNA-seq analysis reveals extensive transcriptional plasticity to temperature stress in a freshwater fish species. BMC Genomics 14(1):375.

Soneson, C., and M. Delorenzi. 2013. A comparison of methods for differential expression analysis of RNA-seq data. BMC Bioinformatics 14(1):91.

Song, J., R. Brill, and J. Mcdowell. 2019. Plasticity in Standard and Maximum Aerobic Metabolic Rates in Two Populations of an Estuarine Dependent Teleost , Spotted Seatrout (*Cynoscion nebulosus*): Biology 8(2):46.

Stamps, J. A. 2007. Growth-mortality tradeoffs and "personality traits" in animals. Ecology Letters 10(5):355–363.

Sun, Z., X. Tan, M. Xu, Q. Liu, H. Ye, C. Zou, and C. Ye. 2019. Liver transcriptome analysis and de novo annotation of the orange-spotted groupers (*Epinephelus coioides*) under cold stress. Comparative Biochemistry and Physiology D-Genomics & Proteomics 29:264–273.

The Gene Ontology Consortium. 2019. The Gene Ontology Resource: 20 years and still GOing strong. Nucleic Acids Research 47(D1):D330--D338.

The Uniprot Consortium. 2019. UniProt: a worldwide hub of protein knowledge. Nucleic Acids Research 47(D1):D506--D515.

Tillander, V., S. E. H. Alexson, and D. E. Cohen. 2017. Deactivating Fatty Acids: Acyl-CoA Thioesterase-Mediated Control of Lipid Metabolism. Trends in Endocrinology & Metabolism 28(7):473–484.

Todd, E. V., M. A. Black, and N. J. Gemmell. 2016. The power and promise of RNA-seq in ecology and evolution. Molecular Ecology 25(6):1224–1241.

Touma, J., K. K. García, S. Bravo, F. Leiva, J. Moya, L. Vargas-Chacoff, A. Reyes, and R. Vidal. 2019. De novo Assembly and Characterization of Patagonian Toothfish Transcriptome and Develop of EST-SSR Markers for Population Genetics. Frontiers in Marine Science 6.

Veilleux, H. D., T. Ryu, J. M. Donelson, T. Ravasi, and P. L. Munday. 2018. Molecular Response to Extreme Summer Temperatures Differs Between Two Genetically Differentiated Populations of a Coral Reef Fish. Frontiers in Marine Science 5.

Wang, Z., M. Gerstein, and M. Snyder. 2009. RNA-Seq: a revolutionary tool for transcriptomics. Nature Reviews Genetics 10(1):57–63.

Weinstein, M., and R. Yerger. 1976. Electrophoretic investigation of subpopulations of the spotted seatrout, *Cynoscion nebulosus* (Cuvier), in the Gulf of Mexico and Atlantic Coast of Florida. Florida Comp. Biochem. Physiol. 54B(97–102).

Wellband, K. W., and D. D. Heath. 2017. Plasticity in gene transcription explains the differential performance of two invasive fish species. Evolutionary Applications 10(6):563–576.

White, C. R., L. A. Alton, and P. B. Frappell. 2012. Metabolic cold adaptation in fishes occurs at the level of whole animal, mitochondria and enzyme. Proceedings of the Royal Society of London B: Biological Sciences 279(1734):1740–1747.

Wiley, B., and R. Chapman. 2003. Population Structure of Spotted Seatrout, *Cynoscion nebulosus*, along the Atlantic Coast of the U.S. Pages 31–40 *in* S. Borton, editor. Biology of the spotted seatrout2. CRC Press, Boca Raton, FL.

Windisch, H. S., S. Frickenhaus, U. John, R. Knust, H. O. Pörtner, and M. Lucassen. 2014. Stress response or beneficial temperature acclimation: Transcriptomic signatures in Antarctic fish (*Pachycara brachycephalum*). Molecular Ecology 23(14):3469–3482.

Wolfe, A. J. 2005. The Acetate Switch. Microbiology and Molecular Biology Reviews 69(1):12–50.

Xie, Y., G. Wu, J. Tang, R. Luo, J. Patterson, S. Liu, W. Huang, G. He, S. Gu, S. Li, X. Zhou, T.-W. Lam, Y. Li, X. Xu, G. K.-S. Wong, and J. Wang. 2014. SOAPdenovo-Trans: de novo transcriptome assembly with short RNA-Seq reads. Bioinformatics 30(12):1660–1666.

Yang, Y., Q. Fu, X. Wang, Y. Liu, Q. Zeng, Y. Li, S. Gao, L. Bao, S. Liu, D. Gao, R. Dunham, and Z. Liu. 2018. Comparative transcriptome analysis of the swimbladder reveals expression signatures in response to low oxygen stress in channel catfish, *Ictalurus punctatus*. Physiological Genomics 50(8):636–647.

Ye, J., G. Coulouris, I. Zaretskaya, I. Cutcutache, S. Rozen, and T. L. Madden. 2012. Primer-BLAST: a tool to design target-specific primers for polymerase chain reaction. BMC bioinformatics 13:134.

2.7 Supplemental Information

https://scholarworks.wm.edu/data/423/

This dataset contains supplemental materials for Chapter 2: Comparative Transcriptomics of Spotted Seatrout (*Cynoscion nebulosus*) Populations to Cold and Heat Stress in the associated publication - Search for Selection: Genomic, Transcriptomic, and Phenotypic Investigations of Spotted Seatrout (*Cynoscion nebulosus).*

Data are contained in a compressed file and include files in FASTA format (.fa), a text-based format representing nucleotide sequences using single-letter codes; data generated by Trinotate v3.1.1, an open source annotation suite designed for automatic functional annotation of transcriptomes (see Bryant et al. 2017, doi: 10.1016/j.celrep.2016.12.063) and data generated by Kallisto v.0.43.1., an open source RNA-seq quantification program. (see Bray et al. 2016, doi: 10.1038/nbt.3519).

File Name | Description:

- **SuppInfo_S1_Transcriptome.fa**: Spotted seatrout (*Cynoscion nebulosus*) liver transcriptome in FASTA format
- **SuppInfo_S2_Trinotate_Report.xls**: Functional annotation report from Trinotate for the liver transcriptome.
- **SuppInfo_S3_20_Common_Transcripts.xls**: Significant common transcripts responsive to both cold and heat stress and in both the southern and northern populations.
- **SuppInfo_S4_DE_contig_names.xlsx**: Transcript names showing significant differential expression to temperature stress, separated by populations
- **SuppInfo_S5_kallisto_matrix**: Transcripts quantification matrix for all samples
- **SuppInfo_S6_KEGG_pathways.xlsx**: Names of common and unique Kyoto Encyclopedia of Genes and Genomes (KEGG) molecular pathways between and within populations.

2.8 Tables

Table 3. Spotted seatrout samples used in RNA-seq.

Treatment Group	Sample ID	Sampling Temperature (°C)	Sample Size
SC cold	SC_c_1 to SC_c_5	5	5
VA cold	VA_c_1 to VA_c_5	5	5
SC heat	SC_h_1 to SC_h_5	30	5
VA heat	VA_h_1 to VA_h_5	30	5
SC control	SC_ctrl_1 to SC_ctrl_5	15	5
VA control	VA_ctrl_1 to VA_ctrl_5	15	5

Table 4. Top 10 KEGG pathways in both northern (VA) and southern (SC) spotted seatrout populations exposed to acute temperature stress. Numbers in the parentheses indicate KEGG Orthology terms identified in that specific pathway.

KEGG	VA	KEGG	SC
	Cold stress		
lco01100	Metabolic pathways (46)	lco01100	Metabolic pathways (69)
lco04210	Apoptosis (9)	lco04010	MAPK signaling pathway (11)
lco04910	Insulin signaling pathway (9)	lco04371	Apelin signaling pathway (9)
lco04068	FoxO signaling pathway (9)	lco04068	FoxO signaling pathway (8)
lco04141	Protein processing in endoplasmic reticulum (9)	lco00100	Steroid biosynthesis (8)
lco04010	MAPK signaling pathway (8)	lco04920	Adipocytokine signaling pathway (7)
lco00561	Glycerolipid metabolism (7)	lco04210	Apoptosis (7)
lco04371	Apelin signaling pathway (7)	lco03320	PPAR signaling pathway (7)
lco04530	Tight junction (6)	lco04910	Insulin signaling pathway (6)
lco04110	Cell cycle (6)	lco04530	Tight junction (6)
	Heat stress		
lco01100	Metabolic pathways (29)	lco01100	Metabolic pathways (24)
lco04141	Protein processing in endoplasmic reticulum (13)	lco04010	MAPK signaling pathway (5)
lco00510	N-Glycan biosynthesis (5)	lco04920	Adipocytokine signaling pathway (4)
lco04010	MAPK signaling pathway (4)	lco03320	PPAR signaling pathway (4)
lco00230	Purine metabolism (4)	lco04218	Cellular senescence (4)
lco00564	Glycerophospholipid metabolism (4)	lco04514	Cell adhesion molecules (CAMs) (3)
lco04210	Apoptosis (3)	lco00071	Fatty acid degradation (3)
lco01230	Biosynthesis of amino acids (3)	lco01212	Fatty acid metabolism (3)
lco04060	Cytokine-cytokine receptor interaction (3)	lco04141	Protein processing in endoplasmic reticulum (3)
lco04625	C-type lectin receptor signaling pathway (4)	lco04310	Wnt signaling pathway (3)

Table S 4. Details of spotted seatrout used in RNA-seq.

RNA-seq ID	Collection date	Location	Coordinates	Group	Acclimation started	Acclimation temp (°C)	Sampling temp (°C)	Experiment date	Weight (g)	Notes
JS01	11/23/2017	SC	32.753055, -79.896670	cold stress	11/23/2017	15	5	1/23/2018	235	
JS02	11/23/2017	SC	32.753055, -79.896670	cold stress	11/23/2017	15	5	2/15/2018	393	
JS03	11/23/2017	SC	32.753055, -79.896670	cold stress	11/23/2017	15	5	2/19/2018	394	
JS04	11/23/2017	SC	32.753055, -79.896670	cold stress	11/23/2017	15	5	2/23/2018	548	
JS05	11/23/2017	SC	32.753055, -79.896670	cold stress	11/23/2017	15	5	2/26/2018	458	
JS06	11/6/2017	VA	37.732985, -76.408968	cold stress	11/6/2017	15	5	1/23/2018	252	
JS07	11/6/2017	VA	37.732985, -76.408968	cold stress	11/6/2017	15	5	2/15/2018	187	
JS08	11/6/2017	VA	37.732985, -76.408968	cold stress	11/6/2017	15	5	2/19/2018	213	
JS09	11/6/2017	VA	37.732985, -76.408968	cold stress	11/6/2017	15	5	2/19/2018	217	
JS10	11/6/2017	VA	37.732985, -76.408968	cold stress	11/6/2017	15	5	2/23/2018	157	
JS11	3/4/2018	SC	32.753055, -79.896670	heat stress	6/6/2018	20	30	7/6/2018	368	
JS12	3/4/2018	SC	32.753055, -79.896670	heat stress	6/6/2018	20	30	7/15/2018	508	
JS13	3/4/2018	SC	32.753055, -79.896670	heat stress	6/6/2018	20	30	7/18/2018	447	
JS14	3/4/2018	SC	32.753055, -79.896670	heat stress	6/6/2018	20	30	7/22/2018	452	
JS15	3/4/2018	SC	32.753055, -79.896670	heat stress	6/6/2018	20	30	7/28/2018	473	
JS16	11/6/2017	VA	37.732985, -76.408968	heat stress	6/6/2018	20	30	7/3/2018	224	
JS17	11/6/2017	VA	37.732985, -76.408968	heat stress	6/6/2018	20	30	7/6/2018	231	
JS18	11/6/2017	VA	37.732985, -76.408968	heat stress	6/6/2018	20	30	7/10/2018	179	
JS19	11/6/2017	VA	37.732985, -76.408968	heat stress	6/6/2018	20	30	7/10/2018	210	
JS20	11/6/2017	VA	37.732985, -76.408968	heat stress	6/6/2018	20	30	7/15/2018	155	
JS21	10/23/2016	SC	32.753055, -79.896670	control	10/25/2016	15	15	3/8/2017	N/A	F1 generation of wild caught parents (courtsey SCDNR)
JS22	10/23/2016	SC	32.753055, -79.896670	control	10/25/2016	15	15	4/23/2017	N/A	
JS23	10/23/2016	SC	32.753055, -79.896670	control	10/25/2016	15	15	4/23/2017	N/A	
JS24	10/23/2016	SC	32.753055, -79.896670	control	10/25/2016	15	15	4/23/2017	N/A	
JS25	10/23/2016	SC	32.753055, -79.896670	control	10/25/2016	15	15	4/23/2017	N/A	
JS26	11/2/2016	VA	37.732985, -76.408968	control	11/2/2016	15	15	3/8/2017	N/A	
JS27	11/2/2016	VA	37.732985, -76.408968	control	11/2/2016	15	15	3/8/2017	N/A	

JS28	11/2/2016	VA	37.732985, -76.408968	control	11/2/2016	15	15	3/8/2017	N/A	
JS29	11/2/2016	VA	37.732985, -76.408968	control	11/2/2016	15	15	3/8/2017	N/A	
JS30	11/2/2016	VA	37.732985, -76.408968	control	11/2/2016	15	15	3/8/2017	N/A	

Table S 5. Primers used in RT-qPCR. 18S rDNA primer sequences were obtained from Brewton et al. (2013). The rest were designed based on assembled contigs in this study.

Oligo Sequence (5' To 3')	Oligo Name
CCAACGAGCGCTGACCTCCG	18S_F
GAGTCACCAAAGCGGCCGGG	18S_R
ACAAAGCTGGATTTGGCAGC	mic2_F
CCGATTCTGGACCCACAGAG	mic2_R
GTTCAAACACGCCACCTGAG	apo2_F
CTACGTCCACACGTCCTGTC	apo2_R
GGCACGGAATTCAAGCTGAC	hsp4_F
GGACCCGTAACCCAGATGAC	hsp4_R
TGGTGGTCACATCATCAGGC	ped2_R
TCGGTTCGGTCAAAGTGGAG	ped2_R
TGGATCAGTGAGCAAAGGGC	lec2_F
TCTGGACGTGGACATGTGAG	lec2_R
ATGGAAGGGGTCCACTTGAG	cea2_F
CCTGCTTGACGAGCTGTACC	cea2_R

Table S 6. QUAST report results for the de novo assembled transcriptome.

# contigs (>= 0 bp)	37398
# contigs (>= 1000 bp)	14669
# contigs (>= 5000 bp)	1674
# contigs (>= 10000 bp)	123
# contigs (>= 25000 bp)	0
# contigs (>= 50000 bp)	0
Total length (>= 0 bp)	51904107
Total length (>= 1000 bp)	42353733
Total length (>= 5000 bp)	11607548
Total length (>= 10000 bp)	1547531
Total length (>= 25000 bp)	0
Total length (>= 50000 bp)	0
# contigs	21316
Largest contig	24504
Total length	47027336
GC (%)	48.98
N50	3121
N75	1840
L50	4735
L75	9620
# N's per 100 kbp	392.15

2.9 Figures

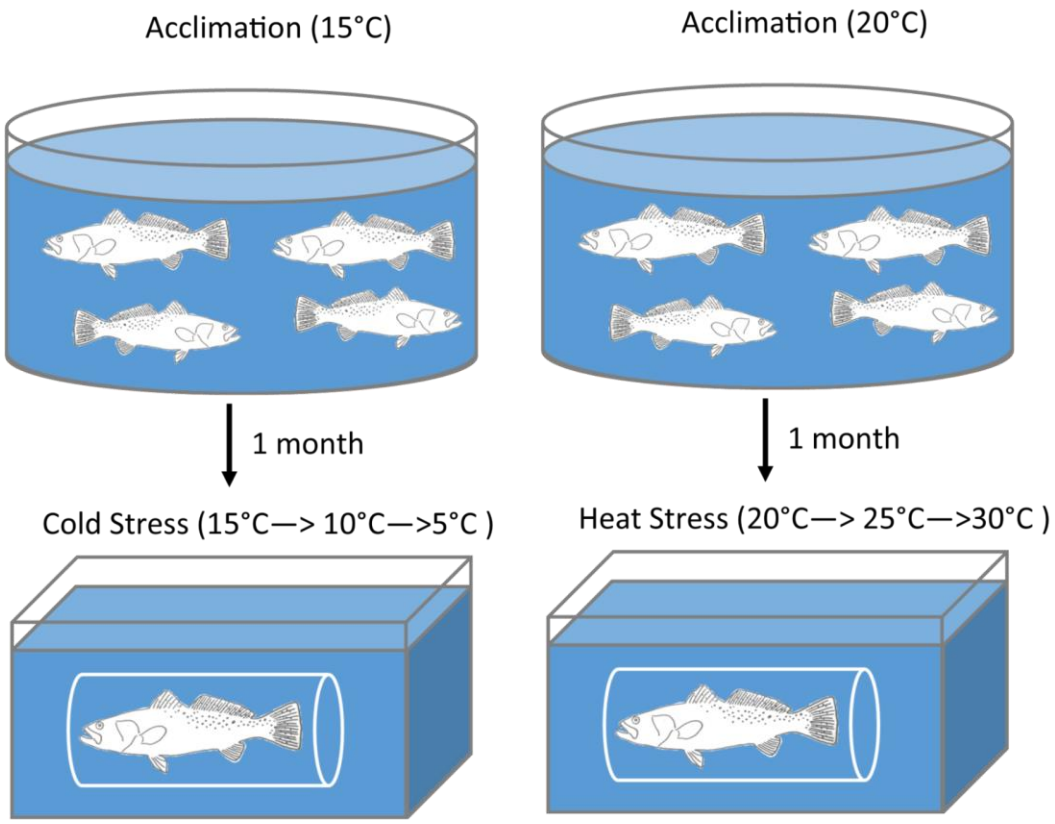

Figure 7. Schematic of the acclimation and experimental setup for the northern population (VA). The southern population (SC) setup was identical.

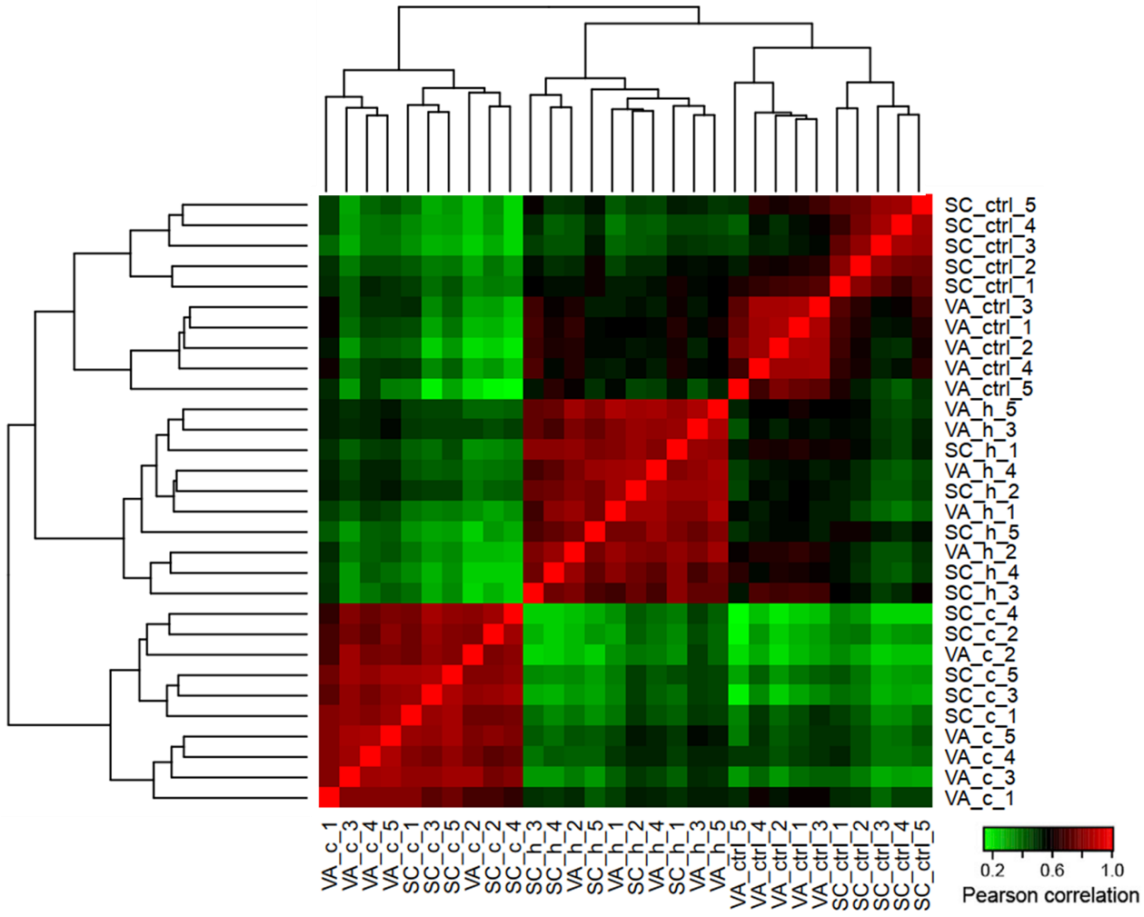

Figure 8. Heatmap showing pairwise Pearson's correlation values of gene expression for all 30 samples. VA=northern population, SC=southern population, c=cold stress, h=heat stress, ctrl=control.

Figure 9. Venn diagram showing number of significant differentially expressed transcripts between the northern (VA) and southern (SC) spotted seatrout populations. a) cold stress b) heat stress.

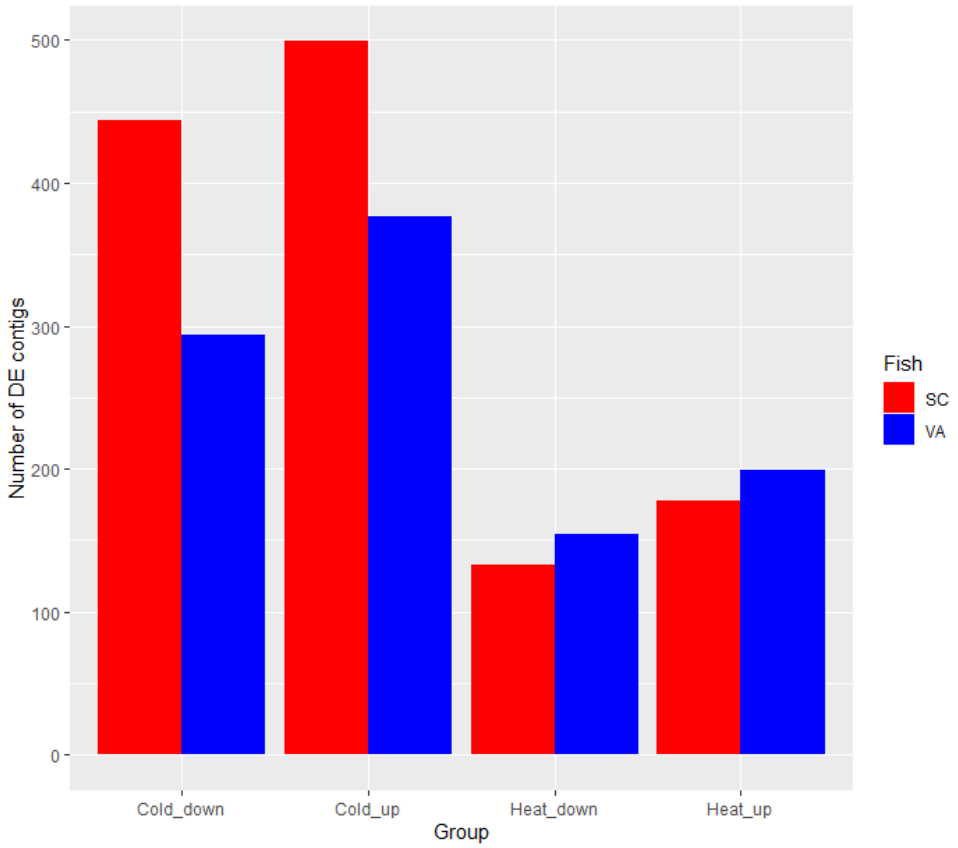

Figure 10 . Number of upregulated and downregulated differerntially expressed (DE) transcripts in cold and heat groups, colors indicate the two spotted seatrout populations.

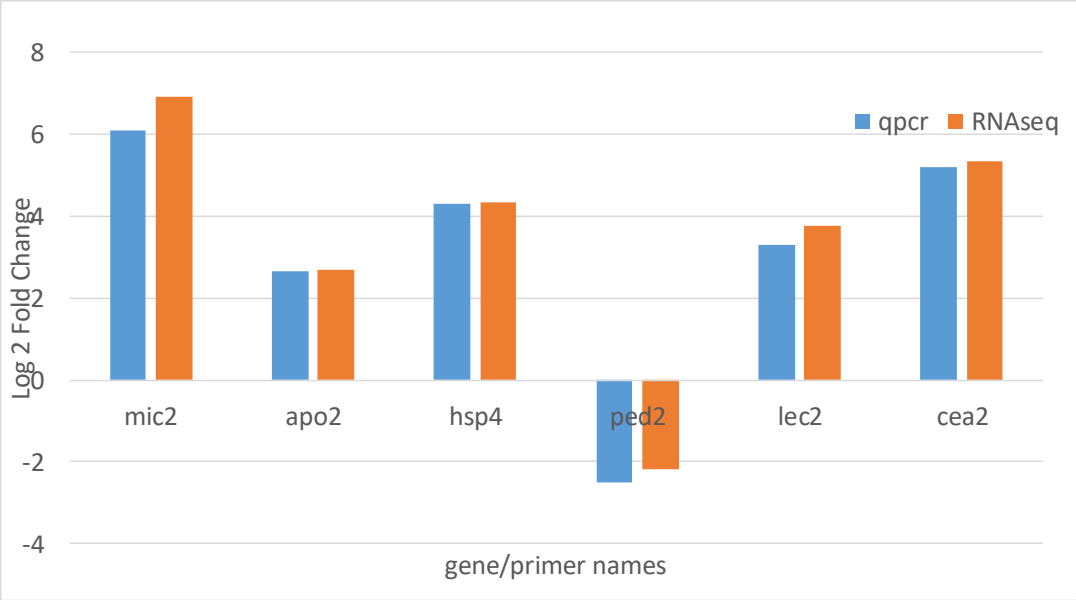

Figure S 1 Comparisons of log_2 fold change between RNA-seq and RT-qPCR results. Primer/sample pairs are as follows: mic2, apo2 (JS01-05 and JS21-25); hsp4, ped2 (JS06-10 and JS26-30); lec2, cea2 (JS11-15 and JS21-25)

3 Chapter 3. Genomic Signatures of Selection of Spotted Seatrout (*Cynoscion nebulosus*)

3.1 Abstract

Local adaptation can mediate species responses to climate change, yet little is known about the existence of local adaptation in many coastal marine species and its genetic basis. Spotted seatrout (*Cynosion nebulosus*) is an estuarine dependent species distributed from the Atlantic coast of the southeastern US and Gulf of Mexico. The genomic signatures of selection were investigated among spotted seatrout sampled from a wide geographic range which consists of a large portion of its current distribution. Using over 15,000 single nucleotide polymorphism (SNP) markers, previously reported genetic break on the US east coast near New River, North Carolina and distinct populations within the Gulf of Mexico were confirmed. Using a combination of population differentiation and environmental association analyses, I discovered SNP markers (n=226) with allele frequencies that are consistent with natural selection by local winter temperatures. A subset of the identified markers (n=24) were matched to transcripts in a recently generated spotted seatrout liver transcriptome (Chapter 2) and thus confirmed their functional roles in the fish. Functional annotation of the 24 transcripts found 18 with significant hits to known coding proteins and enriched in carbohydrate and fatty acid metabolism and transcriptional regulation processes. Among eight candidate genes that showed nonsynonymous substitutions, PRSS1(trypsin) has been shown in other fish species to be involved in cold adaptation. This study serves as a basis for the development of future high-throughput genotyping assays and genetic monitoring programs of spotted seatrout.

3.2 Introduction

Conspecific populations are commonly found in heterogeneous environments and therefore are subject to varying forces of natural selection such as temperature and salinity. Over time, these populations may evolve traits that confer higher fitness to individual organisms in their local habitat. This phenomenon and the process leading to it are called 'local adaptation' (Williams 1966, Kawecki and Ebert 2004). Local adaptation is widespread in the aquatic environment (Conover 1998). For instance, Atlantic silverside (*Menidia menidia*) display elevated growth rates in high latitudes where the growing season is shorter than at low latitudes (Conover and Present 1990) and sockeye salmon (*Oncorhynchus nerka*) populations that encounter more challenging migratory environments have greater aerobic scope, larger hearts, and better blood supply (Eliason et al. 2008). Locally adapted populations are predicted to show different sensitivity to climate change (Jensen et al. 2008), yet the lack of information on the occurrences and mechanisms of local adaptation in many species hinders our ability to more accurately predict population-level responses to climate change (Savolainen et al. 2013; Razgour et al. 2019).

Understanding the genetic basis of adaptation is one of the central questions of evolutionary biology and can provide valuable information for conservation management. Genetic diversity can be broadly divided into two categories: adaptive genetic variation and neutral genetic variation (Holderegger et al. 2006). Adaptive genetic variation refers to those genes and loci underlying fitness and is the direct targets of natural selection, whereas neutral genetic variation has no or very little fitness consequence and therefore is not the direct target of natural selection. Thus, the neutral genetic variation is often used

to infer patterns of gene flow and population structure, while adaptive genetic variation is more appropriate for studying fitness-related traits under selection (Storfer et al. 2018). Genetic studies of natural populations have been concentrated on using markers associated with neutral genetic variation, in part due to the lack of information on adaptive genetic variation for most species.

Studies of adaptive genetic variation have benefited tremendously from advances in DNA sequencing technology. Currently, for species with limited or even no existing genetic information, thousands of single nucleotide polymorphism (SNP) markers can be efficiently identified and genotyped at relatively low cost (Luikart et al. 2003). SNPs have become the genetic marker of choice for many population genomic studies because they are commonly observed in both protein-coding and non-coding regions of a genome, making them ideal markers to study both adaptive and neutral genetic variation (Akey et al. 2002). Higher marker density also means increased resolution and power to search for signatures of selection across the entire genome. For example, 68,182 SNP loci were genotyped in Atlantic herring (*Clupea harengus*) populations and identified hundreds of loci showing signatures of directional selection associated with water temperature and salinity in the Baltic Sea (Guo et al. 2016). Another study identified candidate genes and putative SNP loci under directional selection for temperature tolerance among redband trout (*Oncorhynchus mykiss gairdneri*) populations from contrasting thermal environments (Chen et al. 2018).

There are two main approaches to the discovery of signatures of natural selection using genome-wide SNP markers: genome scan-based and environmental association-based. The first type generally relies on genetic markers (thousands to tens of thousands)

sampled across the genome and scanned for those that show unusual levels of genetic differentiation compared to a genomic background (Lewontin and Krakauer 1973; Beaumont and Nichols 1996). This is because while the allele frequencies of all loci are under the influence of the same demographic processes, loci that are responsible for local adaptation are subject to an additional force of selection. The second approach explicitly incorporates environmental information. In this case, based on the biology and life history of the species, the researcher can propose the mostly likely environmental factors contributing to the observed distribution of genetic diversity. Loci responsible for local adaptation are more likely to be correlated with the environmental axis than neutral loci (Rellstab et al. 2015). Simulations have found that loci independently identified by both methods are more likely to be true targets of selection (Frichot et al. 2014).

Cynoscion nebulosus (Cuvier, 1830), commonly known as spotted seatrout or speckled trout, is a teleostean fish distributed from the Atlantic coast of southeastern US to the Gulf of Mexico (Bortone 2002). The spotted seatrout inhabits estuaries for its entire life cycle and can be found in waters ranging from near freezing to 39.9°C (Jensen 2009; McDonald et al. 2013). Studying the underlying genetic mechanisms of this extreme eurythermal species can provide novel insights into thermal adaptation, which are lacking from previous studies on freshwater and marine fishes (Hemmer-Hansen et al. 2014). Previous genetic studies of spotted seatrout population structure have relied upon a small number of molecular markers (2 to 38) covering a limited subset of the genome (Weinstein and Yerger 1976, King and Pate 1992, Gold and Richardson 1998, Wiley and Chapman 2003, O'Donnell et al. 2014, McDowell et al. 2015, Seyoum et al. 2018). These markers are useful for addressing questions related to demographic processes such as

gene flow and genetic drift, but they have limited power to investigate specific genes and loci that have been subject to selection and adaptive evolution (Narum et al. 2013).

Along the U.S. East Coast, spotted seatrout that from Chesapeake Bay to Pamlico Sound (hereafter called the northern population) are genetically distinct from those in South Carolina and further south (hereafter called the southern population; Wiley and Chapman 2003; McDowell et al. 2015) with a genetic break near New River, North Carolina. One hypothesis to explain the reduced gene flow is a lack of suitable estuarine habitat between New River, NC and Winyah Bay, SC (O'Donnell et al. 2014). Population structure, however, can also be maintained by past and ongoing natural selection (Conover et al. 2006; DeFaveri et al. 2013). A species generally experiences the most stressful abiotic conditions, such as temperature, at its distributional boundaries (Parsons 1991; Hurst 2007). Since North Carolina and Virginia are near the northern range limit of spotted seatrout (Ellis et al. 2017), they experience colder winters than those from the other portions of the species range. There also have been a higher frequency of documented winterkills of the spotted seatrout in the northern region (NCDMF 2014; Ellis et al. 2017) as compared to the southern portion of its range. This leads to an alternative hypothesis that the population structure is maintained, at least in part, due to selection by seasonal minimum water temperature. A better understanding of the factors maintaining population structure can better inform management actions as well as predict performance and distributions in future environmental conditions (Selkoe et al. 2016a; Stanley et al. 2018).

The objective of this Chapter is to test the hypothesis that local adaptation is contributing to population structure in spotted seatrout. Genome-wide SNP markers were

generated for spotted seatrout sampled across a steep temperature gradient along the US East Coast (ATL) and the Gulf of Mexico (GOM). Our null hypothesis was there are no loci showing signatures of selection among genetically distinct populations. If the null hypothesis is false, we predict that at least some of the loci can be functionally annotated and are putatively involved in thermal adaptation among spotted seatrout populations. An improved understanding of the pattern of both adaptive and neutral genetic variation can ultimately lead to sound management decisions for spotted seatrout under climate change.

3.3 Materials and Methods

3.3.1 Sample Collection

Spotted seatrout fin clips (n = 282) were obtained from 17 locations along the U.S. East Coast (ATL) and Gulf of Mexico (GOM) (Table S 7, Figure 11). ATL locations included Corrotoman River (CR), Ware River (WR), York River (YR), Elizabeth River (ER), Lynnhaven River (LR), Rudee Inlet (RI), Oregon Inlet (OI), Pamlico Sound (PS), South River (SR), Bogue Sound (BS), New River (NR), Cape Fear River (CFR), Winyah Bay (WB), James Island (JI), Wassaw Sound (GA); GOM locations included the Gulf side of Florida (FL), and various locations in Mississippi (MS). Fish were captured either by hook and line or gill net. All fin clips were preserved in 95% ethanol until DNA isolation. Total genomic DNA was isolated from tissues using a DNeasy Blood & Tissue Kit following the manufacturer's recommendation (Qiagen, Valencia, CA, USA). To check the integrity of genomic DNA, an aliquot of each extraction (5 ul) was loaded on 1.5% agarose gel mixed with GelRed nucleic acid gel stain (Biotium, Fremont, CA, USA) and included a 1 Kb Plus DNA ladder (Invitrogen Corporation, Carlsbad, CA, USA) as a

size standard. All samples were run in 1X Tris/Borate/EDTA (TBE) buffer at 100 V for 60 minutes. The DNA was then visualized under UV transillumination. Samples with high molecular weight DNA (a single bright band between 10,000 and 15,000 bp) were quantified using a Qubit 2 fluorometer using dsDNA BR assays (Invitrogen, Carlsbad, CA, USA). Samples were normalized to 1,200 ng total DNA and stabilized on a DNA preservation matrix (GenTegra, Pleasanton, CA, USA). Samples were shipped to Diversity Arrays Technology Pty. Ltd. (DArT PL, Canberra, Australia) for high throughput sequencing and SNP genotyping.

3.3.2 DArTseq Genotyping

DArTseq was conducted at DArT PL for the discovery of SNP markers for spotted seatrout. DArTseq combines a genomic complexity reduction step using restriction enzymes (RE) followed by genotyping-by-sequencing (Kilian et al. 2012). The protocol has been successfully applied to a wide range of species, including fishes (Grewe et al. 2015; Georges et al. 2018; Shams et al. 2019). Although DArTseq is conceptually similar to restriction-site associated (RAD) sequencing and double-digest RAD sequencing (ddRAD) (Elshire et al. 2011; Peterson et al. 2012), it preferentially targets genic regions of the genome and therefore is more appropriate for finding genes involved in local adaptation (Kilian et al. 2012). Different restriction enzyme (RE) combinations were tested at the DArT PL (data not shown) and enzymes were selected based on the optimal size distribution of the restriction fragments. Custom proprietary adapters used in ligation reactions were similar to those described by Elshire et al. (2011) and Kilian et al. (2012). A compatible forward adapter included an Illumina flow cell

attachment sequence, a sequencing primer sequence, and a barcode region of variable length. A compatible reverse adapter included an Illumina flow cell attachment sequence. Following double RE digestion and adapter ligation, only the fragments with x-y overhangs were preferentially amplified in polymerase chain reactions (PCR) using the following conditions: 94 ˚C for 1 min, 30 cycles of 94 ˚C for 20 sec, 58 ˚C for 30 sec, and 72 ˚C for 45 sec, and 72 ˚C for 7 min. After PCR, equimolar amounts of amplification product from each sample were pooled and cluster amplification was performed using a HiSeq SR Cluster Kit V4 cBot, followed by 77-bp single-end sequencing on Illumina Hiseq 2500 (Illumina, San Diego, CA, USA). *De novo* SNP discovery was completed using a proprietary bioinformatic pipeline developed by DArT PL (http://www.diversityarrays.com/software.html). Raw sequencing reads, SNP genotypes, and associated marker data for spotted seatrout were downloaded from the DArT PL website.

3.3.3 SNP Filtering

DArTseq genotype data were imported into R version 3.6.3 (R Core Team 2018) using the dartR v1.1.11 package (Gruber et al. 2018) and converted to *genlight* format (Jombart and Ahmed 2011). Quality control is critical for markers generated from genotyping-by-sequencing methods and the filtering steps should be tailored to each dataset and the objective of the study (O'Leary et al. 2018). Filtering steps were conducted to maximize the number of samples retained while maintaining high stringency in the following order: 1) loci with an average reproducibility < 90% were excluded. 2) monomorphic loci (only a single allele across all samples) were excluded. 3)

loci missing > 10% of genotype calls were excluded. 4) In instances where more than one SNP was present within a sequence tag (secondary SNPs), only one SNP was kept at random to reduce linkage. 5) individual samples missing > 10% of genotype calls after initial filtering steps were excluded. 6) loci with a minor allele frequency < 0.01 were excluded. 7) loci with exceedingly low (< 5) and high (> 100) read depth were excluded to mitigate potential issues with allelic dropout (Cooke et al. 2016). Finally, loci were tested for deviation from the expectations of Hardy-Weinberg equilibrium (HWE) for each location using the R package radiator v1.1.5 (Gosselin et al. 2020), which can indicate systematic genotyping errors, the presence of null alleles or other problems related to variation in sequencing depth. Loci that did not conform to the expectations of HWE in one-third of the sampling locations were excluded. This threshold was chosen because loci that do not conform to the expectations of HWE in just one or a few populations may due to biological causes such as selection. The remaining loci were used in the subsequent analyses.

3.3.4 Delineation of Population Structure using the Full Dataset

These summary statistics of each sample location were calculated using the Genodive v3.0 (Meirmans and Van Tiendren 2004):

1. Observed heterozygosity, H_O;
2. Nei's gene diversity, also known as expected heterozygosity, H_S;
3. Inbreeding coefficient, G_{IS}.

Genetic relationships among populations were estimated by calculating pairwise F_{ST} values (Weir and Cockerham 1984) in the R package StAMPP v1.6.1 (Pembleton et

al. 2013). Exploratory principal component analysis (PCA) was conduct to summarize the genetic variability of the dataset using R package adegenet v2.1.2 (Jombart and Ahmed 2011).

The number of clusters (K) contained in the data was assessed using STRUCTURE v2.3.4 (Pritchard et al. 2000). Scenarios for populations from K = 1 to 5 were first tested for all samples with all SNPs. Simulations were run with sampling locations as population priors, and allowing admixture and correlated allele frequencies (Falush et al. 2003). Initial simulations were done three times for each K with a burn-in of 50,000 and 200,000 Markov chain Monte Carlo repetitions. The most likely K was chosen by calculating ΔK, which is based on the rate of change in the log probability of data between successive values of K (Evanno et al. 2005). STRUCTURE may fail to discover weakly differentiated populations in the presence of more strongly differentiated populations (Waples and Gaggiotti 2006; Janes et al. 2017). To achieve a higher resolution for samples along ATL, samples from GOM were excluded for a second round of STRUCTURE simulations with K = 2 to 4. The model parameters were the same as above.

Discriminant analysis of principal components (DAPC) was also used to independently identify the number of clusters that best describe the data. DAPC is a multivariate method developed specifically for genomic data and uses sequential K-means to estimate genetic clusters (Jombart et al. 2010). K was discovered by running the *find.clusters* function in R package *adegenet* v2.1.2 (Jombart and Ahmed 2011) and running 5 iterations each of K = 1 to 17 (the total number of sampling locations). The Bayesian information criterion (BIC) value was used in model selection and was

averaged from the same K. The K with the lowest average BIC value was selected as the most likely scenario (Lee et al. 2009).

Analysis of molecular variance (AMOVA) was used to evaluate a range of population grouping scenarios in terms of the partitioning of genetic variation (Excoffier et al. 1992) in Genodive v3.0 (Meirmans and Van Tiendren 2004). The groupings of sampling locations were informed by the results of the clustering analyses above. Statistical significance of AMOVA results was determined by using 999 permutations of the data.

3.3.5 Outlier Loci Discovery

Isolation by distance (IBD) refers to the spatial autocorrelation of allele frequencies among samples and can lead to an inflated false positive rate when testing for loci putatively under selection (Meirmans 2012). First, a Mantel test which was implemented in adegent v2.1.2 was used to assess whether IBD patterns exist along the U.S. East Coast by using Nei's genetic distance and the shortest distance over water (km) among all sampling locations (Mantel, 1967). Three Mantel tests were run with: 1) All ATL locations. 2) CR-NR (northern ATL). 3) NR-GA (southern ATL).

Two methods based on different statistical methods were used to identify SNP markers that are putatively under selection. Pcadapt v 4.3.1 (Luu et al. 2017) uses genetic markers only and identifies loci that are putatively under selection (outliers) based on their contribution to the population structure. Simulations have shown that *pcadapt* can handle hierarchical population structure better than other genome scan approaches such as BayeScan and OutFlank. *Pcadapt* was chosen specifically for this study because

spotted seatrout is largely non-migratory and are known to exhibit a pattern of hierarchical population structure (Seyoum et al. 2018). The false discovery rate (FDR) was controlled for at $\alpha = 0.05$ (Benjamini and Hochberg 1995).

A second approach to discovery of outlier loci was environmental association analysis (Rellstab et al. 2015). One major advantage of environmental association analysis is that it incorporates *a priori* hypothesis about which environmental variable might be responsible for the observed distribution of genetic diversity. Here, the seasonal minimum water temperature was hypothesized to be the most ecologically relevant environmental variable based on the natural history of spotted seatrout (NCDMF 2014). Therefore, the average water temperature (AWT) in January was obtained for each sampling location from either Coastal Water Temperature Guide (https://www.ncei.noaa.gov/access/data/coastal-water-temperature-guide) or National Estuarine Research Reserve System (http://cdmo.baruch.sc.edu/) (Table S 8). The AWT was standardized by subtracting the mean and dividing by the standard deviation across all sampling locations. For the genetic data, missing genotypes were first imputed by using the default method implemented in the R package *LEA* v2.8.0 (Frichot and François 2015). A Latent factor mixed-effect model (LFMM) was fitted using different subsets of samples to detect loci that are significantly associated with AWT (Frichot and François 2015). First, only samples from ATL were included (LEA1). The Gibbs sampler algorithm was run for 5,000 cycles of burn-in followed by 10,000 iterations of the data. This was performed five times for K = 2 based on DAPC and STRUCTURE clustering results. The second model (LEA2) excluded the southern population on ATL which comprised samples from CFR to GA (see Results) but included GOM samples because

water temperatures in GOM are more similar to those experienced by the southern population, thus we posit that loci that are involved in temperature adaptation should be independently discovered by the two models. Candidate loci were discovered based on the control of FDR at $\alpha = 0.05$ (Benjamini and Hochberg 1995). Only those loci jointly identified as outliers by *pcadapt*, LEA1, and LEA2 were considered putative adaptive loci.

3.3.6 Functional Annotation

The spotted seatrout transcriptome generated in Chapter 2 was used as a reference for functional annotation of the outlier loci. The transcriptome was assembled from liver tissues of fish sampled from CR and JI on ATL after being exposed to acute cold and heat stress (Chapter 2) and is therefore enriched in genes that are expressed in response to temperature stress. To assess whether the outlier SNPs were present in the transcriptome, a custom Basic Local Alignment Search Tool (BLAST) database using the spotted seatrout liver transcriptome as the reference database was constructed. Next, sequence tags (~ 69 bp) from DArTseq containing the outlier SNPs were used as queries in a BLAST nucleotide (BLASTn) analysis (Altschul et al. 1990; Zhang et al. 2000) with E-values set to 1e-10. Significant matches were extracted and for each locus, two transcript sequences (containing the reference or alternate alleles) were prepared and translated into amino acid sequences in all 6 possible reading frames using the Swiss Institute of Bioinformatics Resource Portal (Artimo P, Jonnalagedda M, Arnold K, Baratin D, Csardi G, de Castro E, Duvaud S, Flegel V, Fortier A, Gasteiger E, Grosdidier A, Hernandez C 2012). The longest continuous protein sequence was chosen as the most likely translation

product. The protein sequences were then used in a BLAST protein (BLASTp) analysis on the National Center for Biotechnology Information (NCBI) website to discover homology with known proteins. When there was a significant match to a known protein in the database, two levels of assessments were conducted: 1) whether the nucleotide change resulted in translation of the same or a different amino acid (synonymous/nonsynonymous substitution), and 2) when a nonsynonymous substitution occurred, whether the change in amino acid was a conservative (similar in biochemical properties such as hydrophobicity and charge between the original and the alternative amino acid) or nonconservative replacement.

3.4 Results

3.4.1 SNP Quality Control

Data received from DArT PL included 59,904 SNPs and 282 samples. After the quality filtering steps outlined in the Methods section, a total of 15,187 high-quality SNPs and 277 samples were retained for further analyses. The mean sample size was 16.3 per sample location with a range of 7 (LR) to 35 (CR) (Table 5). Missing genotypes decreased from 14% in the unfiltered dataset to 1% in the final dataset. The highest number of SNPs were removed after "missing > = 10% genotypes by locus" (n = 19,988) and "minor allele frequency < 0.01" (n = 11,946). No loci deviated significantly from the expectations of HWE in more than one-third of the sampling locations (Table 6). Summary statistics for individual samples and SNPs were summarized in boxplots (Figure S 2, Figure S 3). DArTseq data files, a final filtered dataset in *genlight* format,

and associated R scripts are available (https://github.com/sjwu571/Cneb_PopGen) for reproducing the results below.

3.4.2 Delineation of Population Structure using the Full Dataset

Summary statistics were similar among populations (Table 5); effective number of alleles: mean = 1.26, range = 1.254 (MS) to 1.281 (BS); observed heterozygosity: mean = 0.158, range = 0.15 (MS) to 0.174 (SR); expected heterozygosity: mean = 0.173, range = 0.166 (MS) to 0.18 (BS). However, the inbreeding coefficient (G_{is}) had a wider range than other summary statistics among all sampling locations: mean = 0.085, range = 0.019 (WB) to 0.138 (FL).

In the exploratory PCA, PC1 explained 7.8% of the total variation; PC2 explained 2.6% of the total variation; PC3 explained 2.2% of the total variation (Figure 12, Figure 13). The separation between samples from GOM and the samples from ATL was evident along PC1 and PC3. There was evidence of a genetic cline within ATL (Figure 14).

In STRUCTURE analysis, when all samples were included, K = 2 was chosen as the most likely population structure scenario (ΔK = 11,6405). Samples in GOM showed distinct genetic ancestry from samples within ATL, and two genetic ancestries were evident within ATL (Figure 16). When samples in the GOM were excluded, samples from CR to PS were characterized by high posterior probabilities (mean ± SD = 0.936 ± 0.035, blue color) of a northern ATL ancestry (Figure 17). Moving southward, the proportion of southern ancestry started increasing (grey color) and the proportion of northern ancestry decreased slightly in SR and BS (mean ± SD = 0.815 ± 0.109). Admixture was the most pronounced at NR (northern ancestry: mean ± SD = 0.674 ±

0.213; southern ancestry: mean ± SD = 0.326 ± 0.210). South of NR, samples from CFR to GA shifted to a predominantly southern ATL ancestry (mean ± SD = 0.662 ± 0.170), but the northern ancestry was still substantial (mean ± SD = 0.338 ± 0.17). Three samples from southern sampling locations, 2_71 (CFR), 3_65 (JI), and 3_66 (JI), showed high levels of northern ancestries (0.91- 0.948).

Results from DAPC analysis was similar to the results of the STRUCTURE analysis. K = 4 was chosen as the most appropriate number of clusters because it had the lowest BIC score (1819.325), although K = 3 had a similar BIC value (1821.838). In the scenario of K = 3, the three clusters consisted of 1) FL 2) MS and 3) ATL (not shown). In the scenario of K = 4, two clusters within ATL were further discriminated: from north to south, all samples from CR through BS were assigned to cluster 3 (except for two samples from BS, which were assigned to cluster 2) (Table S 9). From CFR to GA, all samples were assigned to cluster 2 (except for one from CFR, two from JI, which were assigned to cluster 3). NR was the only location where samples were near evenly assigned to clusters 2 (n = 15) and 3 (n = 14). Next, DAPC was run using the group assignments defined by the results above, with 50 retained principal components corresponding to 33% of the total variance in the dataset. Discriminant function 1 (DF1) and discriminant function 2 (DF2) explained much of the variance (DF1 = 70.3%, DF2 = 27.9%). Samples within GOM were separated from ATL along DF1, and the FL (cluster 4) was separated from the MS (cluster 1) along DF2 (Figure S 4). Cluster 2 and 3 were separated along DF3, which explained 1.8% of the variation (Figure S 5).

The global F_{ST} value among all locations was 0.077 (95% CI = 0.075-0.079, p =0.001). The magnitude of the pairwise F_{ST} values generally agreed with clustering

results from DAPC and STRUCTURE (Table 7). The two GOM locations (FL, MS) had the highest and all significant pairwise F_{ST} values in comparisons with other sampling locations: mean = 0.143, range = 0.12 (CFR vs. MS) to 0.158 (MS vs. WR) (Table 7). The next highest F_{ST} values were between the northern (north of NR) and southern (south of NR) ATL locations: mean = 0.049, range = 0.023 (BS vs. CFR) to 0.065 (GA vs. WR), $p < 0.0001$. The lowest F_{ST} were among the northern locations: mean = 0.002, range = 0 (CR vs. OR, CR vs. PS, YR vs. OI, PS vs. OI; $p > 0.31$) to 0.005 (WR vs. SR, $p < 0.0001$; WR vs. BS, $p < 0.0001$). Among the southern ATL locations, F_{ST} values were slightly higher than those among the northern ATL locations: mean = 0.008, range = 0.004 (WB vs. GA; $p < 0.0001$) to 0.012 (WB vs. JI, JI vs. GA, both $p < 0.0001$). Comparison of the two northernmost locations, WR and CR, resulted in a small yet significant F_{ST} (0.003, $p < 0.001$). RI was significantly different from every other northern location except LR (0.001, $p = 0.192$). SR and BS, the two geographically closest locations just north of NR, had F_{ST} values that were significantly different from most other northern locations: mean = 0.003, range = 0.002 (SR vs. PS; BS vs. ER; BS vs. LR; BS vs. OI; BS vs. SR) to 0.006 (ER vs. SR); p-values ranged from less than 0.0001 to 0.035. However, SR was not significantly different from LR ($F_{ST} = 0.001$, $p = 0.137$).

A range of grouping scenarios for locations were evaluated using AMOVA: 1. no grouping; 2. (ATL)(GOM); 3. (ATL)(FL)(MS); 4. (CR-BR)(CFR-WB)(FL)(MS). From scenario 2 to 4, variation among populations within groups (F_{SC}) decreased sequentially (0.032 → 0.017 → 0.003, all $p = 0.001$, Table 8). This result suggested that that scenario 4 was the most effective in minimizing variation among groups. The among-group component of variation (F_{CT}) was maximized in scenario 3 (0.123, $p = 0.001$).

3.4.3 Outlier Loci

Mantel tests showed a pattern of IBD when ATL locations were included (r =0.693, p = 0.001, Figure S 6), but IBD was not found either among the northern ATL locations (r = -0.168, p =0.873, Figure S 7) or among the southern ATL locations (r = 0.243, p =0.322, Figure S 8). Tests for loci putatively under selection were completed jointly with *pcadapt* and LEA. Pcadapt identified 2,145 outliers with all samples from ATL. LEA1 identified 1,517 outliers showing a significant correlation with AWT on ATL, and LEA2 identified 1,562 outliers when only the northern population and GOM samples were included. In total, 226 loci were found to be in common among the three lists of outliers, representing 1.5 % of the full filtered data set. Examination of the allele frequencies of these outliers revealed that 25 loci were fixed (100% of the sampled were homozygous for one of the two alleles) in more than one location (Table S 10). For example, the G allele at locus 26155658 is fixed in samples from CR to LR; The C allele at locus 26153792 is fixed in samples from CR to OI; the G allele at locus 26154184 is fixed in samples between FL and MS.

The custom BLASTn searches matched 24 of 226 outlier loci to transcripts within the spotted seatrout liver transcriptome (mean length of transcripts = 2,597 bp, range = 215 to 10,462 bp). A separate BLASTn search of the GenBank database was conducted for the rest of the outlier loci (n = 202) and found five significant GenBank matches (Benson 2013) (Table 10). The 24 outlier loci with matches to known proteins in the liver transcriptome were chosen for further functional analyses because they were not only discovered as outliers but were also being expressed in the cells of spotted seatrout

exposed to acute temperature stress (Chapter 2). The BLASTp search for the longest translated sequences of these 24 transcripts provided 18 significant matches to known proteins (Table 9). From these 18 hits: 1) Eight transcripts (GRF3C4, FDXACB1, PRSS1, CCNJ and Unknown_1 to 4) carried a nonsynonymous mutation at the outlier locus, which resulted in amino acid substitutions, and 2) All eight changes in amino acids were found to be nonconservative replacements (changes in charge or hydrophobicity). The allele frequencies of two of the loci with nonsynonymous substitutions, PRSS1 and FDXACB1, showed strong correlations with AWT (r = -0.85 and -0.87, $p < 0.001$, respectively, Figure S 9). Four of the loci identified as having synonymous substitutions also showed a strong correlation with AWT (PLXC1: r = -0.72, p =0.001; Unknown_5: r = -0.79, $p < 0.001$; ERBB4: r = -0.74, $p < 0.001$; HP55: r = -0.74, $p < 0.001$, Figure S 9, Figure S 10).

3.5 Discussion

Spotted seatrout populations on ATL display differences in a range of life history and physiological traits, yet little is known about whether there is adaptive genetic variation underlying these differences. To fill this knowledge gap, a survey of genome-wide SNP loci was conducted to search for signatures of natural selection based on spotted seatrout sampled across a wide geographic range. Consistent with findings from previous studies, a hierarchical pattern of population structure was found for spotted seatrout (GOM vs ATL and within ATL). Differentiation-based and environmental association-based analyses jointly identified 226 outlier loci as candidates of natural selection. The mapping of these outlier loci to a high-quality liver transcriptome of

spotted seatrout confirmed that 24 resided in actively transcribed genes. Annotation of the 24 outlier loci indicated that they were enriched in biological functions such as transcriptional regulation and metabolic processes, signal transduction, and cell cycle control. In addition, 8 of the 24 outlier loci displayed nonsynonymous substitutions which all resulted in amino acids with different biochemical properties. Specifically, allelic frequencies of six genes (PRSS1, FDXACB1, PLXC1, ERBB4, HP55 and Unknown_5) showed the strongest associations with AWT, suggesting their potential roles in local adaptation of spotted seatrout.

3.5.1 Genetic Diversity

Within the spatial distribution of a species, it is generally expected that the peripheral populations will have low levels of genetic diversity compared to more central populations (Mayr 1963). Fragmented habitats and stronger selective pressure, among other factors, can generate these types of patterns of genetic diversity. In spotted seatrout, Chesapeake Bay is near the northern range limit, yet the lowest level of genetic diversity was not found at the northernmost location, CR. Instead, the effective number of alleles (Eff_num), observed heterozygosity (Ho), heterozygosity within populations (Hs) were all the lowest in GOM samples from MS. In addition, most locations did not appear to have high levels of inbreeding, except for JI (0.113) and FL (0.138). This may be attributable to the smaller neighborhood size of spotted seatrout in the Southeastern U.S., which can result in a higher probability of inbreeding: nearly 100% tagged spotted seatrout were recaptured within 13 km from the point of release in South Carolina (Davy 1994) and within 50 km in Florida (Iversen and Tabb 1962). In contrast, 25% of the

spotted seatrout tagged in Virginia and North Carolina migrated over 100 km (Ellis 2014) and this level of mixing of individuals was enough to allow genetic homogeneity north of Bogue Sound, NC in a previous study (Ellis 2019). Low sample sizes and opportunistic sampling may also be contributing factors; increased sample sizes and repeated sampling will be needed to verify whether the observation of genetic diversity is temporally stable and should be of concern to fisheries managers.

3.5.2 Genetic Population Structure

Analyses of genome-wide SNP loci revealed a similar pattern of population structuring of spotted seatrout as has been reported by previous studies. A recent genetic study of spotted seatrout using 38 microsatellites and sequences of mitochondrial DNA control region delineated three subpopulations: the first population ranged from South Padre Island, TX to Apalachicola River on the western coast of Florida; the second population ranged from Apalachicola River around the panhandle of Florida to Miami and Palm Beach; the third population ranged from Palm Beach northward along the Atlantic coastline to Morehead City, NC (Seyoum et al. 2018). In the GOM, our results agreed with the findings of Seyoum *et al*. (2018): MS is within the western Gulf population and FL is within the eastern Gulf population, and MS and FL are significantly different from each other. This result is expected given the largely non-migratory nature of spotted seatrout and the large geographic distance (ca. 850 km along the coastline) between MS and FL. Two subpopulations of spotted seatrout were resolved on ATL with a genetic break near NR, which was consistent with previous findings using microsatellites (O'Donnell et al. 2014; Ellis et al. 2019). The genetic differentiation between the locations on either side of NR was small (average pairwise $F_{ST} = 0.049$, $p <$

0.0001), relative to the level of differentiation observed between locations in the GOM (average pairwise F_{ST} = 0.143, $p < 0.0001$).

This pattern of population differentiation was also reflected in the visual representation of the two clustering analyses: on the DAPC plot, two ATL clusters (2 and 3) were separated on DF3 (variance explained = 1.8%), in contrast to the separation of GOM and ATL along DF1 (variance explained = 70.3%). Samples from GOM showed distinct ancestry compared to samples from ATL. In the southernmost locations on ATL (CFR, WB, JI, GA), however, the proportions of the northern ancestry were still substantial (~25%) which suggested asymmetric gene flow from north to south. This result was different from previous studies using microsatellite loci which found almost exclusive southern ancestries for samples collected from South Carolina, Georgia, and Florida (O'Donnell et al. 2014; Ellis et al. 2019). This discrepancy could be due to the difference in genome-coverage between the types of genetic markers used. Previous studies used relatively low numbers of microsatellite loci (n = 13, O'Donnell et al. 2013; n= 22, Ellis et al. 2019) compared to over 15,000 SNP loci in this study. This dramatic increase in genome-coverage most likely increased the accuracy of the estimation of genetic ancestry (Allendorf et al. 2010).

3.5.3 Outlier Loci

IBD is an important consideration for testing of outlier loci (Meirmans 2012), and a coastwide pattern of IBD on the U.S. East Coast in spotted seatrout has been found by O'Donnell et al. 2014 and Ellis et al. 2019. A significant IBD when all ATL locations were included was likely an artefact, given that genetic breaks can lead to spurious

patterns of IBD (Meirmans 2012). When either the northern ATL locations or southern ATL locations were tested for IBD separately, the results were no longer significant. Seasonal mixing of spotted seatrout between VA and NC corroborates a lack of IBD pattern. Thus, it was concluded that IBD has minimal impact on outlier tests for spotted seatrout along the U.S. East Coast.

Using a combination of methods, loci that are likely targets of natural selection in spotted seatrout were discovered. About a quarter of the outlier loci (25 of 226) had fixed alleles in more than one sampling location, but a BLASTn search did not result in any significant GenBank matches for these loci. Among the 226 outlier loci, 24 resided in genes that were also discovered in the transcriptome (Chapter 2). Excluding seven genes with unknown function (Unknwon_1 to 6, plus SERTM1), the remaining 17 genes could be categorized into four general functional groups based on the biological processes that they were involved in: 1) Transcriptional regulation (ZN182, Z3H7B, GTF3C4, ERBB4, TOP3A, CIPC, FDXACB1), 2) Metabolism of carbohydrates and lipids (PPCT, FAM135A, CHST7, PRSS1, BHMT, PPN), 3) Signal transduction (PLXC1, HP55), and 4) Cell cycle control (STAG2, CCNJ). These biological pathways have all been associated with stress responses in a variety of fishes (Gracey et al. 2004; Narum et al. 2010; Jeffries et al. 2016). For instance, genes associated with transcriptional regulation were among the largest groups of differentially expressed genes in response to cold stress in common carp, *Cyprinus carpio* (Gracey 2007). In longfin smelt (*Spirinchus thaleichthys*) and delta smelt (*Hypomesus transpacificus*), many differentially expressed genes in response to heat stress were involved in metabolic processes (Jeffries 2016).

Further investigation of the 24 outlier loci revealed eight with nonsynonymous substitutions (GTF3C4, FDXACB1, PRSS1, CCNJ, and Unknown_1 to 4). One of these genes, PRSS1 (trypsin), is a protease found in the digestive system of many vertebrates (Huber and Bode 1978). PRSS1 was involved in cold adaptation of Maori cod (*Paranotothenia magellanica)* (Genicot et al. 1996) and Atlantic cod (*Gadus morhua*) (Amiza and Apenten 1996). PRSS1 also showed significant differential expression in the liver of common carp after exposure to cold stress (Gracey 2007). This evidence suggests that PRSS1 has a conserved role in coping with cold stress across a wide range of fish taxa. CCNJ is a member of the cyclin protein family that controls the progression of cell cycles. In eurythermal goby fish (*Gillichthys mirabilis*), another member of the cyclin family, cyclin D2, was strongly inhibited during acute heat stress (Logan and Somero 2011). GTF3C4 and FDXACB1 have no known functions related to temperature stress responses in fishes, but both play a role in transcription regulation in humans and dogs and may have similar functions in spotted seatrout (Paule and White 2000; Li et al. 2013). The allele frequencies of both PRSS1 and FDXACB1 showed strong correlations with AWT, suggesting potential roles in thermal adaptation in spotted seatrout. Taken together, these eight genes represent good candidates to further investigate mechanisms of thermal adaptation of spotted seatrout.

The rest of the transcribed outlier loci (n = 16) had synonymous substitutions. Although synonymous substitutions do not result in changes in the amino acid during protein translation and therefore no effect on protein structure and function is expected, there is evidence that the use of synonymous codons can impact gene expression (Hershberg and Petrov 2008). Codon-usage bias refers to the findings that synonymous

codons were not used in equal frequencies (Plotkin and Kudla 2011). One possible explanation was that certain codons were favored over others during protein translation due their superior translational efficiency. Thus, one codon may provide a slight selective advantage and thereby, fine-tuning of gene expression could be achieved (Quax et al. 2015). The differential expression of the synonymous loci between VA and SC (Chapter 2) may be attributed to codon-usage bias: 21 transcripts showed differential expression in both VA and SC after cold stress (Figure S 12), and 20 transcripts showed differential expression in both VA and SC after heat stress (Figure S 13). The missing transcripts (three in cold stress and four in heat stress) were due to extremely low expression in either one of the control or treatment groups, thus the differential expression calculation was not possible.

The directions of differential expression (upregulation or downregulation) were generally consistent between VA and SC samples, but there were exceptions such as HP55, F135A, Unknown_6, BHMT, CIPC, and PLXC1 in cold stress (Figure S 12). Similarly, in heat stress, all changes in gene expression were in the same directions except for BHMT, Z3H7B, and CIPC (Figure S 13). In cold stress, Unknown_2 showed the largest differences in log2 fold change between VA and SC samples. In heat stress, ERBB4 showed the largest differences in log2 fold change between VA and SC. However, none of the outlier loci showed significant differential expression in Chapter 2 (log2 fold change $\geq$ two, and a multi-test adjusted p-value ≤ 0.05). This could have two explanations: 1) A mismatch between the genetic variation, which provides a plastic thermal response (significant differential expression) and that provides long-term adaptation to the local environment (outlier loci). 2) An artifact because DArTseq failed

to cover genomic regions that contain genes showing significant differential expression. DArTseq covers only a reduced representation of the genome, similar to other genotyping-by-sequencing methods (Lowry et al. 2017). Thus, both scenarios are plausible and future studies armed with a high-quality spotted seatrout genome assembly would differentiate between the two possibilities.

3.5.4 Outlier Loci vs. Neutral Loci

Neutral and putatively adaptive loci can show distinct patterns of population differentiation because genetic drift, natural selection, and gene flow influence them disproportionately (Matala et al. 2014; Hohenlohe et al. 2018). For example, European flounder (*Platichthys flesus*) populations showed overall low levels of genetic differentiation using largely neutral microsatellite markers (F_{ST} = 0.02), indicating high levels of gene flow among populations. A putatively adaptive gene, the heat-shock cognate 70 (Hsc70), however, shows a much higher level of differentiation (F_{ST} = 0.45) suggesting local adaptation is possible despite a high level of gene flow (Hemmer-Hansen et al. 2007). In this study, PCA of 14,962 neutral loci explained 10% of differentiation among all samples, whereas 226 outlier loci explained 24% (PC1 and PC2 combined, Figure S 14, Figure S 16). This result is comparable to a recent study in redband trout (*Oncorhynchus mykiss gairdneri*), with 13 outlier loci explaining substantially larger variation compared to 5,890 neutral loci (60.6% vs 16.8%) (Chen et al. 2018). Thus, the outlier loci represent good candidates for designing targeted SNP assay panels for high-throughput, repeatable genotyping of spotted seatrout.

Understanding whether adaptive genetic variation exists and its association with environmental variables has important applications for predicting how spotted seatrout will respond to future climate change. For example, spotted seatrout from Virginia and South Carolina displayed different levels of metabolic plasticity after being acclimated at the same temperature (Song et al. 2019). The outlier loci can be included in a generalized linear model (GAM) framework in order to predict whole-organism performance metrics such as metabolic rate. Furthermore, the recent development of mechanistic species distribution models that incorporate adaptive genetic variation is a promising step towards a more realistic projection of the biological consequences of climate change (Fitzpatrick and Keller 2015; Razgour et al. 2019). In conclusion, this study identified adaptive genetic variation in spotted seatrout populations, and it is the hope of the authors that this information can be of some use for fisheries managers to mitigate the negative impact of climate change on this species.

3.6 References

Allendorf, F. W., P. A. Hohenlohe, and G. Luikart. 2010. Genomics and the future of conservation genetics. Nature Reviews Genetics 11(10):697–709.

Altschul, S. F., W. Gish, W. Miller, E. W. Myers, and D. J. Lipman. 1990. Basic local alignment search tool. Journal of Molecular Biology 215(3):403–410.

Amiza, M. A., and R. K. O. Apenten. 1996. Urea and Heat Unfolding of Cold-Adapted Atlantic Cod (*Gadus morhua*) Trypsin and Bovine Trypsin. Journal of the Science of Food and Agriculture 70(1):1–10.

Artimo P, Jonnalagedda M, Arnold K, Baratin D, Csardi G, de Castro E, Duvaud S, Flegel V, Fortier A, Gasteiger E, Grosdidier A, Hernandez C, I. 2012. ExPASy: SIB bioinformatics resource portal. Nucleic Acids Research 40(W1):W597–W603.

Beaumont, M. A., and R. A. Nichols. 1996. Evaluating loci for use in the genetic analysis of population structure. Proc. R. Soc. Lond. B 263(1377):1619–1626.

Benjamini, Y., and Y. Hochberg. 1995. Controlling the false discovery rate: a practical and powerful approach to multiple testing. Journal of the Royal Statistical Society. Series B (Methodological) 57(1): 289-300.

Chen, Z., A. P. Farrell, A. Matala, and S. R. Narum. 2018. Mechanisms of thermal adaptation and evolutionary potential of conspecific populations to changing environments. Molecular Ecology 27(3):659–674.

Conover, D. 1998. Local adaptation in marine fishes -evidence and implications for stock enhancement. Bulletin of Marine Science 62(2):477–493.

Cooke, T. F., M.-C. Yee, M. Muzzio, A. Sockell, R. Bell, O. E. Cornejo, J. L. Kelley, G.

Bailliet, C. M. Bravi, C. D. Bustamante, and E. E. Kenny. 2016. GBStools: A Statistical Method for Estimating Allelic Dropout in Reduced Representation Sequencing Data. PLOS Genetics 12(2):e1005631.

Davy, K. B. 1994. South Carolina Marine Game Fish Tagging Program 1974-1992.

Ellis, T. A. 2014. Mortality and Movement of Spotted Seatrout at Its Northern Latitudinal Limits. North Carolina State University.

Ellis, T. A., J. A. Buckel, J. E. Hightower, and S. J. Poland. 2017. Relating cold tolerance to winterkill for spotted seatrout at its northern latitudinal limits. Journal of Experimental Marine Biology and Ecology 490:42–51.

Ellis, T. A., J. R. McDowell, and J. A. Buckel. 2019. Stock structure of spotted seatrout: assessing genetic connectivity at northern latitudinal limits. North Carolina Coastal Recreational Fishing License Fund Final Report.

Elshire, R. J., J. C. Glaubitz, Q. Sun, J. A. Poland, K. Kawamoto, E. S. Buckler, and S. E. Mitchell. 2011. A robust, simple genotyping-by-sequencing (GBS) approach for high diversity species. PLoS ONE 6(5):1–10.

Evanno, G., S. Regnaut, and J. Goudet. 2005. Detecting the number of clusters of individuals using the software STRUCTURE: A simulation study. Molecular Ecology 14(8):2611–2620.

Excoffier, L., P. E. Smouse, and J. M. Quattro. 1992. Analysis of molecular variance inferred from metric distances among DNA haplotypes: application to human mitochondrial DNA restriction data. Genetics 131(2):479–491.

Falush, D., M. Stephens, and J. K. Pritchard. 2003. Inference of population structure

using multilocus genotype data: Linked loci and correlated allele frequencies. Genetics 164(4):1567–1587.

Fitzpatrick, M. C., and S. R. Keller. 2015. Ecological genomics meets community-level modelling of biodiversity: Mapping the genomic landscape of current and future environmental adaptation. Ecology Letters 18(1):1–16.

Frichot, E., and O. François. 2015. LEA: An R package for landscape and ecological association studies. Methods in Ecology and Evolution 6(8):925–929.

Frichot, É., O. François, O. E. Gaggiotti, P. de Villemereuil, and É. Bazin. 2014. Genome scan methods against more complex models: when and how much should we trust them? Molecular Ecology 23(8):2006–2019.

Genicot, S., F. Rentier-Delrue, D. Edwards, J. VanBeeumen, and C. Gerday. 1996. Trypsin and trypsinogen from an Antarctic fish: Molecular basis of cold adaptation. Biochimica et Biophysica Acta - Protein Structure and Molecular Enzymology 1298(1):45–57.

Georges, A., B. Gruber, G. B. Pauly, D. White, M. Adams, M. J. Young, A. Kilian, X. Zhang, H. B. Shaffer, and P. J. Unmack. 2018. Genomewide SNP markers breathe new life into phylogeography and species delimitation for the problematic short-necked turtles (Chelidae: Emydura) of eastern Australia. Molecular Ecology 27(24):5195–5213.

Gosselin, T., L. M, D.-D. F, and P. Grewe. 2020. radiator: RADseq Data Exploration, Manipulation and Visualization using R. https://thierrygosselin.github.io/radiator/.

Gracey, A. Y., E. J. Fraser, W. Li, Y. Fang, R. R. Taylor, J. Rogers, A. Brass, and A. R.

Cossins. 2004. Coping with cold: An integrative, multitissue analysis of the transcriptome of a poikilothermic vertebrate. Proceedings of the National Academy of Sciences of the United States of America 101(48):16970–16975.

Grewe, P. M., P. Feutry, P. L. Hill, R. M. Gunasekera, K. M. Schaefer, D. G. Itano, D. W. Fuller, S. D. Foster, and C. R. Davies. 2015. Evidence of discrete yellowfin tuna (*Thunnus albacares*) populations demands rethink of management for this globally important resource. Scientific Reports 5(1):16916.

Gruber, B., P. J. Unmack, O. F. Berry, and A. Georges. 2018. dartr: An R package to facilitate analysis of SNP data generated from reduced representation genome sequencing. Molecular Ecology Resources 18(3):691–699.

Hemmer-Hansen, J., E. E. Nielsen, J. Frydenberg, and V. Loeschcke. 2007. Adaptive divergence in a high gene flow environment: Hsc70 variation in the European flounder (*Platichthys flesus* L.). Heredity 99(6):592–600.

Hemmer-Hansen, J., N. O. Therkildsen, and J. M. Pujolar. 2014. Population genomics of marine fishes: next-generation prospects and challenges. The Biological Bulletin 227(2):117–132.

Hershberg, R., and D. A. Petrov. 2008. Selection on Codon Bias. Annual Review of Genetics 42(1):287–299.

Hohenlohe, P. A., B. K. Hand, K. R. Andrews, and G. Luikart. 2018. Population Genomics Provides Key Insights in Ecology and Evolution. Pages 483–510 Population Genomics: Concepts, Approaches and Applications. Springer Switzerland.

Holderegger, R., U. Kamm, and F. Gugerli. 2006. Adaptive vs. neutral genetic diversity: Implications for landscape genetics. Landscape Ecology 21(6):797–807.

Iversen, E., and D. C. Tabb. 1962. Subpopulations based on growth and tagging studies of spotted seatrout, *Cynoscion nebulosus*, in Florida. Copeia 3:544–548.

Janes, J. K., J. M. Miller, J. R. Dupuis, R. M. Malenfant, J. C. Gorrell, C. I. Cullingham, and R. L. Andrew. 2017. The K = 2 conundrum. Molecular Ecology 26(14):3594–3602.

Jeffries, K. M., R. E. Connon, B. E. Davis, L. M. Komoroske, M. T. Britton, T. Sommer, A. E. Todgham, and N. A. Fangue. 2016. Effects of high temperatures on threatened estuarine fishes during periods of extreme drought. The Journal of Experimental Biology 219(11):1705–1716.

Jensen, L. F., M. M. Hansen, C. Pertoldi, G. Holdensgaard, K.-L. D. Mensberg, and V. Loeschcke. 2008. Local adaptation in brown trout early life-history traits: implications for climate change adaptability. Proceedings of the Royal Society B: Biological Sciences 275(1653):2859–2868.

Jombart, T., and I. Ahmed. 2011. adegenet 1.3-1: new tools for the analysis of genome-wide SNP data. Bioinformatics 27(21):3070–3071. R Foundation for Statistical Computing, Vienna, Austria.

Jombart, T., S. Devillard, and F. Balloux. 2010. Discriminant analysis of principal components: a new method for the analysis of genetically structured populations. BMC Genetics 11(1):94.

Kilian, A., P. Wenzl, E. Huttner, J. Carling, L. Xia, H. Blois, V. Caig, K. Heller-

Uszynska, D. Jaccoud, C. Hopper, M. Aschenbrenner-Kilian, M. Evers, K. Peng, C. Cayla, P. Hok, and G. Uszynski. 2012. Diversity arrays technology: A generic genome profiling technology on open platforms. Methods in Molecular Biology 888:67–89.

Lee, C., A. Abdool, and C.-H. Huang. 2009. PCA-based population structure inference with generic clustering algorithms. BMC bioinformatics 10 Suppl 1:S73.

Lewontin, R. C., and J. Krakauer. 1973. Distribution of gene frequency as a test of the theory of the selective neutrality of polymorphisms. Genetics 74(1):175–95.

Li, Y., B. M. vonHoldt, A. Reynolds, A. R. Boyko, R. K. Wayne, D.-D. Wu, and Y.-P. Zhang. 2013. Artificial Selection on Brain-Expressed Genes during the Domestication of Dog. Molecular Biology and Evolution 30(8):1867–1876.

Logan, C. A., and G. N. Somero. 2011. Effects of thermal acclimation on transcriptional responses to acute heat stress in the eurythermal fish *Gillichthys mirabilis* (Cooper). AJP: Regulatory, Integrative and Comparative Physiology 300(6):R1373–R1383.

Lowry, D. B., S. Hoban, J. L. Kelley, K. E. Lotterhos, L. K. Reed, M. F. Antolin, and A. Storfer. 2017. Breaking RAD: an evaluation of the utility of restriction site-associated DNA sequencing for genome scans of adaptation. Molecular Ecology Resources 17(2):142–152.

Luu, K., E. Bazin, and M. G. B. Blum. 2017. pcadapt: an R package to perform genome scans for selection based on principal component analysis. Molecular Ecology Resources 17(1):67–77.

Mantel, N. 1967. The Detection of Disease Clustering and a Generalized Regression

Approach. Cancer Research 27(2):209–220.

Matala, A. P., M. W. Ackerman, M. R. Campbell, and S. R. Narum. 2014. Relative contributions of neutral and non-neutral genetic differentiation to inform conservation of steelhead trout across highly variable landscapes. Evolutionary Applications 7(6):682–701.

Mayr, E. 1963. Animal species and evolution. Harvard University Press.

Meirmans, P. G. 2012. The trouble with isolation by distance. Molecular Ecology 21(12):2839–2846.

Meirmans, P. G., and P. H. Van Tiendren. 2004. genotype and genodive: two programs for the analysis of genetic diversity of asexual organisms. Molecular Ecology Notes 4(4):792–794.

Narum, S. R., N. R. Campbell, C. C. Kozfkay, and K. A. Meyer. 2010. Adaptation of redband trout in desert and montane environments. Molecular Ecology 19(21):4622–4637.

NCDMF. 2014. Stock Assessment of Spotted Seatrout , *Cynoscion nebulosus* , in Virginia and North Carolina Waters.

O'Donnell, T. P., M. R. Denson, and T. L. Darden. 2014. Genetic population structure of spotted seatrout *Cynoscion nebulosus* along the south-eastern U.S.A. Journal of Fish Biology 85(2):374–393.

O'Leary, S. J., J. B. Puritz, S. C. Willis, C. M. Hollenbeck, and D. S. Portnoy. 2018. These aren't the loci you'e looking for: Principles of effective SNP filtering for molecular ecologists. Molecular Ecology 27(16):3193–3206.

Paule, M. R., and R. J. White. 2000. Transcription by RNA polymerases I and III. Nucleic Acids Research 28(6):1283–1298.

Pembleton, L. W., N. O. I. Cogan, and J. W. Forster. 2013. StAMPP: an R package for calculation of genetic differentiation and structure of mixed-ploidy level populations. Molecular Ecology Resources 13(5):946–952.

Peterson, B. K., J. N. Weber, E. H. Kay, H. S. Fisher, and H. E. Hoekstra. 2012. Double digest RADseq: An inexpensive method for de novo SNP discovery and genotyping in model and non-model species. PLoS ONE 7(5).

Plotkin, J. B., and G. Kudla. 2011. Synonymous but not the same: The causes and consequences of codon bias. Nature Reviews Genetics 12(1):32–42.

Pritchard, J. K., M. Stephens, and P. Donnelly. 2000. Inference of population structure using multilocus genotype data. Genetics 155(2):945–959.

Quax, T. E. F., N. J. Claassens, D. Söll, and J. van der Oost. 2015. Codon Bias as a Means to Fine-Tune Gene Expression. Molecular Cell 59(2):149–161.

Razgour, O., B. Forester, J. B. Taggart, M. Bekaert, J. Juste, C. Ibáñez, S. J. Puechmaille, R. Novella-Fernandez, A. Alberdi, and S. Manel. 2019. Considering adaptive genetic variation in climate change vulnerability assessment reduces species range loss projections. Proceedings of the National Academy of Sciences 116(21):10418–10423.

Rellstab, C., F. Gugerli, A. J. Eckert, A. M. Hancock, and R. Holderegger. 2015. A practical guide to environmental association analysis in landscape genomics. Molecular Ecology 24(17):4348–4370.

Savolainen, O., M. Lascoux, and J. Merilä. 2013. Ecological genomics of local adaptation. Nature Reviews Genetics 14(11):807–820.

Seifu Seyoum, Richard S McBride, Michael D Tringali, Vicki L Villanova, Cecilia Puchutulegui, Samantha Gray, and Nathan Van Bibber. (n.d.). Genetic population structure of the spotted seatrout (*Cynoscion nebulosus*): simultaneous examination of the mtDNA control region and microsatellite marker results. Bulletin of marine science. 94(1):47–71.

Seyoum, S., R. S. McBride, M. D. Tringali, V. L. Villanova, C. Puchutulegui, S. Gray, and N. Van Bibber. 2018. Genetic population structure of the spotted seatrout (*Cynoscion nebulosus*): simultaneous examination of the mtDNA control region and microsatellite marker results. Bulletin of Marine Science 94(1):47–71.

Shams, F., F. Dyer, R. Thompson, R. P. Duncan, J. D. Thiem, A. Kilian, and T. Ezaz. 2019. Application of DArT seq derived SNP tags for comparative genome analysis in fishes; An alternative pipeline using sequence data from a non-traditional model species, *Macquaria ambigua*. PLoS ONE 14(12):1–13.

Song, J., R. Brill, and J. Mcdowell. 2019. Plasticity in Standard and Maximum Aerobic Metabolic Rates in Two Populations of an Estuarine Dependent Teleost , Spotted Seatrout (*Cynoscion nebulosus*):1–19.

Storfer, A., A. Patton, and A. K. Fraik. 2018. Navigating the interface between landscape genetics and landscape genomics. Frontiers in Genetics 9(MAR).

Waples, R. S., and O. Gaggiotti. 2006. What is a population? An empirical evaluation of some genetic methods for identifying the number of gene pools and their degree of

connectivity. Molecular Ecology 15(6):1419–1439.

Weir, B. S., and C. C. Cockerham. 1984. Estimating F-Statistics for the Analysis of Population Structure. Evolution 38(6):1358–1370.

Zhang, Z., S. Schwartz, L. Wagner, and W. Miller. 2000. A greedy algorithm for aligning DNA sequences. Journal of Computational Biology: A Journal of Computational Molecular Cell Biology 7(1–2):203–214.

3.7 Tables

Table 5. Sampling locations (n = 17) and summary statistics for each sampling location: Number of alleles (Num), effective number of alleles (Eff_num), observed heterozygosity (Ho), heterozygosity within populations (Hs), inbreeding coefficient (Gis) (Nei, 1987).

Abbreviation	Location	n	Num	Eff_num	Ho	Hs	Gis
CR	Corrotoman River, VA	35	1.772	1.276	0.161	0.174	0.076
WR	Ware River, VA	9	1.541	1.259	0.153	0.169	0.096
YR	York River, VA	14	1.59	1.262	0.152	0.167	0.094
ER	Elizabeth River, VA	10	1.557	1.263	0.153	0.171	0.102
LR	Lynnhaven River, VA	7	1.503	1.258	0.154	0.17	0.098
RI	Rudee Inlet, VA	16	1.638	1.267	0.153	0.171	0.101
OI	Oregon Inlet, NC	8	1.529	1.26	0.156	0.171	0.088
PS	Pamlico Sound, NC	12	1.598	1.267	0.157	0.172	0.085
SR	South River, NC	8	1.559	1.271	0.174	0.178	0.022
BS	Bogue Sound, NC	20	1.737	1.281	0.167	0.18	0.072
NR	New River, NC	29	1.753	1.279	0.158	0.177	0.107
CFR	Cape Fear River, NC	16	1.669	1.275	0.162	0.177	0.084
WB	Winyah Bay, SC	10	1.592	1.27	0.172	0.175	0.019
JI	James Island, SC	11	1.58	1.267	0.154	0.173	0.113
GA	Wassaw Sound, GA	10	1.595	1.269	0.166	0.175	0.051
FL	Florida	31	1.822	1.268	0.151	0.175	0.138
MS	Mississippi	31	1.781	1.254	0.15	0.166	0.095
Total		277					

Table 6. Number of SNP loci retained after each filtering step.

Filter	Retained loci
Loci received from DArT Pty. Ltd.	59,904
Average reproducibility < 90%	59,884
Monomorphic	59,884
Missing ≥ 10% genotypes by locus	39,896
More than one SNP per locus (secondary SNPs)	29,457
Missing ≥ 10% genotypes by individual sample	29,452
Minor allele frequency < 0.01	17,506
Read depth >5 and <100	15,187
Hardy-Weinberg Equilibrium	
P < 0.05 in one thirds of all locations (n = 6)	15,187
Outlier identification	
Putatively neutral	14,961
Putatively under selection	226

Table 7. Pairwise genetic distance (F_{ST}) (Weir & Cockerham, 1984) among all 17 sampling locations (below diagonal) and p-values associated with the pairwise genetic distance (above diagonal). Italicized numbers indicate statistical significance ($p < 0.05$). Corrotoman River (CR), Ware River (WR), York River (YR), Elizabeth River (ER), Lynnhaven River (LR), Rudee Inlet (RI), Oregon Inlet (OI), Pamlico Sound (PS), South River (SR), Bogue Sound (BS), New River (NR), Cape Fear River (CFR), Winyah Bay (WB), James Island (JI), Wassaw Sound (GA), Florida (FL), and Mississippi (MS).

	CR	WR	YR	ER	LR	RI	OI	PS	SR	BS	NR	CFR	WB	JI	GA	FL	MS
CR		<0.001	0.105	0.022	0.897	<0.001	0.306	0.45	<0.001	<0.001	<0.001	<0.001	<0.001	<0.001	<0.001	<0.001	<0.001
WR	*0.003*		0.006	0.151	0.031	<0.001	<0.001	0.101	<0.001	<0.001	<0.001	<0.001	<0.001	<0.001	<0.001	<0.001	<0.001
YR	0.001	*0.002*		0.135	0.829	<0.001	0.425	0.168	<0.001	<0.001	<0.001	<0.001	<0.001	<0.001	<0.001	<0.001	<0.001
ER	*0.001*	0.001	0.001		0.669	0.005	0.156	0.214	<0.001	0.001	<0.001	<0.001	<0.001	<0.001	<0.001	<0.001	<0.001
LR	0.001	*0.002*	0.001	0.000		0.192	0.86	0.897	0.137	0.004	<0.001	<0.001	<0.001	<0.001	<0.001	<0.001	<0.001
RI	*0.002*	*0.003*	*0.002*	0.002	0.001		0.001	<0.001	<0.001	<0.001	<0.001	<0.001	<0.001	<0.001	<0.001	<0.001	<0.001
OI	0.000	*0.004*	0.000	*0.001*	*0.001*	0.003		0.527	0.001	0.02	<0.001	<0.001	<0.001	<0.001	<0.001	<0.001	<0.001
PS	0.000	0.001	0.001	0.001	0.001	0.002	0.000		0.035	<0.001	<0.001	<0.001	<0.001	<0.001	<0.001	<0.001	<0.001
SR	*0.003*	*0.005*	*0.004*	0.006	0.001	*0.004*	*0.003*	*0.002*		0.006	<0.001	<0.001	<0.001	<0.001	<0.001	<0.001	<0.001
BS	*0.003*	*0.005*	*0.004*	*0.002*	*0.002*	0.005	0.002	*0.002*	*0.002*		<0.001	<0.001	<0.001	<0.001	<0.001	<0.001	<0.001
NR	*0.011*	*0.014*	*0.011*	*0.011*	*0.007*	0.013	0.009	*0.008*	*0.005*	*0.003*		<0.001	<0.001	<0.001	<0.001	<0.001	<0.001
CFR	*0.041*	*0.044*	*0.042*	*0.041*	*0.038*	*0.042*	*0.040*	*0.036*	*0.029*	*0.023*	*0.011*		<0.001	<0.001	<0.001	<0.001	<0.001
WB	*0.059*	*0.064*	*0.061*	*0.061*	*0.060*	*0.061*	*0.059*	*0.052*	*0.047*	*0.037*	*0.021*	*0.005*		<0.001	<0.001	<0.001	<0.001
JI	*0.049*	*0.051*	*0.051*	*0.048*	*0.048*	*0.050*	*0.048*	*0.044*	*0.035*	*0.031*	*0.019*	*0.009*	*0.012*		<0.001	<0.001	<0.001
GA	*0.060*	*0.065*	*0.063*	*0.062*	*0.060*	*0.062*	*0.059*	*0.054*	*0.047*	*0.039*	*0.023*	*0.005*	*0.004*	*0.012*		<0.001	<0.001
FL	*0.154*	*0.156*	*0.155*	*0.155*	*0.152*	*0.155*	*0.152*	*0.151*	*0.142*	*0.14*	*0.133*	*0.128*	*0.131*	*0.133*	*0.128*		<0.001
MS	*0.152*	*0.158*	*0.155*	*0.156*	*0.152*	*0.153*	*0.155*	*0.151*	*0.143*	*0.138*	*0.126*	*0.12*	*0.125*	*0.126*	*0.123*	*0.108*	

Table 8. Summary statistics from Analysis of Molecular Variance (AMOVA), with four different grouping scenarios (no cluster; two clusters; three cluster; four clusters) informed by STRUCTURE analysis. ATL = U.S. East Coast, GOM = Gulf of Mexico, FL = Florida, MS = Mississippi, CR = Corrotoman River, BS = Bogue Sound, CFR = Cape Fear River, WB = Winyah Bay.

Groups	Source of variation	Nested in	%var	F-stat	F-value	p-value
None	Within Individual	--	0.825	F_{IT}	0.175	--
	Among Individual	Population	0.098	F_{IS}	0.106	0.001
	Among Population	--	0.077	F_{ST}	0.077	0.001
ATL, GOM	Within Individual	--	0.769	F_{IT}	0.231	--
	Among Individual	Population	0.091	F_{IS}	0.106	0.001
	Among Population	Groups	0.032	F_{SC}	0.035	0.001
	Among Groups	--	0.108	F_{CT}	0.108	0.001
ATL, FL, MS	Within Individual	--	0.783	F_{IT}	0.217	--
	Among Individual	Population	0.077	F_{IS}	0.089	0.001
	Among Population	Groups	0.017	F_{SC}	0.019	0.001
	Among Groups	--	0.123	F_{CT}	0.123	0.001
CR-BS, CFR-WB, FL, MS	Within Individual	--	0.812	F_{IT}	0.188	--
	Among Individual	Population	0.078	F_{IS}	0.087	0.001
	Among Population	Groups	0.003	F_{SC}	0.003	0.001
	Among Groups	--	0.108	F_{CT}	0.108	0.001

Table 9. Summary of a subset of outlier loci (n = 24) with matching transcripts in the spotted seatrout liver transcriptome.

	Dartseq Locus Name	RNA-Seq Transcript Name	Substitution (Y= Synonymous)	Change in Amino Acid Properties	Gene	Gene Product Name	Uniprot Biological Processes
1	26147674-11-G/T	SOAP_k35_C550755	N(Alanine -> Serine)	non-polar -> polar	GTF3C4	General transcription factor 3C polypeptide 4	Transcription
2	26154314-11-C/T	TransAb_k35_R132148	N(Arginine -> Cysteine)	positive charge -> non-polar	FDXACB1	Ferredoxin-fold anticodon binding domain containing 1	rRNA base methylation
3	26155422-29-G/A	TRINITY_DN32064_c3_g1_i2	N(Aspartic acid-> Asparagine)	negative charge -> polar	PRSS1	Trypsin	Digestion, proteolysis
4	26147731-26-A/G	TRINITY_DN23422_c0_g1_i2	N(Glycine -> Serine)	non-polar -> polar	CCNJ	Cyclin-J	Mitotic cell cycle phase transition, regulation of cyclin-dependent protein serine/threonine kinase activity
5	26160889-44-A/T	Velvet_k55_Locus_44852_Transcript_22_Confidence_0.667_Length_584	N(Isoleucine -> Asparagine)	non-polar -> polar	Unknown_1		
6	26157694-	SOAP_k45_scaffold2537	N(Lysine ->	positive	Unknow		

	56-G/T		Asparagine)	charge -> polar	n_2		
7	26153166-10-C/T	SOAP_k55_scaffold27393	N(Tyrosine -> Cysteine)	polar -> non-polar	Unknown_3		
8	26146437-30-G/A	TRINITY_DN24384_c0_g2_i1	N(Glycine -> Glutamic acid)	non-polar -> negative charge	Unknown_4		
9	100020377-63-G/T	Velvet_k35_Locus_14851_Transcript_11_Confidence_1.000_Length_1492	Y	N/A	BHMT	Betaine--homocysteine S-methyltransferase 1	Amino acids metabolism
10	100074958-10-C/T	TRINITY_DN28123_c7_g1_i3	Y	N/A	ZN182	Zinc finger protein 182	Transcription regulation
11	26146515-30-T/G	TransAb_k35_S86005	Y	N/A	SERTM1	Serine rich and transmembrane domain containing protein 1	N/A
12	26146747-7-C/T	Velvet_k55_Locus_8750_Transcript_17_Confidence_0.600_Length_7492	Y	N/A	PLXC1	Plexin C1	Cell adhesion, regulation of axongenesis
13	26147170-7-T/C	SOAP_k35_C528161	Y	N/A	Unknown_5		
14	26149882-19-C/T	TRINITY_DN27532_c3_g1_i11	Y	N/A	FAM135A	Protein FAM135A	Lipid metabolism

15	26152460-8-C/A	Velvet_k35_Locus_37784_Transcript_24_Confidence_0.143_Length_1733	Y	N/A	CHST7	Carbohydrate sulfotransferase 7	Carbohydrate metabolism
16	26153232-56-A/C	Velvet_k35_Locus_6487_Transcript_23_Confidence_0.714_Length_2389	Y	N/A	Z3H7B	Zinc finger CCCH domain-containing protein 7B	Host-virus interaction, post-transcriptional regulation of gene expression
17	26154516-53-A/G	TRINITY_DN33331_c0_g1_i1	Y	N/A	PPN	Papilin	Extracellular matrix organization, multicellular organism development
18	26154796-57-C/A	TRINITY_DN29888_c2_g3_i3	Y	N/A	ERBB4	Receptor tyrosine-protein kinase	Transcription regulation, central nervous system morphogenesis
19	26156106-24-G/C	SOAP_k35_scaffold180	Y	N/A	STAG2	Cohesin subunit SA-2	Cell cycle, cell division
20	26156658-57-C/T	SOAP_k35_C488787	Y	N/A	PPCT	Phosphatidylcholine transfer protein	Lipid transport
21	26157558-30-C/T	TRINITY_DN31664_c2_g2_i4	Y	N/A	TOP3A	Topoisomerase 3-alpha	Chromosome separation,

							DNA replication
22	26158335-37-A/G	Velvet_k45_Locus_14520_Transcript_22_Confidence_0.667_Length_3009	Y	N/A	CIPC	CLOCK-interacting pacemaker	Biological rhythms, transcription regulation
23	26158827-54-G/A	TRINITY_DN30515_c0_g3_i3	Y	N/A	Unknown_6		
24	26160230-27-A/G	TransAb_k35_TransAb_k35_R31972	Y	N/A	HP55	Hibernation-specific plasma protein	Hibernation

Table 10. A subset of the outlier loci (n = 5) with significant matches in GenBank but without a matching transcript in the spotted seatrout liver transcriptome.

	Locus name	Synonymous Substitution?	Gene name	Gene product name	Uniprot biological processes
1	26153444-32-G/A	No continuous amino acid product	GPR132	G-protein coupled receptor 132	Mitotic cell cycle control, stress response
2	26160511-32-C/T	No continuous amino acid product	LOC106527740	Trace amine-associated receptor 13c-like	G protein-coupled receptor activity
3	26157246-12-A/G	Outside open reading frame	PCLO	Piccolo presynaptic cytomatrix protein a	cAMP-mediated signaling, presynapse to nucleus signaling pathway
4	26157480-51-G/A	No continuous amino acid product	RGS17	Regulator of G protein signaling 17	G protein-coupled receptor signaling pathway, negative regulation of signal transduction
5	26157740-30-T/A	N(Arginine->Tryptophan)	JCAD	Junctional cadherin 5 associated	Cell adhesion

Table S 7. Details on the spotted seatrout samples used in this study and well positions on DArTseq plates.

Plate ID	Well	Sample ID	Box (sample #)	Sample Location	Date of capture	TL length (mm)
1	A1	1_1	544_1	Corrotoman, VA	11/1/2016	.
1	B1	1_2	544_2	Corrotoman, VA	11/1/2016	.
1	C1	1_3	544_3	Corrotoman, VA	11/1/2016	.
1	D1	1_4	544_5	Corrotoman, VA	11/1/2016	.
1	E1	1_5	544_6	Corrotoman, VA	11/1/2016	.
1	F1	1_6	544_7	Corrotoman, VA	11/1/2016	.
1	G1	1_7	544_8	Corrotoman, VA	11/1/2016	.
1	H1	1_8	544_9	Corrotoman, VA	11/1/2016	.
1	A2	1_9	544_10	Corrotoman, VA	11/1/2016	.
1	B2	1_10	544_11	Corrotoman, VA	11/1/2016	.
1	C2	1_11	544_12	Corrotoman, VA	11/1/2016	.
1	D2	1_12	527_2	Corrotoman, VA	9/28/2016	>305
1	E2	1_13	527_3	Corrotoman, VA	10/1/2016	>305
1	F2	1_14	527_4	Corrotoman, VA	10/31/2015	>305
1	G2	1_15	527_5	Corrotoman, VA	9/25/2016	<305
1	H2	1_16	527_6	Corrotoman, VA	9/25/2016	<305
1	A3	1_17	527_7	Corrotoman, VA	9/25/2016	<305
1	B3	1_18	527_9	Corrotoman, VA	9/28/2016	<305
1	C3	1_19	527_10	Corrotoman, VA	9/28/2016	<305
1	D3	1_20	527_11	Corrotoman, VA	9/28/2016	<305
1	E3	1_21	542_31	Corrotoman, VA	10/7/2016	.
1	F3	1_22	542_32	Corrotoman, VA	10/7/2016	.
1	G3	1_23	542_33	Corrotoman, VA	10/5/2016	.
1	H3	1_24	542_34	Corrotoman, VA	10/5/2016	.
1	A4	1_25	542_35	Corrotoman, VA	10/7/2016	.
1	B4	1_26	542_36	Corrotoman, VA	10/5/2016	.

1	C4	1_27	542_37	Corrotoman, VA	10/5/2016	.
1	D4	1_28	542_38	Corrotoman, VA	10/7/2016	.
1	E4	1_29	542_40	Corrotoman, VA	10/18/2016	.
1	F4	1_30	542_41	Corrotoman, VA	10/18/2016	.
1	G4	1_31	542_42	Corrotoman, VA	10/13/2016	.
1	H4	1_32	542_43	Corrotoman, VA	10/18/2016	.
1	A5	1_33	542_44	Corrotoman, VA	10/25/2016	.
1	B5	1_34	542_45	Corrotoman, VA	10/18/2016	.
1	C5	1_35	542_46	Corrotoman, VA	10/18/2016	.
1	D5	1_36	451_26	Ware River, VA	8/15/2015	.
1	E5	1_37	451_27	Ware River, VA	8/15/2015	.
1	F5	1_38	451_28	Ware River, VA	8/15/2015	.
1	G5	1_39	451_29	Ware River, VA	8/15/2015	.
1	H5	1_40	451_30	Ware River, VA	8/15/2015	.
1	A6	1_41	451_31	Ware River, VA	8/15/2015	.
1	B6	1_42	451_33	Ware River, VA	8/15/2015	.
1	C6	1_43	451_34	Ware River, VA	8/15/2015	.
1	D6	1_44	451_35	Ware River, VA	8/15/2015	.
1	E6	1_45	488_1	York River, VA	10/15/2015	.
1	F6	1_46	488_2	York River, VA	10/15/2015	.
1	G6	1_47	488_3	York River, VA	10/15/2015	.
1	H6	1_48	488_4	York River, VA	10/15/2015	.
1	A7	1_49	488_5	York River, VA	10/15/2015	.
1	B7	1_50	488_6	York River, VA	10/15/2015	.
1	C7	1_51	488_7	York River, VA	10/15/2015	.
1	D7	1_52	488_8	York River, VA	10/15/2015	.
1	E7	1_53	488_9	York River, VA	10/15/2015	.
1	F7	1_54	488_10	York River, VA	10/15/2015	.
1	G7	1_55	488_11	York River, VA	10/15/2015	.

1	H7	1_56	488_12	York River, VA	10/15/2015	.
1	A8	1_57	488_13	York River, VA	10/15/2015	.
1	B8	1_58	488_14	York River, VA	10/15/2015	.
1	C8	1_59	481_1	Elizabeth River, VA	10/15/2015	.
1	D8	1_60	481_2	Elizabeth River, VA	10/15/2015	.
1	E8	1_61	481_3	Elizabeth River, VA	10/15/2015	.
1	F8	1_62	481_4	Elizabeth River, VA	10/15/2015	.
1	G8	1_63	481_5	Elizabeth River, VA	10/15/2015	.
1	H8	1_64	481_6	Elizabeth River, VA	10/15/2015	.
1	A9	1_65	481_7	Elizabeth River, VA	10/15/2015	.
1	B9	1_66	481_8	Elizabeth River, VA	10/15/2015	.
1	C9	1_67	481_9	Elizabeth River, VA	10/15/2015	.
1	D9	1_68	481_10	Elizabeth River, VA	10/15/2015	.
1	E9	1_69	471_1	Lynnhaven River, VA	10/15/2015	.
1	F9	1_70	471_26	Lynnhaven River, VA	10/15/2015	.
1	G9	1_71	471_27	Lynnhaven River, VA	10/15/2015	.
1	H9	1_72	471_45	Lynnhaven River, VA	10/15/2015	.
1	A10	1_73	471_46	Lynnhaven River, VA	10/15/2015	.
1	B10	1_74	471_48	Lynnhaven River, VA	10/15/2015	.
1	C10	1_75	471_49	Lynnhaven River, VA	10/15/2015	.
1	D10	1_76	516_50	Rudee Inlet, VA	04 & 08/2016	.
1	E10	1_77*	516_2	Rudee Inlet, VA	04 & 08/2016	.
1	F10	1_78*	471_26	Lynnhaven River, VA	10/15/2015	.
1	G10	1_79	516_6	Rudee Inlet, VA	04 & 08/2016	.
1	H10	1_80	516_6	Rudee Inlet, VA	04 & 08/2016	.
1	A11	1_81	516_8	Rudee Inlet, VA	04 & 08/2016	.
1	B11	1_82	516_9	Rudee Inlet, VA	04 & 08/2016	.
1	C11	1_83	516_10	Rudee Inlet, VA	04 & 08/2016	.
1	D11	1_84	516_11	Rudee Inlet, VA	04 & 08/2016	.

1	E11	1_85	516_12	Rudee Inlet, VA	04 & 08/2016	.
1	F11	1_86	516_15	Rudee Inlet, VA	04 & 08/2016	.
1	G11	1_87	516_16	Rudee Inlet, VA	04 & 08/2016	.
1	H11	1_88	516_20	Rudee Inlet, VA	04 & 08/2016	.
1	A12	1_89	516_21	Rudee Inlet, VA	04 & 08/2016	.
1	B12	1_90	516_22	Rudee Inlet, VA	04 & 08/2016	.
1	C12	1_91	516_23	Rudee Inlet, VA	04 & 08/2016	.
1	D12	1_92	516_24	Rudee Inlet, VA	04 & 08/2016	.
1	E12	1_93	516_25	Rudee Inlet, VA	04 & 08/2016	.
1	F12	1_94	506_1454	Oregon Inlet, NC	6/15/2016	362
2	A1	2_1	506_1457	Oregon Inlet, NC	6/15/2016	305
2	B1	2_2	506_1458	Oregon Inlet, NC	6/15/2016	343
2	C1	2_3	506_1459	Oregon Inlet, NC	6/15/2016	330
2	D1	2_4	506_1462	Oregon Inlet, NC	6/15/2016	330
2	E1	2_5	506_1463	Oregon Inlet, NC	6/15/2016	305
2	F1	2_6	506_1465	Oregon Inlet, NC	7/15/2016	356
2	G1	2_7	506_1466	Oregon Inlet, NC	7/15/2016	432
2	H1	2_8	492_1329	Pamlico Sound, NC	6/2/2015	504
2	A2	2_9	492_1331	Pamlico Sound, NC	7/7/2015	396
2	B2	2_10	492_1332	Pamlico Sound, NC	7/23/2015	432
2	C2	2_11	492_1333	Pamlico Sound, NC	8/5/2015	427
2	D2	2_12	492_1334	Pamlico Sound, NC	8/5/2015	460
2	E2	2_13	492_1338	Pamlico Sound, NC	8/13/2015	486
2	F2	2_14	492_1339	Pamlico Sound, NC	8/24/2015	422
2	G2	2_15	492_1341	Pamlico Sound, NC	8/24/2015	463
2	H2	2_16	492_1343	Pamlico Sound, NC	8/24/2015	430
2	A3	2_17	492_1344	Pamlico Sound, NC	8/24/2015	420
2	B3	2_18	492_1345	Pamlico Sound, NC	8/24/2015	425
2	C3	2_19	492_1355	Pamlico Sound, NC	8/27/2015	450

2	D3	2_20	421_277	South River, NC	8/14/2014	420
2	E3	2_21	421_278	South River, NC	8/14/2014	402
2	F3	2_22	421_285	South River, NC	8/25/2014	410
2	G3	2_23	421_286	South River, NC	8/25/2014	421
2	H3	2_24	421_292	South River, NC	8/25/2014	464
2	A4	2_25	421_294	South River, NC	8/25/2014	433
2	B4	2_26	421_295	South River, NC	8/25/2014	410
2	C4	2_27	421_297	South River, NC	8/25/2014	437
2	D4	2_28	421_243	Bogue Sound, NC	8/14/2014	394
2	E4	2_29	421_245	Bogue Sound, NC	8/14/2014	581
2	F4	2_30	421_246	Bogue Sound, NC	8/14/2014	413
2	G4	2_31	421_247	Bogue Sound, NC	8/14/2014	404
2	H4	2_32	421_248	Bogue Sound, NC	8/14/2014	422
2	A5	2_33	421_249	Bogue Sound, NC	8/14/2014	434
2	B5	2_34	421_250	Bogue Sound, NC	8/14/2014	374
2	C5	2_35	421_251	Bogue Sound, NC	8/14/2014	385
2	D5	2_36	421_252	Bogue Sound, NC	8/14/2014	406
2	E5	2_37	421_253	Bogue Sound, NC	8/14/2014	527
2	F5	2_38	421_254	Bogue Sound, NC	8/14/2014	396
2	G5	2_39	421_256	Bogue Sound, NC	8/14/2014	456
2	H5	2_40	421_257	Bogue Sound, NC	8/14/2014	393
2	A6	2_41	421_259	Bogue Sound, NC	8/14/2014	416
2	B6	2_42	421_260	Bogue Sound, NC	8/14/2014	411
2	C6	2_43	421_262	Bogue Sound, NC	8/14/2014	369
2	D6	2_44	421_263	Bogue Sound, NC	8/14/2014	411
2	E6	2_45	421_264	Bogue Sound, NC	8/14/2014	373
2	F6	2_46	421_265	Bogue Sound, NC	8/14/2014	425
2	G6	2_47	421_266	Bogue Sound, NC	8/14/2014	398
2	H6	2_48	506_1547	New River, NC	8/8/2016	610

2	A7	2_49	506_1549	New River, NC	8/13/2016	432
2	B7	2_50	506_1550	New River, NC	8/13/2016	406
2	C7	2_51	506_1552	New River, NC	8/13/2016	432
2	D7	2_52	506_1553	New River, NC	8/13/2016	457
2	E7	2_53	506_1554	New River, NC	8/13/2016	406
2	F7	2_54	506_1555	New River, NC	8/13/2016	406
2	G7	2_55	506_1556	New River, NC	8/13/2016	432
2	H7	2_56	506_1557	New River, NC	8/13/2016	457
2	A8	2_57	506_1559	New River, NC	9/9/2016	362
2	B8	2_58	506_1407	Cape Fear River, NC	4/23/2016	394
2	C8	2_59	506_1408	Cape Fear River, NC	4/23/2016	394
2	D8	2_60	506_1409	Cape Fear River, NC	4/23/2016	406
2	E8	2_61	506_1410	Cape Fear River, NC	4/23/2016	387
2	F8	2_62	506_1411	Cape Fear River, NC	5/16/2016	432
2	G8	2_63	506_1412	Cape Fear River, NC	5/16/2016	387
2	H8	2_64	506_1413	Cape Fear River, NC	5/16/2016	362
2	A9	2_65	506_1414	Cape Fear River, NC	5/27/2016	432
2	B9	2_66	506_1415	Cape Fear River, NC	6/10/2016	533
2	C9	2_67	506_1416	Cape Fear River, NC	6/10/2016	495
2	D9	2_68	506_1419	Cape Fear River, NC	6/13/2016	362
2	E9	2_69	506_1420	Cape Fear River, NC	6/13/2016	362
2	F9	2_70	506_1421	Cape Fear River, NC	6/13/2016	356
2	G9	2_71	506_1422	Cape Fear River, NC	6/13/2016	356
2	H9	2_72	506_1423	Cape Fear River, NC	6/14/2016	356
2	A10	2_73	506_1427	Cape Fear River, NC	6/20/2016	457
2	B10	2_74	427_3070	Winyah Bay, SC	03 to 12/2012	.
2	C10	2_75	427_3117	Winyah Bay, SC	03 to 12/2012	.
2	D10	2_76	427_3158	Winyah Bay, SC	03 to 12/2012	.
2	E10	2_77	427_3159	Winyah Bay, SC	03 to 12/2012	.

2	F10	2_78	427_3203	Winyah Bay, SC	03 to 12/2012	.
2	G10	2_79	427_3204	Winyah Bay, SC	03 to 12/2012	.
2	H10	2_80	427_3237	Winyah Bay, SC	03 to 12/2012	.
2	A11	2_81	427_3238	Winyah Bay, SC	03 to 12/2012	.
2	B11	2_82	427_3239	Winyah Bay, SC	03 to 12/2012	.
2	C11	2_83	427_3240	Winyah Bay, SC	03 to 12/2012	.
2	D11	2_84	426_2	Wassaw Sound, GA	06 to 10/2014	.
2	E11	2_85	426_3	Wassaw Sound, GA	06 to 10/2014	.
2	F11	2_86	426_6	Wassaw Sound, GA	06 to 10/2014	.
2	G11	2_87	426_7	Wassaw Sound, GA	06 to 10/2014	.
2	H11	2_88	426_9	Wassaw Sound, GA	06 to 10/2014	.
2	A12	2_89	426_10	Wassaw Sound, GA	06 to 10/2014	.
2	B12	2_90	426_12	Wassaw Sound, GA	06 to 10/2014	.
2	C12	2_91	426_15	Wassaw Sound, GA	06 to 10/2014	.
2	D12	2_92	426_18	Wassaw Sound, GA	06 to 10/2014	.
2	E12	2_93	426_19	Wassaw Sound, GA	06 to 10/2014	.
2	F12	2_94	426_22	Wassaw Sound, GA	06 to 10/2014	.
3	A 1	3_1	750_2	Mississippi	10/4/2018	338
3	A 2	3_2	750_3	Mississippi	10/4/2018	240
3	A 3	3_3	750_4	Mississippi	10/4/2018	330
3	A 4	3_4	750_5	Mississippi	10/4/2018	334
3	A 5	3_5	750_6	Mississippi	10/4/2018	333
3	A 6	3_6	750_7	Mississippi	10/5/2018	356
3	A 7	3_7	750_8	Mississippi	10/8/2018	406
3	A 8	3_8	750_9	Mississippi	10/8/2018	325
3	A 9	3_9	750_10	Mississippi	10/16/2018	269
3	A 10	3_10	750_11	Mississippi	10/16/2018	266
3	A 11	3_11	750_12	Mississippi	10/16/2018	354
3	A 12	3_12	750_13	Mississippi	10/16/2018	356

3	B 1	3_13	750_14	Mississippi	10/16/2018	298
3	B 2	3_14	750_16	Mississippi	10/16/2018	389
3	B 3	3_15	750_17	Mississippi	10/16/2018	369
3	B 4	3_16	750_19	Mississippi	12/7/2018	494
3	B 5	3_17	750_20	Mississippi	12/18/2018	498
3	B 6	3_18	750_21	Mississippi	12/18/2018	275
3	B 7	3_19	750_22	Mississippi	12/18/2018	235
3	B 8	3_20	750_23	Mississippi	2/4/2019	490
3	B 9	3_21	750_24	Mississippi	2/6/2019	516
3	B 10	3_22	750_25	Mississippi	2/6/2019	565
3	B 11	3_23	750_26	Mississippi	2/6/2019	394
3	B 12	3_24	750_27	Mississippi	2/7/2019	425
3	C 1	3_25	750_28	Mississippi	2/7/2019	358
3	C 2	3_26	750_30	Mississippi	2/7/2019	380
3	C 3	3_27	750_32	Mississippi	2/28/2019	335
3	C 4	3_28	750_33	Mississippi	2/28/2019	333
3	C 5	3_29	750_34	Mississippi	3/11/2019	343
3	C 6	3_30	750_35	Mississippi	3/11/2019	323
3	C 7	3_31	750_36	Mississippi	3/21/2019	494
3	C 8	3_32	751_3	Florida	4/5/2019	254
3	C 9	3_33	751_4	Florida	4/5/2019	318
3	C 10	3_34	751_5	Florida	4/5/2019	292
3	C 11	3_35	751_6	Florida	4/5/2019	356
3	C 12	3_36	751_7	Florida	4/5/2019	356
3	D 1	3_37	751_8	Florida	4/5/2019	394
3	D 2	3_38	751_9	Florida	4/5/2019	368
3	D 3	3_39	751_10	Florida	4/5/2019	318
3	D 4	3_40	751_11	Florida	4/5/2019	356
3	D 5	3_41	751_12	Florida	4/5/2019	368

3	D 6	3_42	751_13	Florida	4/5/2019	279
3	D 7	3_43	751_14	Florida	4/5/2019	305
3	D 8	3_44	751_15	Florida	4/5/2019	356
3	D 9	3_45	751_16	Florida	4/5/2019	356
3	D 10	3_46	751_18	Florida	4/5/2019	381
3	D 11	3_47	751_20	Florida	4/5/2019	406
3	D 12	3_48	751_21	Florida	4/5/2019	445
3	E 1	3_49	751_23	Florida	4/5/2019	368
3	E 2	3_50	751_25	Florida	4/5/2019	457
3	E 3	3_51	761_25	Florida	2/18/2019	381
3	E 4	3_52	761_26	Florida	3/25/2019	305
3	E 5	3_53	761_27	Florida	3/25/2019	356
3	E 6	3_54	761_28	Florida	3/25/2019	356
3	E 7	3_55	761_29	Florida	5/7/2019	343
3	E 8	3_56	761_30	Florida	2/18/2019	356
3	E 9	3_57	761_31	Florida	2/18/2019	298
3	E 10	3_58	761_32	Florida	3/14/2019	343
3	E 11	3_59	761_34	Florida	2/18/2019	298
3	E 12	3_60	761_35	Florida	5/7/2019	318
3	F 1	3_61	761_37	Florida	5/7/2019	394
3	F 2	3_62	761_38	Florida	5/7/2019	368
3	F 3	3_63	654_25	James Island, SC	11/23/2017	370
3	F 4	3_64	654_28	James Island, SC	11/23/2017	350
3	F 5	3_65	654_31	James Island, SC	11/23/2017	400
3	F 6	3_66	654_35	James Island, SC	11/23/2017	373
3	F 7	3_67	654_39	James Island, SC	11/23/2017	.
3	F 8	3_68	654_40	James Island, SC	3/4/2018	.
3	F 9	3_69	654_41	James Island, SC	3/4/2018	.
3	F 10	3_70	654_44	James Island, SC	3/4/2018	350

3	F 11	3_71	654_45	James Island, SC	3/4/2018	450
3	F 12	3_72	654_48	James Island, SC	3/4/2018	380
3	G 1	3_73	654_51	James Island, SC	3/4/2018	395
3	G 2	3_74	505_914	New River, NC	7/22/2016	378
3	G 3	3_75	505_1117	New River, NC	7/22/2016	400
3	G 4	3_76	505_1118	New River, NC	7/22/2016	370
3	G 5	3_77	505_1119	New River, NC	7/22/2016	379
3	G 6	3_78	505_1120	New River, NC	7/22/2016	364
3	G 7	3_79	505_1298	New River, NC	4/13/2016	575
3	G 8	3_80	505_1300	New River, NC	4/26/2016	566
3	G 9	3_81	505_1304	New River, NC	5/25/2016	582
3	G 10	3_82	505_1306	New River, NC	7/12/2016	603
3	G 11	3_83	505_1308	New River, NC	7/14/2016	665
3	H 1	3_84	493_1538	New River, NC	4/28/2016	610
3	H 2	3_85	493_1539	New River, NC	4/28/2016	610
3	H 3	3_86	493_1540	New River, NC	4/28/2016	457
3	H 4	3_87	493_1541	New River, NC	4/28/2016	406
3	H 5	3_88	493_1542	New River, NC	4/28/2016	432
3	H 6	3_89	506_1543	New River, NC	7/27/2016	610
3	H 7	3_90	506_1544	New River, NC	7/27/2016	406
3	H 8	3_91	506_1545	New River, NC	7/27/2016	381
3	H 9	3_92	506_1546	New River, NC	7/27/2016	381
3	H 10	3_93	531_1717	New River, NC	7/26/2016	499
3	H 11	3_94	419_64	New River, NC	9/5/2014	434

Table S 8. Average water temperature in January for all sampling locations and data source.

Sample location	°F	Buoy location	Retrieved from
CR	39	Lewisetta, VA	https://www.ncei.noaa.gov/access/data/coastal-water-temperature-guide/all_meanT.html
WR	42	York Town, VA	https://www.ncei.noaa.gov/access/data/coastal-water-temperature-guide/all_meanT.html
YR	42	York Town, VA	https://www.ncei.noaa.gov/access/data/coastal-water-temperature-guide/all_meanT.html
ER	49	money point, VA	https://www.ncei.noaa.gov/access/data/coastal-water-temperature-guide/all_meanT.html
LR	46	CBBT	https://www.ncei.noaa.gov/access/data/coastal-water-temperature-guide/all_meanT.html
RI	46	CBBT	https://www.ncei.noaa.gov/access/data/coastal-water-temperature-guide/all_meanT.html
OI	45	Duck, NC	https://www.ncei.noaa.gov/access/data/coastal-water-temperature-guide/all_meanT.html
PS	47.66	USCG Station Hatteras, NC	https://www.ndbc.noaa.gov/data/climatic/HCGN7.txt
SR	49.64	Beaufort, NC	https://www.ndbc.noaa.gov/data/climatic/BFTN7.txt
BS	49.64	Beaufort, NC	https://www.ndbc.noaa.gov/data/climatic/BFTN7.txt
NR	49.4	Zeke's Basin	http://cdmo.baruch.sc.edu/dges/
CFR	49.4	Zeke's Basin	http://cdmo.baruch.sc.edu/dges/
WB	49.82	Springmaid Pier, SC	https://www.ndbc.noaa.gov/data/climatic/MROS1.txt
JI	50	Charleston, SC	https://www.ncei.noaa.gov/access/data/coastal-water-temperature-guide/all_meanT.html
GA	51	Savannah Beach, GA	https://www.ncei.noaa.gov/access/data/coastal-water-temperature-guide/all_meanT.html
FL	63.86	Venice, FL	https://www.ndbc.noaa.gov/data/climatic/VENF1.txt
MS	57.2	Bay Waveland Yacht Club, MS	https://www.ndbc.noaa.gov/data/climatic/WYCM6.txt

Table S 9. Sample assignments based on Discriminant Analysis of Principal Components (DAPC). Corrotoman River (CR), Ware River (WR), York River (YR), Elizabeth River (ER), Lynnhaven River (LR), Rudee Inlet (RI), Oregon Inlet (OI), Pamlico Sound (PS), South River (SR), Bogue Sound (BS), New River (NR), Cape Fear River (CFR), Winyah Bay (WB), James Island (JI), Wassaw Sound (GA), Florida (FL), and Mississippi (MS).

	Cluster			
	1	2	3	4
CR	0	0	35	0
WR	0	0	9	0
YR	0	0	14	0
ER	0	0	10	0
LR	0	0	7	0
RI	0	0	16	0
OI	0	0	8	0
PS	0	0	12	0
SR	0	0	8	0
BS	0	2	18	0
NR	0	15	14	0
CFR	0	15	1	0
WB	0	10	0	0
JI	0	9	2	0
GA	0	10	0	0
FL	0	0	0	31
MS	31	0	0	0

Table S 10. Allele frequencies of 226 outlier loci in all 17 sampling locations. Corrotoman River (CR), Ware River (WR), York River (YR), Elizabeth River (ER), Lynnhaven River (LR), Rudee Inlet (RI), Oregon Inlet (OI), Pamlico Sound (PS), South River (SR), Bogue Sound (BS), New River (NR), Cape Fear River (CFR), Winyah Bay (WB), James Island (JI), Wassaw Sound (GA), Florida (FL), and Mississippi (MS). Fixed alleles are shaded in grey.

Locus name	CR	WR	YR	ER	LR	RI	OI	PS	SR	BS	NR	CFR	WB	JI	GA	FL	MS
26150445-43-G/C	0.81	0.83	0.93	0.90	0.93	0.94	0.75	0.71	0.63	0.63	0.71	0.59	0.50	0.55	0.50	0.63	0.97
26156078-18-A/G	0.87	0.94	0.82	1.00	1.00	0.94	1.00	0.96	1.00	0.95	0.91	0.88	0.67	0.75	0.95	0.94	0.93
26157376-8-A/G	0.93	1.00	0.96	1.00	1.00	1.00	1.00	0.96	0.94	0.80	0.66	0.59	0.30	0.41	0.40	0.08	0.82
26159850-11-C/A	0.97	1.00	0.93	1.00	0.93	0.94	0.94	0.96	0.81	0.85	0.76	0.75	0.65	0.45	0.55	0.00	0.21
26152909-31-C/G	0.30	0.56	0.46	0.50	0.43	0.59	0.50	0.58	0.38	0.48	0.62	0.81	0.95	0.82	0.95	0.94	0.95
26152976-20-C/T	0.50	0.50	0.46	0.65	0.79	0.53	0.75	0.75	0.56	0.73	0.60	0.75	0.90	0.55	1.00	0.41	0.48
26158393-56-C/G	0.61	0.33	0.57	0.15	0.29	0.56	0.57	0.58	0.63	0.43	0.48	0.33	0.60	0.55	0.45	0.39	0.45
26159595-47-T/C	0.58	0.63	0.82	0.90	0.79	0.69	0.75	0.77	1.00	0.73	0.79	0.72	0.45	0.55	0.65	0.48	0.38
26150224-60-G/A	0.39	0.61	0.50	0.55	0.57	0.50	0.56	0.58	0.56	0.65	0.59	0.53	0.40	0.45	0.85	1.00	0.84
26157511-53-C/T	1.00	1.00	1.00	0.89	1.00	0.86	1.00	1.00	1.00	0.85	0.89	0.86	0.75	0.56	0.75	0.87	0.81
26159204-37-G/C	0.86	0.72	0.96	0.70	1.00	0.73	0.88	0.82	0.63	0.73	0.75	0.54	0.50	0.41	0.30	0.56	0.81
26153232-56-A/C	0.69	0.72	0.71	0.60	0.43	0.59	0.50	0.54	0.50	0.68	0.48	0.34	0.44	0.50	0.55	0.32	0.40
26157906-42-G/A	0.76	0.78	0.86	0.90	0.64	0.91	0.88	0.92	0.94	0.85	0.83	0.94	0.80	0.77	0.95	0.95	0.84
26159661-10-A/G	0.34	0.33	0.57	0.45	0.36	0.60	0.31	0.38	0.69	0.70	0.48	0.69	0.70	0.65	0.60	0.84	0.90
26146361-28-T/C	0.77	0.78	0.75	0.75	0.64	0.69	0.81	0.75	0.56	0.75	0.66	0.72	0.30	0.64	0.55	0.37	0.16
26153030-35-C/T	0.86	0.56	0.89	0.70	0.90	0.86	0.64	0.92	0.63	0.78	0.77	0.57	0.75	0.22	0.72	0.60	0.60
26153444-32-G/A	0.73	0.83	0.57	0.95	0.71	0.75	0.50	0.96	0.88	0.73	0.78	0.81	0.80	0.68	0.95	0.84	0.92
26147893-65-C/T	0.31	0.22	0.32	0.50	0.43	0.38	0.31	0.33	0.31	0.45	0.47	0.56	0.65	0.59	0.70	0.79	0.97
26154382-6-C/T	0.59	0.56	0.75	0.70	0.71	0.63	0.63	0.67	0.94	0.65	0.86	0.97	1.00	0.95	1.00	0.90	1.00
26149529-21-A/G	0.95	1.00	0.92	0.80	0.86	0.93	0.71	0.96	0.94	0.79	0.90	0.84	0.61	0.90	0.81	0.67	0.55
26156106-24-G/C	0.20	0.33	0.18	0.25	0.21	0.28	0.38	0.21	0.19	0.43	0.31	0.28	0.40	0.36	0.65	0.32	0.35
26148857-65-G/A	0.40	0.56	0.45	0.56	0.33	0.36	0.56	0.50	0.56	0.61	0.64	0.67	0.40	0.65	0.56	0.40	0.27
26160511-32-C/T	0.13	0.28	0.21	0.25	0.08	0.27	0.07	0.25	0.19	0.50	0.36	0.73	0.85	0.73	1.00	0.74	0.48
26147862-67-G/A	0.79	0.72	0.75	0.85	0.79	0.69	0.63	0.63	0.69	0.55	0.57	0.22	0.25	0.23	0.30	0.06	0.00
26150095-30-C/T	0.67	0.72	0.68	0.85	0.50	0.69	0.81	0.71	0.75	0.90	0.88	0.91	0.80	0.82	0.90	0.84	0.81
26158386-56-C/T	0.91	0.94	0.96	0.80	1.00	0.91	0.94	0.96	0.88	0.80	0.76	0.88	0.65	0.68	0.80	0.03	0.22

26150562-59-T/G	0.32	0.22	0.43	0.30	0.21	0.53	0.29	0.42	0.38	0.63	0.66	0.75	0.80	0.77	0.90	0.27	1.00
26151817-18-G/A	0.77	0.78	0.89	0.85	0.86	0.81	0.75	0.83	0.63	0.50	0.53	0.31	0.40	0.50	0.15	0.10	0.37
26154048-29-C/G	0.69	0.61	0.71	0.33	0.57	0.59	0.75	0.59	0.36	0.55	0.48	0.37	0.30	0.36	0.70	0.35	0.42
26148628-51-T/C	0.87	0.67	0.89	0.85	0.79	0.84	0.81	0.75	0.75	0.80	0.67	0.69	0.60	0.50	0.40	0.00	0.00
26149468-45-A/C	0.93	0.72	0.86	0.65	0.93	0.81	0.81	0.83	0.63	0.83	0.86	0.91	0.90	0.77	0.85	0.19	0.77
26150086-32-T/A	0.87	0.94	0.82	0.90	1.00	0.72	0.94	0.67	0.38	0.65	0.60	0.28	0.30	0.59	0.40	0.73	0.87
26149676-23-C/T	0.41	0.31	0.46	0.40	0.43	0.28	0.50	0.29	0.75	0.55	0.68	0.72	0.90	0.86	0.95	0.74	0.50
26155658-21-G/A	1.00	1.00	1.00	1.00	1.00	0.97	1.00	0.96	1.00	0.95	0.71	0.47	0.55	0.55	0.45	0.37	0.97
26157246-12-A/G	0.89	0.72	0.89	0.75	0.79	0.81	0.88	0.63	0.69	0.89	0.74	0.56	0.35	0.36	0.50	0.74	0.58
26150615-35-C/T	0.54	0.44	0.54	0.60	0.64	0.63	0.44	0.63	0.63	0.68	0.79	0.81	0.95	0.73	0.85	1.00	0.98
26152305-65-G/A	0.70	0.83	0.71	0.75	0.64	0.44	0.81	0.46	0.63	0.45	0.55	0.25	0.15	0.27	0.20	0.29	0.22
26145901-50-C/T	0.74	0.72	0.71	0.65	0.64	0.53	0.69	0.63	0.69	0.50	0.31	0.16	0.30	0.18	0.25	0.45	0.50
26152784-27-C/T	0.66	0.83	0.57	0.60	0.64	0.63	0.69	0.58	0.44	0.50	0.38	0.41	0.40	0.45	0.25	0.18	0.32
26145864-68-A/G	0.81	0.94	0.89	0.80	0.79	0.88	0.94	0.83	0.75	0.73	0.67	0.66	0.30	0.59	0.45	0.60	0.65
26149484-26-T/G	0.70	0.72	0.54	0.60	0.71	0.59	0.38	0.58	0.75	0.60	0.55	0.50	0.40	0.45	0.55	0.10	0.15
26147754-54-C/T	0.79	0.78	0.64	0.70	0.86	0.72	0.63	0.58	0.69	0.60	0.66	0.63	0.70	0.64	0.60	0.76	0.73
26158335-37-A/G	0.44	0.44	0.50	0.65	0.50	0.34	0.44	0.50	0.44	0.65	0.57	0.67	0.50	0.45	0.25	0.67	0.81
26149675-61-A/G	0.97	1.00	0.89	0.95	1.00	0.94	0.88	0.92	0.94	0.80	0.88	0.75	0.75	0.86	0.85	0.77	0.97
26148490-34-G/A	0.40	0.39	0.18	0.25	0.50	0.56	0.44	0.50	0.38	0.48	0.53	0.84	0.90	0.82	0.80	0.97	0.84
26159924-45-T/C	0.64	0.67	0.46	0.45	0.36	0.56	0.69	0.42	0.50	0.35	0.48	0.44	0.30	0.45	0.40	0.53	0.23
26157558-30-C/T	0.80	0.78	0.71	0.65	0.71	0.69	0.81	0.63	0.69	0.75	0.69	0.72	0.85	0.77	0.85	0.44	0.37
26155603-22-C/G	0.86	0.72	0.93	0.70	0.86	0.75	0.69	0.79	0.81	0.68	0.76	0.59	0.80	0.82	0.60	0.14	0.25
26146293-64-T/C	0.63	0.72	0.79	0.85	0.71	0.72	0.69	0.83	0.75	0.70	0.81	0.88	0.95	0.77	0.75	0.79	0.81
26146515-30-T/G	0.74	0.67	0.50	0.70	0.86	0.75	0.50	0.63	0.50	0.58	0.59	0.50	0.55	0.41	0.20	0.29	0.47
26152157-16-C/T	0.54	0.56	0.54	0.44	0.75	0.63	0.69	0.63	0.63	0.63	0.69	0.50	0.70	0.77	0.60	0.93	0.97
100028347-45-A/G	0.91	0.94	1.00	0.95	0.93	0.97	0.88	0.88	0.75	0.83	0.67	0.63	0.40	0.82	0.55	0.44	0.31
26161191-5-G/A	0.24	0.25	0.27	0.33	0.29	0.04	0.38	0.38	0.25	0.48	0.63	0.77	0.75	0.45	0.80	0.57	0.85
26149232-45-C/T	0.66	0.67	0.45	0.55	0.64	0.43	0.56	0.50	0.69	0.60	0.38	0.50	0.30	0.68	0.44	0.38	0.39
26158752-30-A/T	0.53	0.44	0.54	0.60	0.71	0.69	0.75	0.79	0.56	0.65	0.67	0.53	0.45	0.50	0.45	0.87	0.85
26149818-25-G/A	0.78	0.50	0.92	0.67	0.71	0.66	0.83	0.65	0.69	0.58	0.75	0.69	0.75	0.59	0.45	0.61	0.74
26154257-62-G/T	0.49	0.61	0.71	0.70	0.43	0.41	0.75	0.63	0.63	0.65	0.67	0.84	0.85	0.59	0.90	0.60	0.47
26149520-63-T/C	0.61	0.61	0.68	0.55	0.57	0.75	0.81	0.50	0.50	0.58	0.48	0.22	0.30	0.23	0.10	0.11	0.85

26154465-10-T/A	0.94	0.83	0.92	0.95	0.75	0.90	0.94	0.79	0.71	0.71	0.88	0.73	0.90	0.73	0.60	0.61	0.45
26154793-13-C/T	0.83	0.78	0.93	1.00	1.00	0.88	0.94	0.88	0.94	0.93	1.00	0.94	0.95	0.86	0.95	0.94	0.95
26155313-38-A/G	0.61	0.61	0.61	0.65	0.79	0.63	0.81	0.79	0.75	0.85	0.64	0.81	0.95	0.86	0.90	0.71	0.27
26147400-24-A/G	0.91	1.00	0.93	1.00	1.00	0.88	0.94	0.96	0.81	0.75	0.78	0.66	0.55	0.50	0.45	0.66	1.00
26150662-10-G/A	0.90	0.78	0.89	0.85	0.71	0.78	0.88	0.79	0.69	0.70	0.53	0.38	0.35	0.27	0.15	0.05	0.18
26161192-14-A/G	0.53	0.44	0.46	0.50	0.71	0.64	0.56	0.50	0.44	0.38	0.33	0.22	0.15	0.15	0.10	0.20	0.02
26152094-37-A/G	0.87	0.78	0.93	1.00	0.79	0.91	0.88	0.79	0.75	0.70	0.69	0.66	0.70	0.59	0.60	0.44	0.56
26153711-53-G/C	0.89	1.00	0.86	0.80	0.86	0.81	0.88	0.83	0.81	0.78	0.63	0.50	0.20	0.64	0.30	0.25	0.63
26146294-63-A/T	0.84	0.78	0.75	0.65	0.86	0.84	0.75	0.71	0.63	0.68	0.71	0.66	0.65	0.64	0.65	0.67	0.55
26153792-5-T/C	0.00	0.00	0.00	0.00	0.00	0.00	0.00	0.08	0.06	0.23	0.33	0.72	0.95	0.82	1.00	1.00	0.14
26146044-37-T/G	0.71	0.83	0.75	0.65	0.71	0.69	0.81	0.75	0.69	0.55	0.59	0.19	0.30	0.23	0.30	0.24	0.11
26149999-30-T/C	0.70	0.72	0.86	0.60	0.71	0.66	0.75	0.67	0.56	0.53	0.57	0.47	0.40	0.35	0.50	0.00	0.00
26153261-37-C/T	0.36	0.19	0.21	0.39	0.67	0.28	0.13	0.38	0.25	0.50	0.41	0.40	0.65	0.36	0.55	0.61	0.45
26146014-19-G/T	0.61	0.39	0.61	0.45	0.71	0.78	0.50	0.63	0.69	0.73	0.74	0.53	0.65	0.64	0.60	0.92	0.65
26145909-64-A/G	0.75	0.78	0.57	0.40	0.64	0.63	0.63	0.58	0.69	0.65	0.52	0.44	0.45	0.32	0.45	0.42	0.53
26149648-52-C/T	0.57	0.83	0.54	0.75	0.71	0.63	0.50	0.71	0.56	0.73	0.74	0.72	0.65	0.55	0.85	0.66	0.76
26157359-41-T/C	0.69	0.67	0.61	0.60	0.79	0.50	0.56	0.54	0.56	0.55	0.53	0.59	0.45	0.27	0.30	0.15	0.18
26152797-39-G/A	0.77	0.94	0.86	0.80	0.86	0.88	1.00	1.00	0.94	0.93	0.79	0.84	0.75	0.86	0.85	0.95	0.95
26150203-42-T/C	0.63	0.72	0.68	0.45	0.57	0.56	0.63	0.54	0.56	0.63	0.47	0.47	0.45	0.36	0.40	0.05	0.19
26145976-45-A/G	0.64	0.72	0.61	0.60	0.71	0.69	0.44	0.67	0.56	0.50	0.40	0.06	0.05	0.18	0.05	0.21	0.00
26155293-11-G/A	0.93	0.83	1.00	0.75	1.00	0.91	0.88	0.79	0.81	0.80	0.72	0.19	0.30	0.59	0.40	0.42	0.98
26152215-62-C/T	0.93	1.00	0.96	0.90	0.93	0.91	0.81	0.92	0.69	0.88	0.83	0.75	0.85	0.64	0.75	0.63	0.56
26149015-16-C/T	0.81	0.94	0.86	0.95	0.79	0.78	0.75	0.79	0.63	0.73	0.62	0.53	0.50	0.36	0.15	0.13	0.47
26149218-40-G/C	0.80	0.61	0.89	0.60	0.50	0.75	0.63	0.54	0.75	0.63	0.66	0.56	0.55	0.50	0.50	0.02	0.08
26152107-48-G/A	0.49	0.67	0.50	0.55	0.29	0.59	0.13	0.68	0.69	0.53	0.66	0.91	1.00	0.95	0.90	0.98	0.98
26157480-51-G/A	0.70	0.72	0.71	0.60	0.71	0.78	0.69	0.71	0.50	0.58	0.38	0.13	0.00	0.18	0.05	0.29	0.00
26149537-68-A/G	0.61	0.67	0.57	0.60	0.71	0.56	0.69	0.54	0.50	0.53	0.47	0.44	0.20	0.45	0.30	0.16	0.45
26156658-57-C/T	0.76	0.67	0.82	0.95	0.71	0.75	0.75	0.92	1.00	0.88	0.86	0.84	0.75	0.77	1.00	0.87	0.93
26146747-7-C/T	0.84	0.94	0.75	0.85	0.71	0.84	0.81	0.67	0.75	0.68	0.72	0.56	0.40	0.50	0.50	0.48	0.24
26153122-49-A/C	0.51	0.28	0.64	0.20	0.64	0.50	0.69	0.58	0.50	0.40	0.33	0.09	0.05	0.32	0.15	0.19	0.00
26157740-30-T/A	0.42	0.50	0.38	0.45	0.21	0.08	0.25	0.46	0.13	0.68	0.64	0.39	0.56	0.41	0.61	0.76	0.76
26154520-18-A/C	0.86	0.81	0.73	0.83	0.58	0.68	0.88	0.86	0.81	0.72	0.65	0.90	0.65	0.70	0.72	0.63	0.45

26147286-58-C/A	0.41	0.50	0.46	0.55	0.29	0.47	0.25	0.58	0.31	0.68	0.53	0.78	0.90	0.73	0.90	0.90	0.94
26156898-25-G/A	0.70	0.78	0.71	0.45	0.50	0.70	0.75	0.71	0.50	0.60	0.52	0.43	0.15	0.18	0.11	0.44	0.21
26149095-54-C/T	0.96	1.00	0.93	1.00	0.86	0.91	0.94	0.92	0.81	0.88	0.79	0.53	0.35	0.41	0.45	0.19	0.95
26147247-38-C/T	0.83	0.72	0.86	0.90	0.93	0.91	0.88	0.92	1.00	0.88	0.91	0.81	0.95	0.91	0.80	0.94	0.95
26146808-26-G/A	0.87	0.89	0.96	0.75	0.93	0.97	1.00	0.75	0.69	0.75	0.79	0.84	0.55	0.73	0.65	0.12	0.89
26146246-31-G/T	0.94	0.89	1.00	0.95	0.93	0.97	1.00	0.88	0.81	0.73	0.79	0.44	0.30	0.45	0.40	0.58	0.98
26147612-14-A/C	0.64	0.61	0.61	0.60	0.71	0.59	0.56	0.42	0.56	0.60	0.63	0.44	0.45	0.27	0.40	0.39	0.27
26160230-27-A/G	0.70	0.44	0.85	0.65	0.64	0.50	0.50	0.63	0.75	0.55	0.46	0.47	0.35	0.50	0.40	0.16	0.18
26154229-29-C/G	0.96	1.00	0.93	0.95	0.93	0.91	1.00	0.88	0.81	0.83	0.74	0.28	0.60	0.55	0.45	0.06	0.98
26158374-5-G/A	0.55	0.39	0.50	0.30	0.33	0.34	0.29	0.29	0.56	0.37	0.35	0.19	0.28	0.41	0.39	0.39	0.40
26148114-5-T/C	0.47	0.44	0.46	0.40	0.57	0.50	0.38	0.29	0.38	0.38	0.38	0.22	0.20	0.27	0.25	0.11	0.21
26147787-61-C/A	0.56	0.50	0.46	0.60	0.57	0.72	0.31	0.79	0.75	0.83	0.67	0.97	0.95	0.91	0.90	0.76	1.00
26157694-56-G/T	0.46	0.44	0.29	0.50	0.21	0.59	0.31	0.46	0.69	0.50	0.57	0.63	0.50	0.50	0.55	0.78	0.48
26154406-29-G/A	0.57	0.61	0.39	0.60	0.36	0.56	0.50	0.58	0.81	0.73	0.64	0.69	0.80	0.64	0.75	0.84	0.60
26146202-24-A/G	0.41	0.44	0.64	0.55	0.36	0.72	0.75	0.58	0.63	0.60	0.50	0.44	0.40	0.59	0.65	0.66	0.74
26156936-7-G/A	0.61	0.67	0.50	0.45	0.36	0.59	0.44	0.33	0.44	0.45	0.45	0.50	0.55	0.50	0.75	0.37	0.29
100020377-63-G/T	0.86	0.72	0.89	0.65	0.86	0.75	0.88	0.79	0.75	0.73	0.81	0.91	0.80	0.77	0.90	0.77	0.81
26160229-22-C/T	0.70	0.50	0.85	0.65	0.64	0.50	0.50	0.63	0.75	0.55	0.45	0.50	0.35	0.50	0.40	0.13	0.13
26154617-38-A/G	0.59	0.50	0.43	0.50	0.43	0.53	0.63	0.54	0.44	0.45	0.50	0.50	0.50	0.50	0.45	0.39	0.42
26146437-30-G/A	0.66	0.61	0.64	0.70	0.79	0.63	0.88	0.63	0.56	0.50	0.45	0.34	0.20	0.14	0.20	0.19	0.89
26154125-38-A/C	0.61	0.72	0.64	0.70	0.57	0.66	0.69	0.54	0.75	0.70	0.78	0.88	0.90	0.68	0.75	1.00	1.00
26145936-61-G/A	0.96	0.89	1.00	0.75	0.93	0.97	0.94	0.88	0.69	0.85	0.76	0.56	0.20	0.45	0.50	0.47	0.90
26157795-34-A/G	0.69	0.94	0.75	0.94	1.00	0.75	0.79	0.88	0.94	0.92	0.89	1.00	0.95	0.82	0.90	1.00	1.00
100080350-9-G/A	0.84	0.83	0.89	0.80	0.93	0.78	0.81	0.75	0.81	0.83	0.52	0.41	0.10	0.35	0.20	0.10	0.56
26147674-11-G/T	0.96	0.94	0.96	0.85	0.71	1.00	0.88	0.92	0.94	0.83	0.91	0.72	0.55	0.73	0.65	0.76	0.71
26152471-22-A/T	0.54	0.56	0.61	0.65	0.57	0.69	0.38	0.79	0.56	0.60	0.69	0.50	0.55	0.41	0.70	0.94	0.37
26148483-44-T/C	0.85	0.94	0.86	0.80	0.86	0.81	0.79	0.79	0.75	0.71	0.64	0.82	0.56	0.55	0.69	0.61	0.75
26156120-32-A/G	0.76	0.72	0.75	0.75	0.71	0.91	0.88	0.71	0.63	0.53	0.40	0.25	0.10	0.23	0.20	0.38	0.00
26158927-56-G/C	0.44	0.61	0.57	0.60	0.36	0.56	0.69	0.42	0.81	0.63	0.39	0.44	0.50	0.55	0.05	0.37	0.43
26148806-23-A/G	0.99	1.00	1.00	0.90	1.00	1.00	0.94	0.96	0.94	0.78	0.79	0.72	0.65	0.59	0.65	0.85	1.00
26157067-57-T/A	0.69	0.61	0.57	0.55	0.50	0.56	0.69	0.58	0.31	0.60	0.59	0.47	0.50	0.50	0.50	0.53	0.52
26156092-17-A/T	0.46	0.61	0.36	0.50	0.57	0.50	0.63	0.71	0.50	0.63	0.57	0.81	1.00	0.86	0.85	0.92	1.00

26158325-22-T/A	0.76	0.67	0.71	0.70	0.79	0.69	0.75	0.71	0.56	0.53	0.60	0.43	0.44	0.40	0.55	0.47	0.50
26150393-64-G/A	0.64	0.50	0.57	0.50	0.43	0.53	0.56	0.54	0.56	0.45	0.38	0.41	0.30	0.36	0.30	0.15	0.85
26155422-29-G/A	0.77	0.50	0.79	0.60	0.43	0.59	0.69	0.58	0.63	0.55	0.53	0.47	0.50	0.41	0.30	0.02	0.35
26149533-31-A/C	0.88	0.81	0.95	0.85	0.86	0.82	0.93	0.83	0.69	0.76	0.82	0.56	0.40	0.55	0.55	0.50	0.84
26146894-29-A/T	0.31	0.44	0.25	0.45	0.43	0.56	0.44	0.29	0.38	0.58	0.55	0.78	0.75	0.82	0.95	0.97	0.93
26146997-5-C/T	0.63	0.89	0.64	0.75	0.79	0.69	0.81	0.79	0.56	0.80	0.79	0.84	0.85	0.77	0.80	0.97	0.94
26146839-9-A/C	0.99	0.83	0.93	0.90	0.93	0.88	1.00	0.83	0.63	0.85	0.86	0.81	0.75	0.82	0.80	0.95	1.00
26161175-9-C/T	0.13	0.28	0.23	0.15	0.14	0.31	0.14	0.21	0.19	0.40	0.48	0.66	0.55	0.73	0.75	0.37	0.92
26154561-14-A/G	0.41	0.56	0.50	0.60	0.29	0.59	0.44	0.42	0.44	0.50	0.66	0.84	0.85	0.82	0.90	0.97	0.79
26157145-7-T/C	0.94	1.00	0.93	0.90	0.93	0.88	0.94	0.92	0.88	0.90	0.76	0.47	0.45	0.73	0.50	0.24	0.27
26146825-35-C/A	0.61	0.83	0.68	0.70	0.43	0.50	0.69	0.63	0.31	0.63	0.48	0.41	0.40	0.45	0.35	0.10	0.16
26149848-41-T/C	0.93	0.78	0.96	0.90	0.93	0.94	0.88	0.83	0.81	0.88	0.71	0.50	0.50	0.41	0.40	0.16	0.40
26146611-38-A/G	0.19	0.11	0.18	0.20	0.14	0.31	0.25	0.29	0.13	0.30	0.48	0.56	0.55	0.50	0.60	0.53	0.63
26153523-63-C/T	0.86	0.89	0.86	0.75	0.79	0.84	0.75	0.88	0.88	0.78	0.59	0.38	0.30	0.36	0.30	0.52	0.19
26155338-43-A/G	0.91	1.00	0.79	0.90	0.86	0.84	0.88	0.83	0.81	0.85	0.62	0.41	0.75	0.50	0.45	0.12	0.03
26150315-40-G/A	0.69	0.56	0.73	0.90	0.79	0.50	0.75	0.67	0.57	0.78	0.75	0.86	0.90	0.77	0.89	0.98	0.95
26147652-57-C/T	0.90	0.89	0.68	0.80	0.64	0.91	0.88	0.75	0.75	0.48	0.52	0.31	0.30	0.27	0.20	0.13	0.86
26156938-48-G/T	0.63	0.78	0.57	0.40	0.50	0.44	0.56	0.75	0.69	0.40	0.50	0.28	0.45	0.45	0.60	0.05	0.07
26156951-18-A/T	0.63	1.00	0.69	0.44	0.83	0.47	0.75	0.64	0.44	0.55	0.53	0.60	0.60	0.41	0.65	0.27	0.44
26152888-51-G/A	0.14	0.33	0.14	0.35	0.36	0.25	0.31	0.25	0.19	0.25	0.28	0.22	0.30	0.32	0.35	0.73	0.77
26150567-7-G/C	0.59	0.78	0.68	0.65	0.79	0.75	0.81	0.67	0.88	0.68	0.57	0.44	0.35	0.50	0.60	0.94	0.82
100074958-10-C/T	0.94	0.94	0.86	0.80	0.86	0.88	0.81	0.83	0.75	0.88	0.84	0.91	0.85	0.77	0.80	0.82	0.79
26152266-13-A/G	0.93	0.83	0.82	0.95	0.86	0.75	0.88	0.83	0.75	0.80	0.71	0.47	0.60	0.73	0.70	0.39	0.68
26149573-12-A/C	0.83	0.89	0.71	0.65	0.71	0.59	0.63	0.67	0.88	0.80	0.48	0.66	0.60	0.59	0.40	0.42	0.35
26152354-15-A/G	0.56	0.61	0.61	0.40	0.64	0.47	0.56	0.46	0.44	0.48	0.43	0.31	0.35	0.14	0.15	0.00	0.00
26152278-34-G/A	0.89	0.83	0.86	0.65	0.86	0.88	0.88	0.79	0.81	0.78	0.74	0.56	0.45	0.41	0.65	0.05	0.44
26154372-59-A/G	0.26	0.44	0.21	0.17	0.57	0.50	0.50	0.33	0.31	0.33	0.43	0.41	0.30	0.45	0.70	0.55	0.60
26147731-26-A/G	0.49	0.33	0.64	0.55	0.57	0.53	0.63	0.58	0.81	0.65	0.62	0.72	0.80	0.64	0.70	0.76	0.84
26149835-6-C/A	0.66	0.61	0.61	0.45	0.86	0.53	0.50	0.67	0.56	0.50	0.54	0.63	0.65	0.55	0.45	0.56	0.58
26153918-62-A/C	0.41	0.67	0.18	0.40	0.50	0.34	0.50	0.63	0.75	0.45	0.43	0.59	0.45	0.64	0.65	0.61	0.69
26146801-32-T/A	0.77	0.67	0.71	0.75	0.64	0.72	0.75	0.75	0.44	0.60	0.45	0.22	0.05	0.23	0.25	0.29	0.05
26149399-65-C/G	0.90	0.78	0.89	0.80	0.86	0.78	0.88	0.83	0.63	0.78	0.78	0.81	0.80	0.82	0.65	0.77	0.78

26149607-66-T/C	0.74	0.78	0.68	0.60	0.64	0.69	0.63	0.79	0.69	0.53	0.53	0.66	0.75	0.50	0.60	0.48	0.94
26148029-50-T/C	0.63	0.39	0.61	0.70	0.57	0.44	0.56	0.67	0.63	0.68	0.89	0.88	0.95	0.77	1.00	0.94	0.93
26152460-8-C/A	0.76	0.83	0.82	0.90	0.93	0.91	0.56	0.79	0.94	0.88	0.79	0.75	1.00	0.77	0.80	0.98	0.97
26159991-19-A/G	0.68	0.67	0.61	0.55	0.67	0.72	0.69	0.73	0.50	0.60	0.54	0.61	0.40	0.41	0.45	0.06	0.28
26159804-29-A/G	0.64	0.72	0.69	0.50	0.64	0.50	0.63	0.58	0.44	0.60	0.63	0.43	0.70	0.50	0.50	0.05	0.12
26148923-29-G/A	0.56	0.61	0.39	0.60	0.36	0.63	0.50	0.54	0.75	0.73	0.64	0.69	0.80	0.67	0.75	0.85	0.58
26152610-52-A/T	0.79	0.72	0.73	0.75	0.43	0.81	0.79	0.71	0.56	0.73	0.69	0.78	0.75	0.64	0.40	0.58	0.73
26160099-51-A/T	0.89	0.89	1.00	0.69	1.00	0.72	0.75	0.91	0.81	0.64	0.85	0.71	0.63	0.70	0.95	0.37	0.43
26152232-66-C/T	0.40	0.31	0.46	0.55	0.21	0.40	0.36	0.54	0.44	0.48	0.48	0.34	0.60	0.55	0.75	0.83	0.88
26149633-6-G/A	0.67	0.61	0.50	0.35	0.57	0.73	0.63	0.83	0.56	0.63	0.45	0.56	0.40	0.27	0.50	0.10	0.20
26152164-46-T/C	0.57	0.72	0.50	0.60	0.71	0.66	0.56	0.63	0.75	0.63	0.72	0.69	0.65	0.55	0.60	0.81	0.98
26149372-26-C/G	0.49	0.78	0.57	0.80	0.50	0.69	0.69	0.63	0.75	0.60	0.71	0.81	0.95	0.77	0.85	0.95	0.90
26146001-60-T/C	0.29	0.33	0.07	0.35	0.43	0.53	0.50	0.46	0.31	0.43	0.50	0.78	0.85	0.77	0.90	0.37	0.89
100032220-53-T/C	0.93	0.83	1.00	0.90	0.86	0.97	1.00	0.88	0.81	0.68	0.78	0.38	0.20	0.50	0.40	0.81	0.98
26152796-27-C/T	0.71	0.94	0.75	0.70	0.57	0.72	0.56	0.79	0.56	0.65	0.47	0.44	0.55	0.55	0.40	0.18	0.26
26147170-7-T/C	0.86	0.67	0.79	0.80	0.93	0.72	0.75	0.83	0.88	0.60	0.53	0.38	0.30	0.27	0.35	0.00	0.02
100023336-47-C/T	0.18	0.06	0.21	0.11	0.29	0.28	0.06	0.29	0.19	0.25	0.48	0.50	0.55	0.50	0.60	0.97	0.93
26156691-38-T/G	0.13	0.28	0.25	0.40	0.14	0.22	0.25	0.29	0.38	0.43	0.36	0.69	0.65	0.55	0.80	1.00	0.98
26153141-18-G/A	0.71	0.78	0.82	0.35	0.57	0.75	0.56	0.71	0.75	0.58	0.69	0.69	0.55	0.41	0.60	0.50	0.62
26147196-6-A/G	0.70	0.72	0.57	0.55	0.64	0.50	0.56	0.41	0.44	0.50	0.74	0.63	0.65	0.73	0.70	0.32	0.32
26158500-18-A/G	0.74	0.75	0.61	0.80	0.86	0.66	0.63	0.83	0.50	0.58	0.64	0.63	0.30	0.45	0.15	0.31	0.35
26149692-54-T/A	0.89	0.89	0.96	0.90	0.86	0.81	0.75	0.75	0.63	0.73	0.62	0.28	0.05	0.36	0.10	0.31	0.00
26152053-15-A/G	0.91	1.00	0.96	0.90	0.86	0.84	0.88	0.88	0.63	0.63	0.52	0.22	0.10	0.27	0.10	0.82	0.09
26158254-15-G/T	0.57	0.61	0.68	0.90	0.64	0.66	0.69	0.58	0.88	0.68	0.57	0.63	0.55	0.68	0.75	0.72	0.76
26148152-63-C/T	0.94	0.89	0.96	0.90	0.79	0.91	0.94	0.83	0.75	0.83	0.74	0.75	0.80	0.82	0.45	0.71	0.74
26155237-30-C/T	0.93	0.94	0.86	0.95	0.86	0.88	1.00	0.92	0.81	0.78	0.79	0.75	0.80	0.77	0.65	0.03	0.08
26146077-44-C/T	0.86	0.83	0.89	0.78	0.71	0.84	0.88	0.67	0.69	0.63	0.69	0.31	0.20	0.36	0.20	0.16	0.68
26149882-19-C/T	0.39	0.56	0.39	0.55	0.57	0.34	0.44	0.50	0.63	0.45	0.66	0.88	0.95	0.77	0.95	0.52	0.84
26152885-18-G/A	0.90	0.78	0.89	0.90	0.93	0.88	0.94	0.83	0.75	0.68	0.78	0.69	0.83	0.59	0.75	0.66	0.44
26159739-38-G/A	0.84	1.00	0.73	0.80	0.64	0.73	0.69	0.71	0.75	0.78	0.55	0.40	0.45	0.40	0.35	0.21	0.56
26153384-39-G/T	0.57	0.63	0.43	0.60	0.50	0.69	0.50	0.79	0.75	0.58	0.72	0.81	0.75	0.82	0.85	0.63	0.95
100032289-66-C/T	0.76	0.78	0.82	0.60	0.64	0.66	0.79	0.71	0.69	0.68	0.69	0.47	0.50	0.68	0.35	0.16	0.97

26155278-30-A/G	0.37	0.39	0.32	0.10	0.43	0.41	0.31	0.33	0.25	0.23	0.21	0.03	0.00	0.05	0.05	0.08	0.16
26145668-59-T/C	0.83	0.83	0.86	0.90	0.86	0.78	0.94	0.79	0.81	0.65	0.64	0.69	0.55	0.64	0.55	0.05	0.31
26150658-68-T/A	0.77	0.78	0.82	0.75	0.79	0.84	0.88	0.67	0.38	0.58	0.73	0.63	0.55	0.65	0.35	0.44	0.72
26149408-14-T/C	0.70	0.56	0.79	0.60	0.71	0.63	0.44	0.63	0.63	0.35	0.40	0.28	0.05	0.25	0.00	0.09	0.44
26149101-60-C/T	0.56	0.61	0.64	0.70	0.71	0.69	0.38	0.75	0.50	0.70	0.64	0.66	0.70	0.68	0.75	0.87	0.90
26158567-46-T/A	0.09	0.00	0.14	0.30	0.07	0.06	0.25	0.04	0.38	0.10	0.17	0.28	0.20	0.36	0.25	0.37	0.39
26151756-26-G/A	0.87	0.89	0.96	0.95	0.86	0.94	1.00	0.88	0.75	0.85	0.60	0.47	0.40	0.41	0.30	0.18	0.87
26153736-7-T/C	0.80	0.78	0.79	0.75	0.79	0.72	0.81	0.71	0.81	0.40	0.64	0.50	0.30	0.41	0.25	0.53	0.35
26148579-58-T/A	0.59	0.56	0.61	0.45	0.50	0.56	0.50	0.42	0.44	0.35	0.41	0.22	0.35	0.55	0.30	0.02	0.19
26153311-32-T/G	0.94	0.89	0.86	0.80	1.00	0.87	0.81	0.92	0.75	0.82	0.84	0.97	0.95	0.86	0.80	0.82	0.90
26147454-57-A/C	0.76	0.61	0.79	0.45	0.50	0.69	0.56	0.75	0.56	0.55	0.55	0.47	0.17	0.55	0.45	0.55	0.42
26158827-54-G/A	0.51	0.11	0.43	0.45	0.36	0.50	0.25	0.21	0.06	0.45	0.47	0.59	0.55	0.45	0.55	0.44	0.69
26159101-18-G/C	0.77	0.50	0.71	0.60	0.93	0.63	0.50	0.68	0.43	0.63	0.65	0.72	0.65	0.55	0.50	0.58	0.50
26159167-32-T/G	0.76	1.00	0.83	0.95	0.70	0.62	0.88	0.86	0.56	0.42	0.62	0.43	0.60	0.15	0.50	0.20	0.32
26160889-44-A/T	0.46	0.61	0.29	0.35	0.50	0.56	0.31	0.38	0.50	0.30	0.29	0.47	0.15	0.50	0.28	0.08	0.05
26152627-59-G/A	0.86	0.83	0.89	0.80	0.93	0.88	0.88	0.75	0.75	0.73	0.79	0.91	0.72	0.68	0.80	0.73	0.74
26154939-18-T/C	0.70	0.75	0.68	0.55	0.64	0.78	0.67	0.63	0.44	0.73	0.57	0.50	0.25	0.20	0.25	0.38	0.46
26154796-57-C/A	0.81	0.78	0.71	0.70	0.79	0.78	0.69	0.71	0.81	0.75	0.64	0.63	0.40	0.64	0.55	0.44	0.39
26147263-51-A/G	0.40	0.11	0.43	0.45	0.64	0.47	0.69	0.42	0.44	0.58	0.64	0.84	0.90	0.73	0.90	0.90	0.95
26149864-35-C/T	0.43	0.67	0.43	0.45	0.57	0.43	0.33	0.50	0.56	0.61	0.64	0.59	0.83	0.60	0.85	0.85	0.81
26154184-14-G/A	0.64	0.67	0.79	0.75	0.79	0.75	0.69	0.79	0.75	0.70	0.86	0.84	0.85	0.86	0.90	1.00	1.00
26146053-37-A/T	0.40	0.56	0.43	0.60	0.43	0.41	0.56	0.46	0.63	0.55	0.66	0.84	0.95	0.82	0.95	0.74	1.00
26145563-54-A/C	0.70	0.67	0.61	0.65	0.71	0.75	0.75	0.71	0.44	0.60	0.48	0.34	0.30	0.36	0.25	0.03	0.73
26145960-34-C/T	0.94	0.83	0.96	0.90	1.00	0.88	0.94	0.92	0.94	0.85	0.76	0.63	0.50	0.59	0.50	0.13	0.90
26154725-24-G/A	0.44	0.44	0.36	0.30	0.29	0.50	0.44	0.58	0.50	0.58	0.52	0.81	0.90	0.82	0.85	0.82	0.61
26154816-68-T/G	0.63	0.61	0.68	0.65	0.50	0.69	0.63	0.63	0.75	0.80	0.76	0.72	0.80	0.45	0.65	0.98	0.89
26154314-11-C/T	0.84	0.94	0.79	0.75	0.90	0.88	0.75	0.75	0.56	0.73	0.62	0.69	0.60	0.65	0.60	0.26	0.11
100067909-23-C/T	0.63	0.78	0.82	0.70	0.79	0.84	0.88	0.75	0.94	0.85	0.71	0.69	0.80	0.86	0.85	0.94	0.94
26146947-24-G/A	0.86	0.83	0.82	0.65	0.71	0.78	0.69	0.79	0.56	0.85	0.64	0.50	0.55	0.73	0.50	0.39	0.44
26156708-9-T/C	0.54	0.56	0.50	0.80	0.57	0.72	0.50	0.75	0.63	0.65	0.66	0.91	0.80	0.94	0.80	0.81	0.60
26148163-56-C/T	0.67	0.67	0.64	0.75	0.71	0.75	0.69	0.79	0.69	0.73	0.72	0.66	0.60	0.59	0.55	0.92	0.89
26157721-60-A/C	0.77	0.83	0.68	0.75	0.71	0.72	0.75	0.75	0.75	0.50	0.50	0.53	0.50	0.55	0.65	0.10	0.02

26156937-61-G/A	0.31	0.50	0.43	0.55	0.43	0.41	0.50	0.38	0.25	0.53	0.50	0.47	0.55	0.36	0.55	0.79	0.56
26153166-10-C/T	0.47	0.17	0.46	0.17	0.43	0.13	0.06	0.33	0.19	0.19	0.43	0.56	0.44	0.55	0.55	0.56	0.55
26152301-34-A/C	0.89	0.88	0.83	0.72	1.00	0.81	0.79	0.88	1.00	0.75	0.84	0.59	0.75	0.50	0.75	0.44	0.27
26155051-64-T/G	0.90	1.00	0.88	0.95	0.92	0.78	0.92	0.70	0.69	0.84	0.55	0.42	0.55	0.55	0.83	0.04	0.10
26150461-27-C/T	0.74	0.72	0.68	0.65	0.71	0.63	0.88	0.46	0.63	0.55	0.50	0.34	0.20	0.36	0.20	0.03	0.05
26154946-24-T/A	0.57	0.72	0.50	0.65	0.57	0.41	0.38	0.75	0.69	0.40	0.41	0.28	0.25	0.27	0.10	0.16	0.10
26153342-50-G/A	0.62	0.50	0.77	0.50	0.57	0.61	0.58	0.42	0.44	0.38	0.43	0.25	0.25	0.45	0.15	0.48	0.65
26154516-53-A/G	0.70	0.44	0.54	0.55	0.43	0.81	0.69	0.79	0.19	0.63	0.50	0.34	0.40	0.36	0.50	0.08	0.03

3.8 Figures

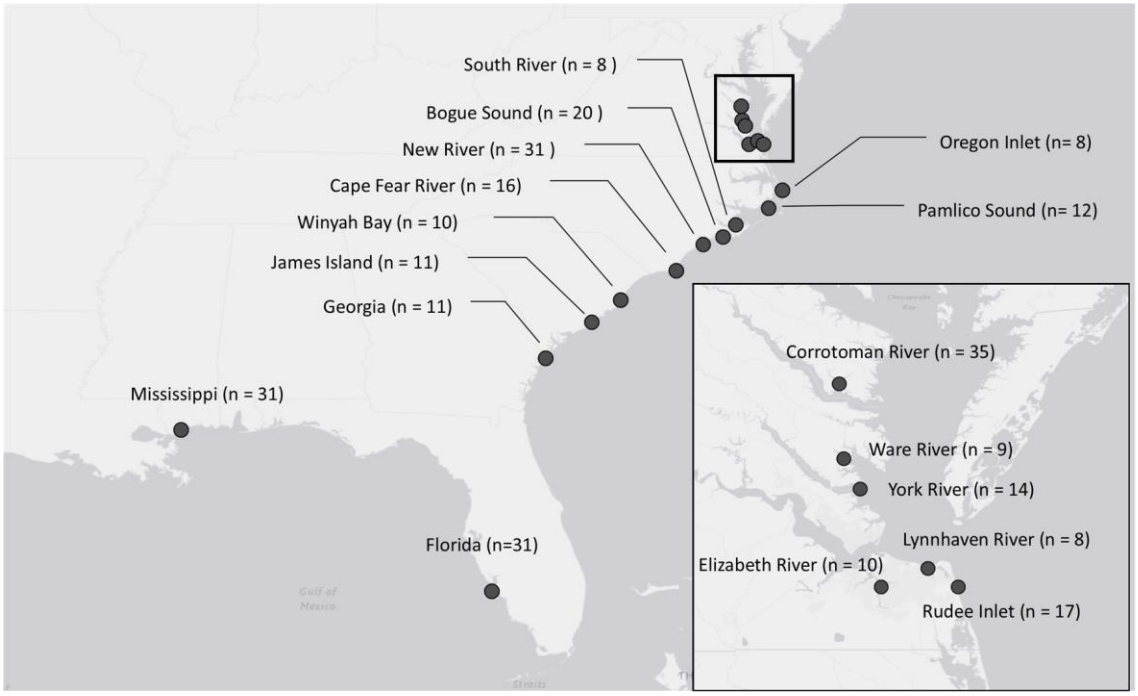

Figure 11. Spotted seatrout sampling locations. Corrotoman River (CR), Ware River (WR), York River (YR), Elizabeth River (ER), Lynnhaven River (LR), Rudee Inlet (RI), Oregon Inlet (OI), Pamlico Sound (PS), South River (SR), Bogue Sound (BS), New River (NR), Cape Fear River (CFR), Winyah Bay (WB), James Island (JI), Wassaw Sound (GA), Florida (FL), and Mississippi (MS). Sample sizes are in the parenthesis.

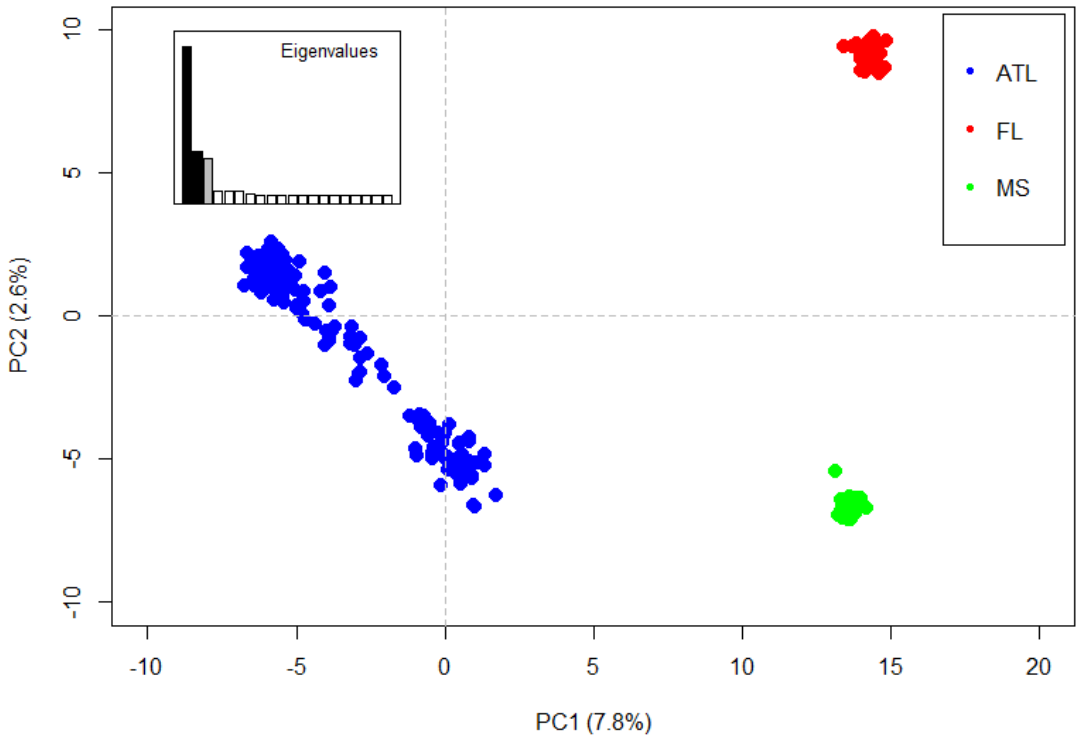

Figure 12. Principal Component Analysis (PCA) using all filtered SNP loci (n = 15,187). ATL = U.S. East Coast, FL = Florida, MS = Mississippi. Each dot represents one sample. X and Y axes represent Principal Component 1 and Principal Component 2.

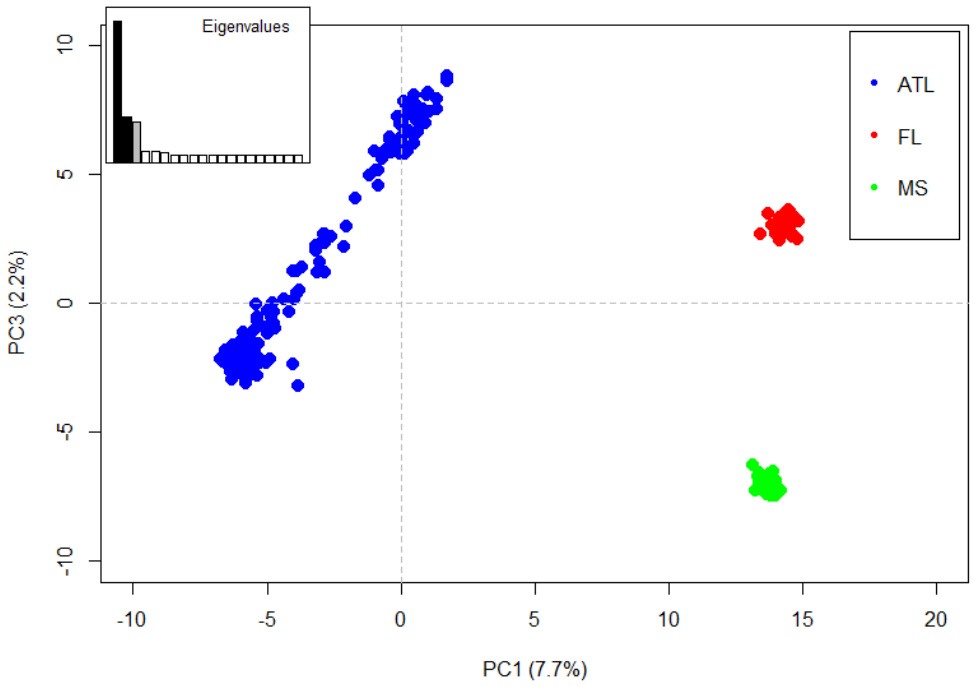

Figure 13. Principal Component Analysis (PCA) using all filtered SNP loci (n = 15,187). ATL = U.S. East Coast, FL = Florida, MS = Mississippi. Each dot represents one sample. X and Y axes represent Principal Component 1 and Principal Component 3.

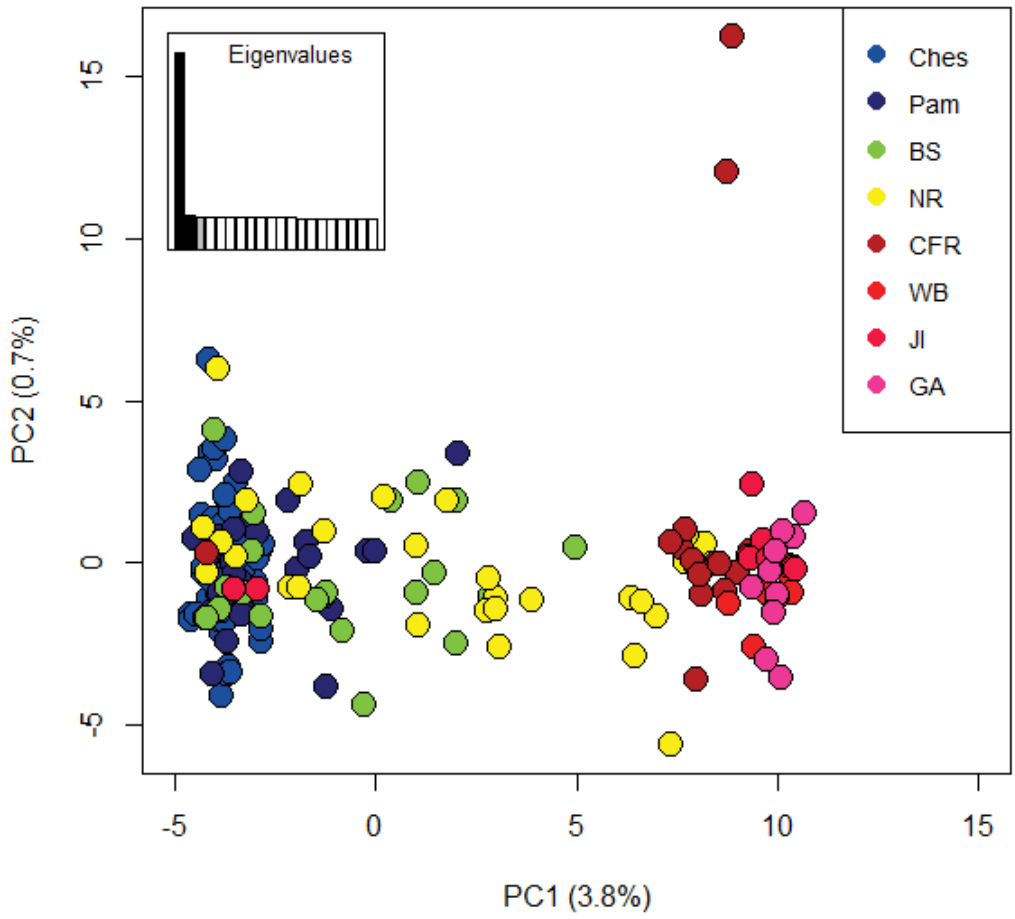

Figure 14. Principal Component Analysis (PCA, PC1 vs. PC2) using all filtered SNP loci (n = 15,187), excluding samples from Gulf of Mexico. To help with visualization: Ches = Corrotoman River (CR), Ware River (WR), York River (YR), Elizabeth River (ER), Lynnhaven River (LR), Rudee Inlet (RI); Pam = Oregon Inlet (OI), Pamlico Sound (PS), and South River (SR); BS = Bogue Sound; NR = New River; CFR = Cape Fear River; WB = Winyah Bay; JI = James Island; GA = Wassaw Sound. Four samples from JI were removed for this plot due to significant deviation from the rest of the samples, likely having hatchery origins.

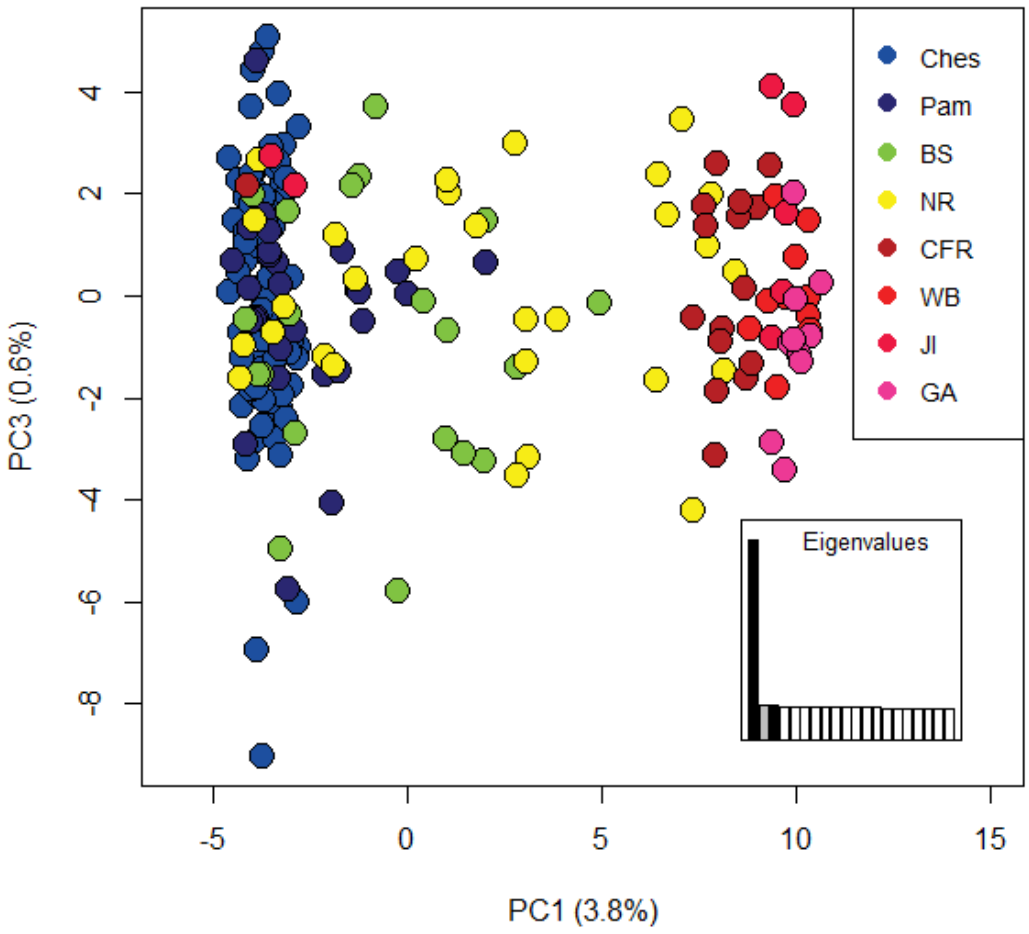

Figure 15. Principal Component Analysis (PCA, PC1 vs. PC3) using all filtered SNP loci (n = 15,187), excluding samples from Gulf of Mexico. To help with visualization: Ches = Corrotoman River (CR), Ware River (WR), York River (YR), Elizabeth River (ER), Lynnhaven River (LR), Rudee Inlet (RI); Pam = Oregon Inlet (OI), Pamlico Sound (PS), and South River (SR); BS = Bogue Sound; NR = New River; CFR = Cape Fear River; WB = Winyah Bay; JI = James Island; GA = Wassaw Sound. Four samples from JI were removed for this plot due to significant deviation from the rest of the samples, likely having hatchery origins.

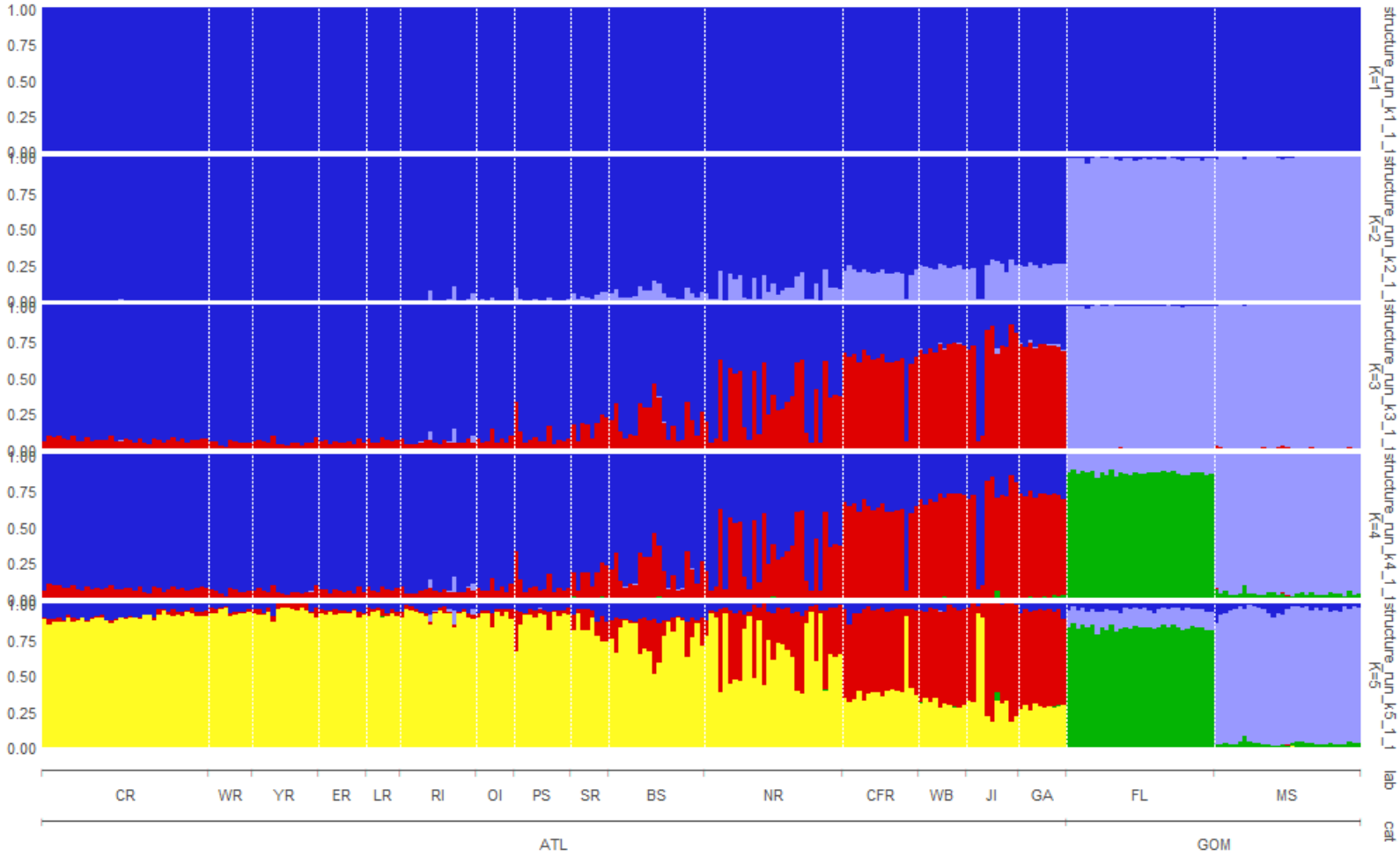

Figure 16. Barplot displaying individual admixture proportions inferred from STRUCTURE analyses. From top to bottom: K = 1 to 5. K =2 was the most likely scenario. Corrotoman River (CR), Ware River (WR), York River (YR), Elizabeth River (ER), Lynnhaven River (LR), Rudee Inlet (RI), Oregon Inlet (OI), Pamlico Sound (PS), South River (SR), Bogue Sound (BS), New River (NR), Cape Fear River (CFR), Winyah Bay (WB), James Island (JI), Wassaw Sound (GA), Florida (FL), and Mississippi (MS); ATL = U.S. East Coast, GOM = Gulf of Mexico.

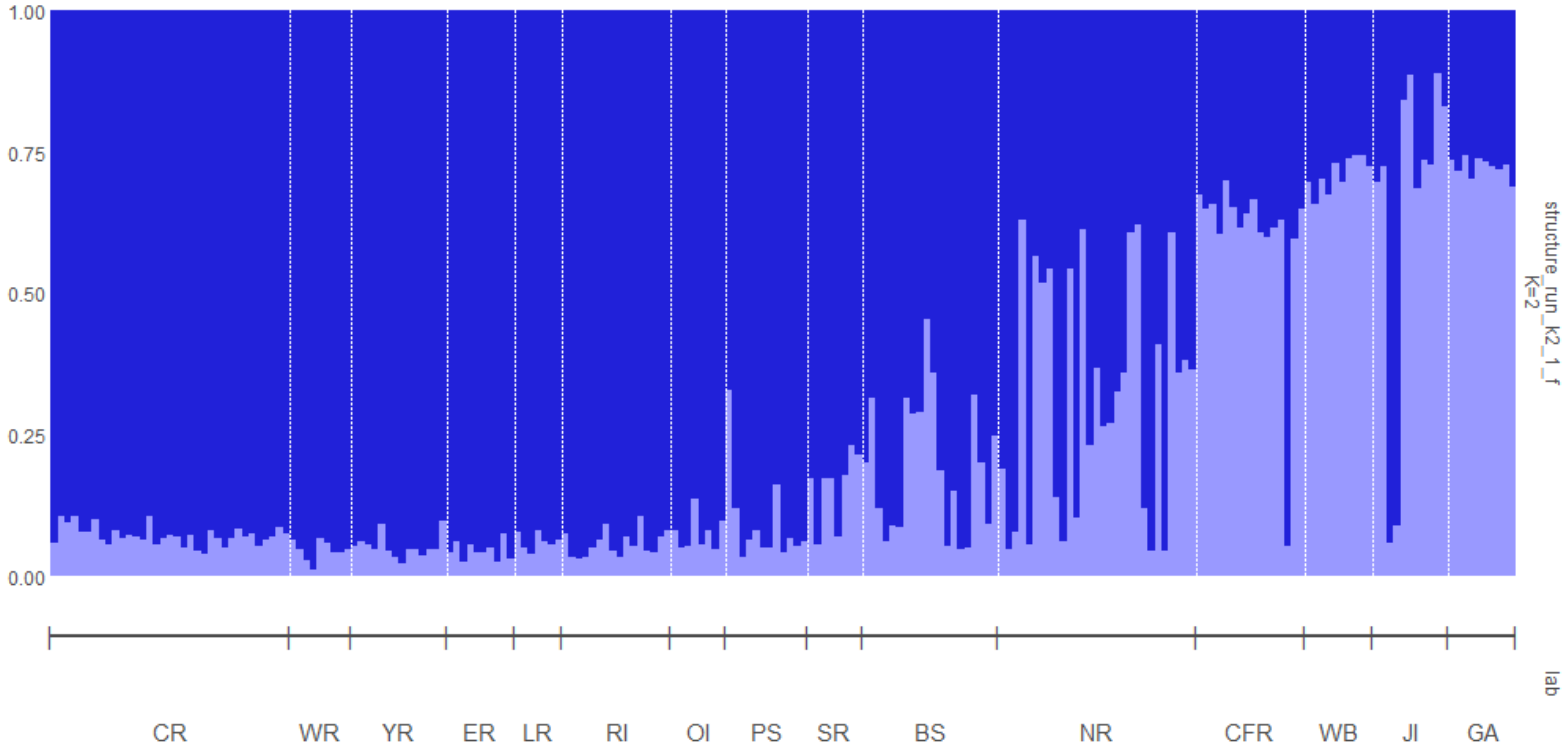

Figure 17. Barplot displaying individual admixture proportions inferred from STRUCTURE analyses with GOM samples excluded. From left to right = north to south. Corrotoman River (CR), Ware River (WR), York River (YR), Elizabeth River (ER), Lynnhaven River (LR), Rudee Inlet (RI), Oregon Inlet (OI), Pamlico Sound (PS), South River (SR), Bogue Sound (BS), New River (NR), Cape Fear River (CFR), Winyah Bay (WB), James Island (JI), Wassaw Sound (GA).

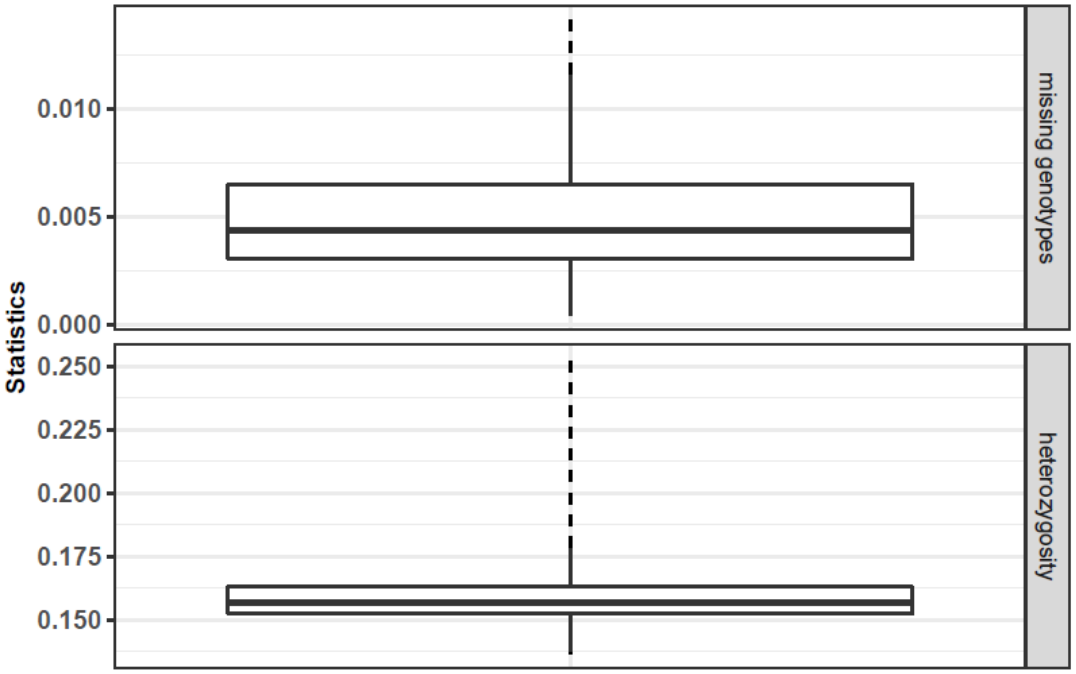

Figure S 2. Boxplots summarizing missing genotypes (%) and heterozygosity for all samples (n = 277).

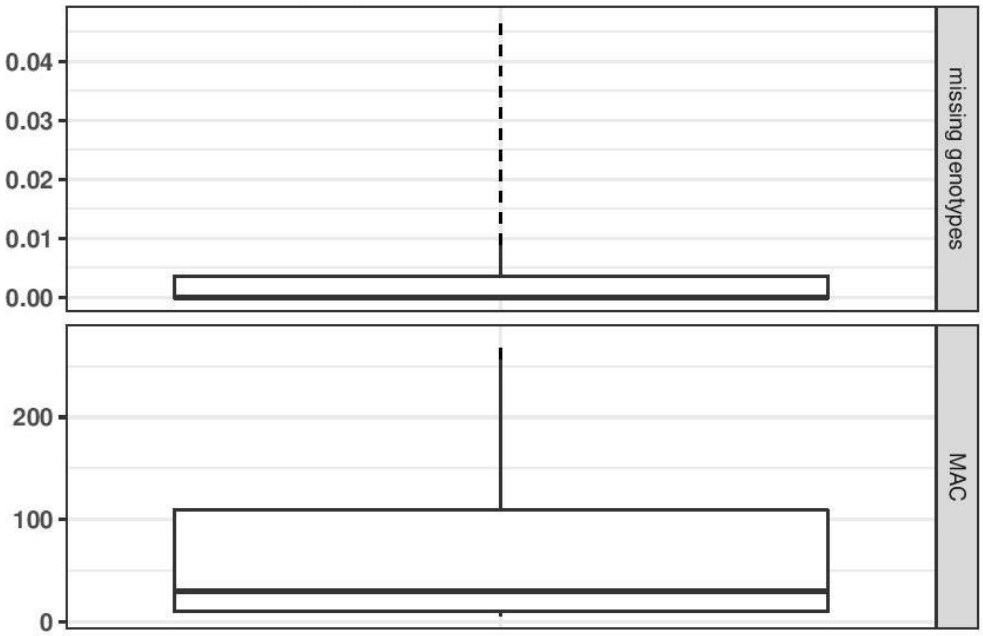

Figure S 3. Boxplots summarizing missing genotypes (%) and minor allele counts (MAC) for all SNP loci (n = 15,187).

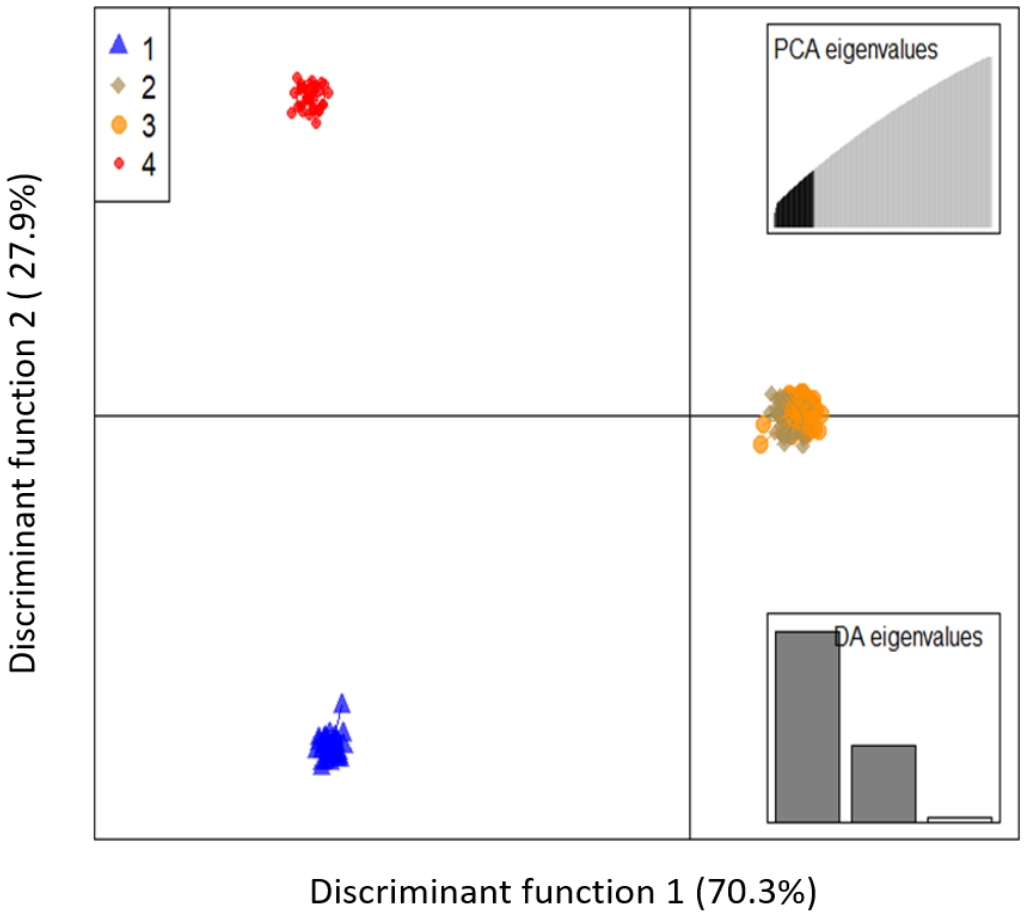

Figure S 4. Discriminant analysis of principal components (DAPC) of spotted seatrout (function 1 vs 2) from 15,187 SNP loci. Cluster membership: 1 = Mississippi (MS), 2 and 3 = U.S. East Coast (ATL), 4 = Florida (FL)

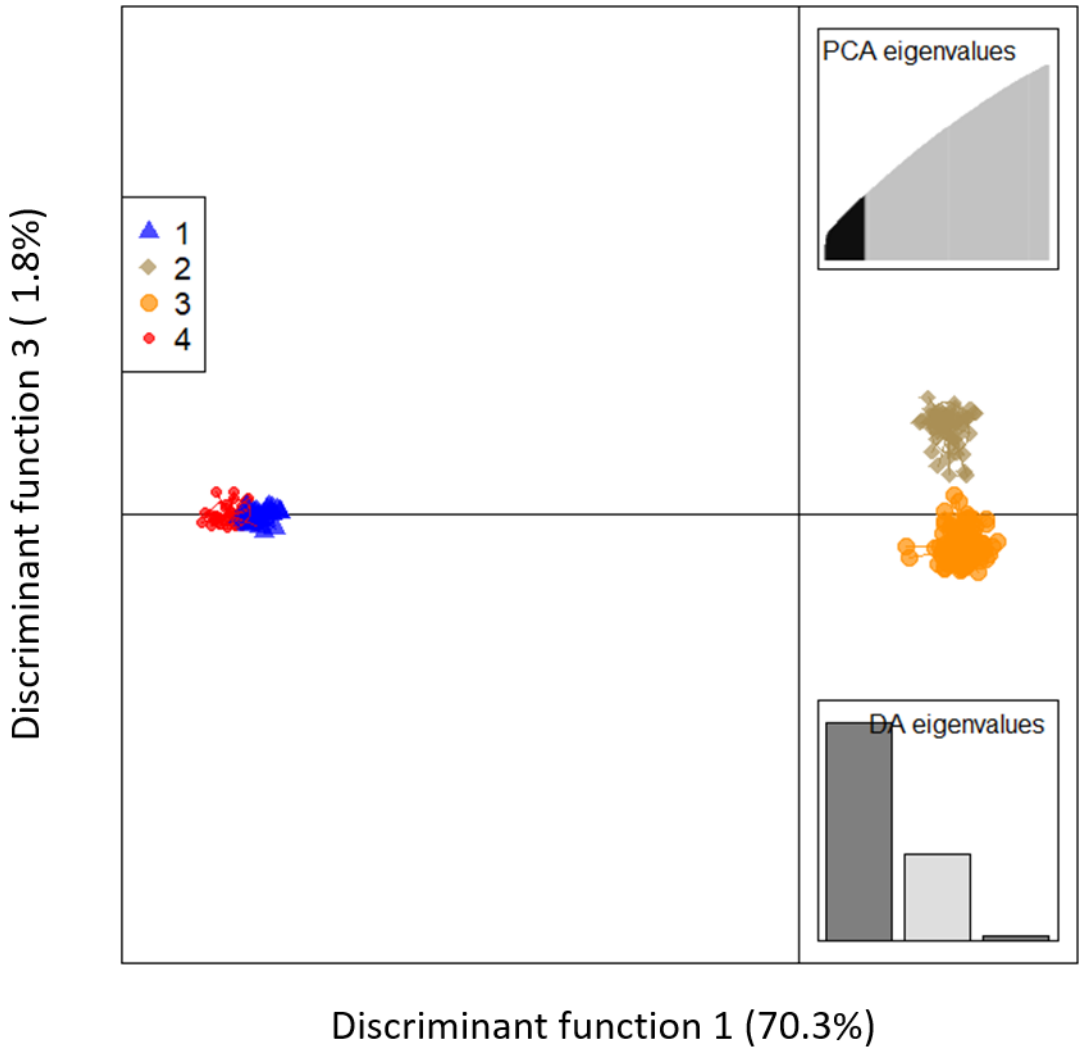

Figure S 5. Discriminant analysis of principal components (DAPC) of spotted seatrout (function 1 vs 3) from 15,187 SNP loci. Cluster membership: 1 = Mississippi (MS), 2 and 3 = U.S. East Coast (ATL), 4 = Florida (FL)

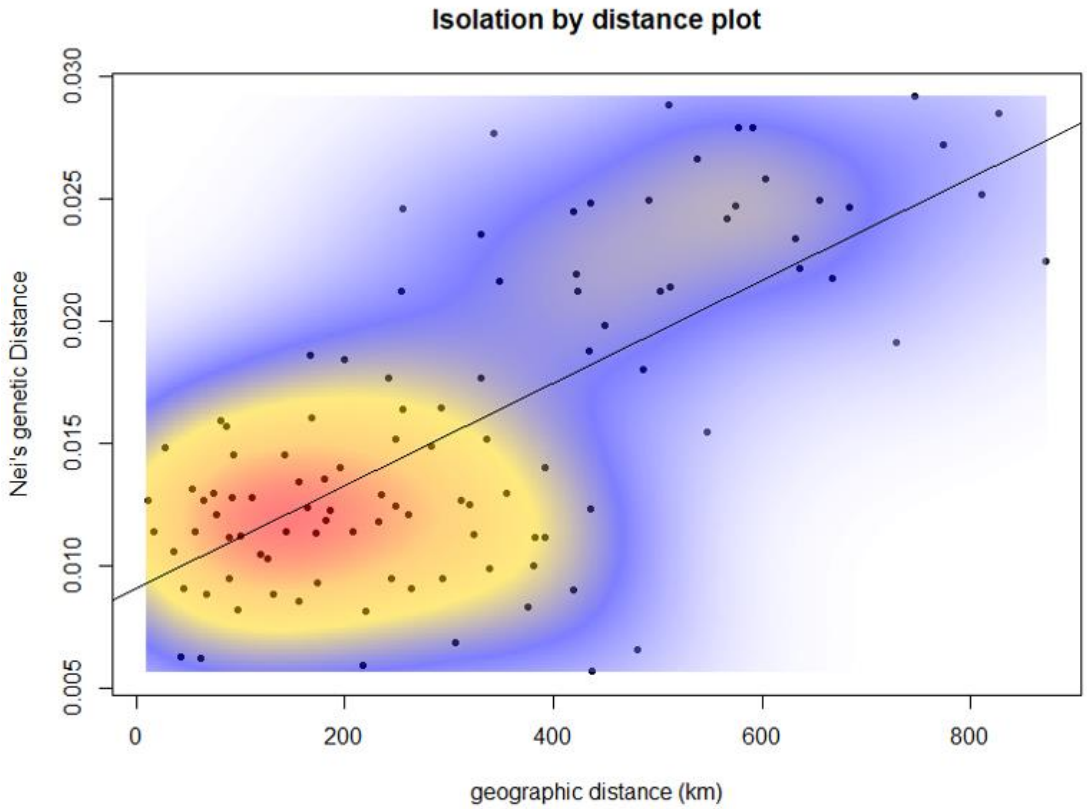

Figure S 6. Isolation by distance (IBD) plot with all sampling locations on the U.S. East Coast. Mantel test: $r = 0.693$, $p = 0.001$.

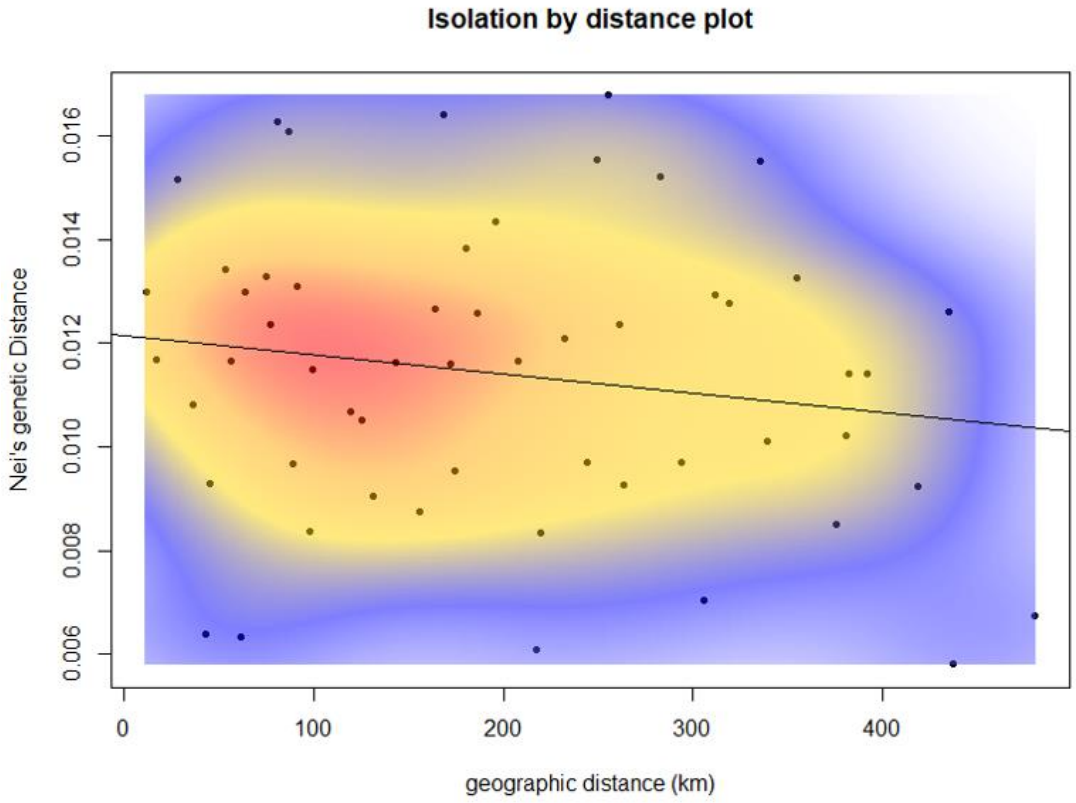

Figure S 7. Isolation by distance (IBD) plot with sample from Corrotoman River (CR) to New River (NR) in the northern part of the U.S. East Coast. Mantel test: r = -0.168, p =0.873.

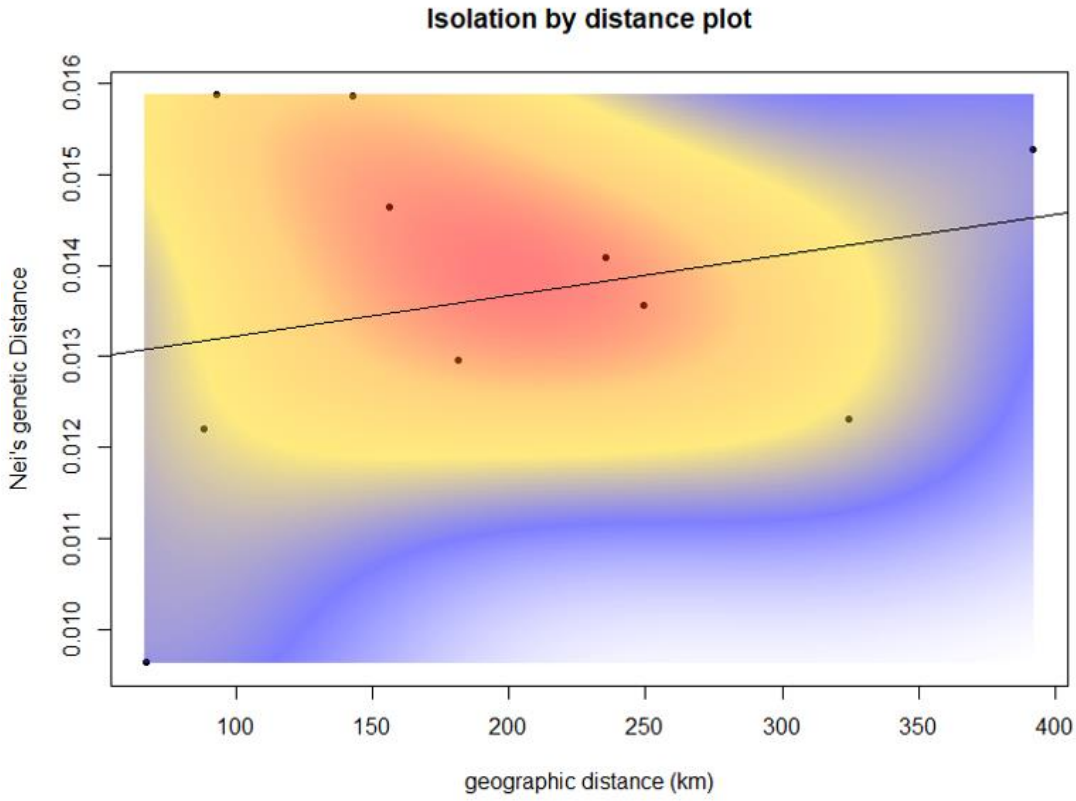

Figure S 8. Isolation by distance (IBD) plot with sample from Wassaw Sound (GA) to New River (NR) in the southern part of the U.S. East Coast. Mantel test: $r = 0.243$, $p = 0.322$.

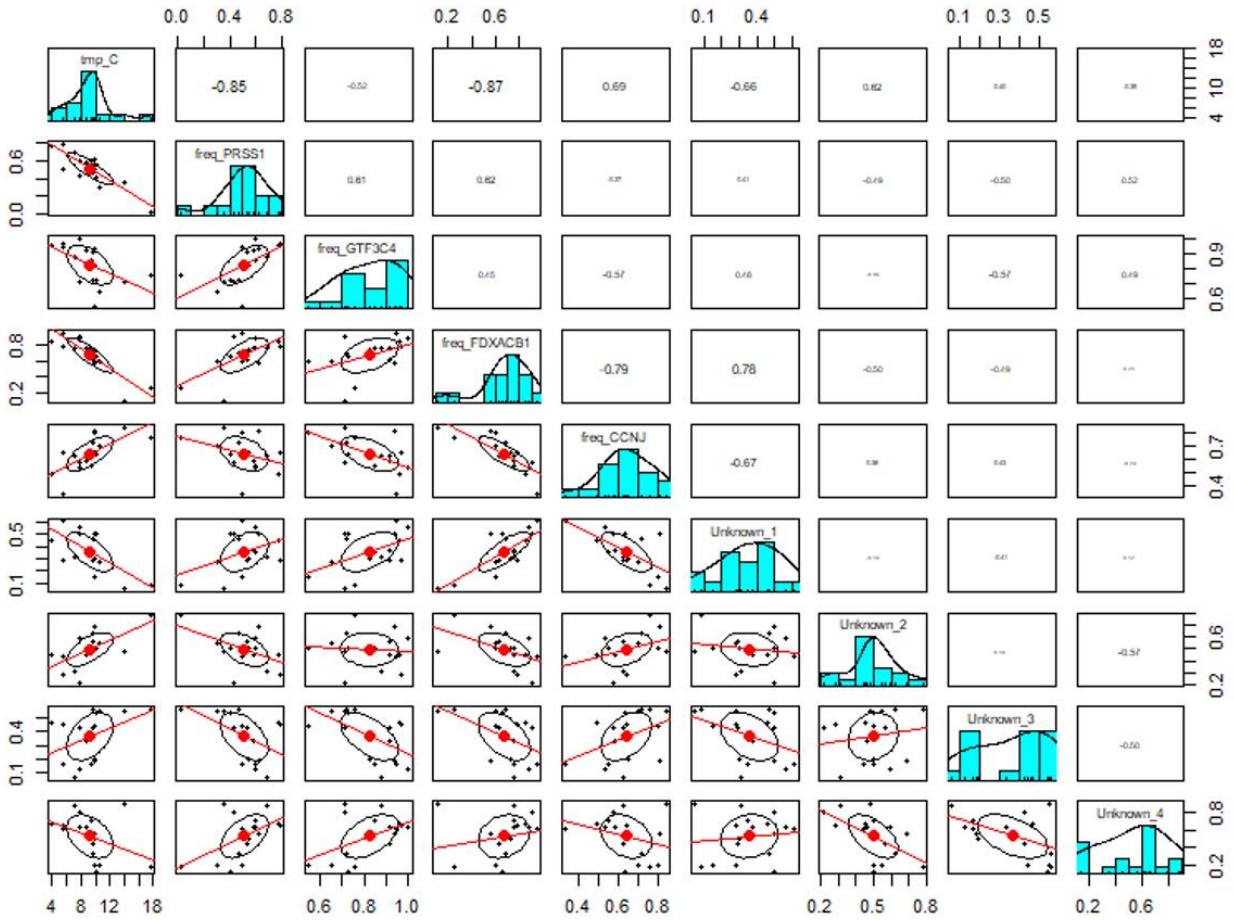

Figure S 9. Scatter plots showing relationships between the allele frequencies (Y axis) of eight nonsynonymous SNP loci with AWT (x axis, first column). On the diagonal are histograms of the allele frequencies. Above diagnol, scaled correlation coefficient (*r*).

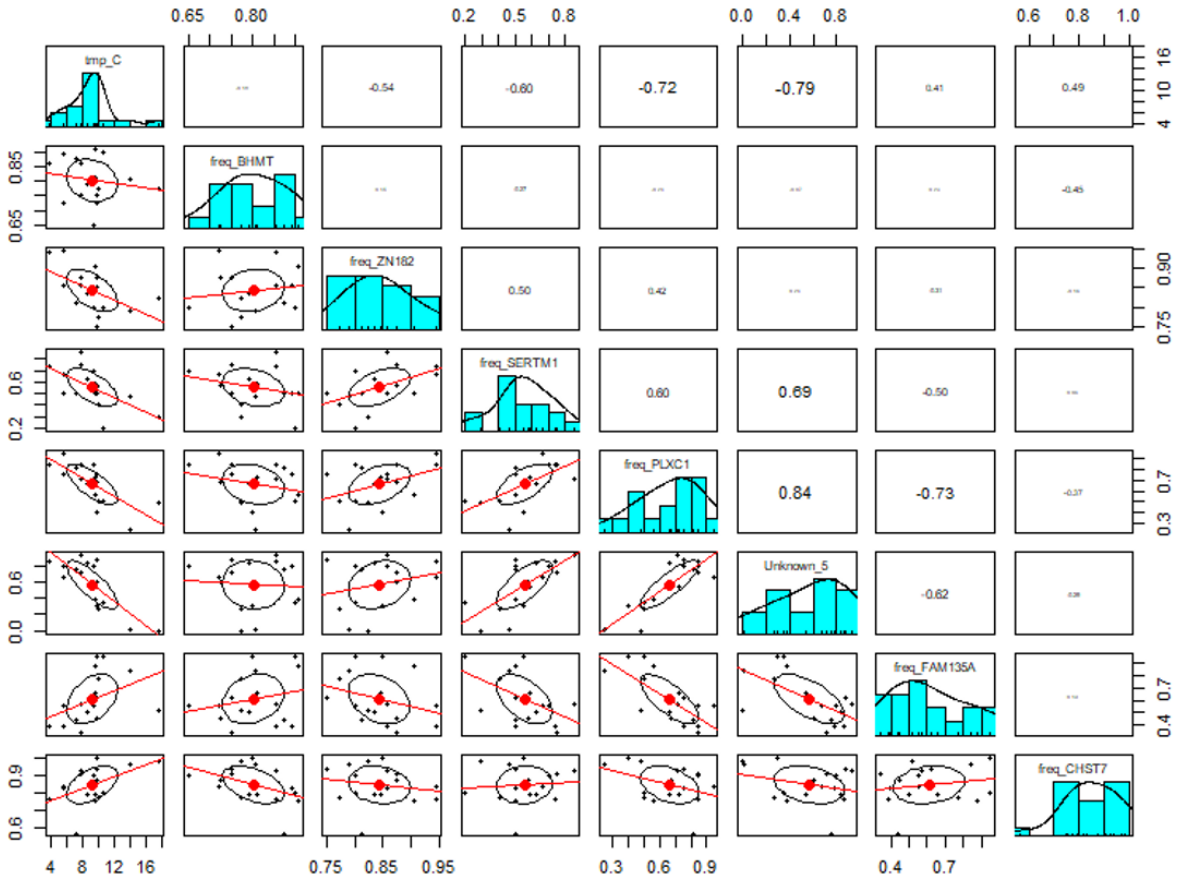

Figure S 10. Scatter plots showing relationship between the allele frequencies (y axis) of the first seven synonymous SNP loci with AWT (x axis, first column). On the diagonal are histograms of the allele frequencies. Above diagnol, scaled correlation coefficient (*r*).

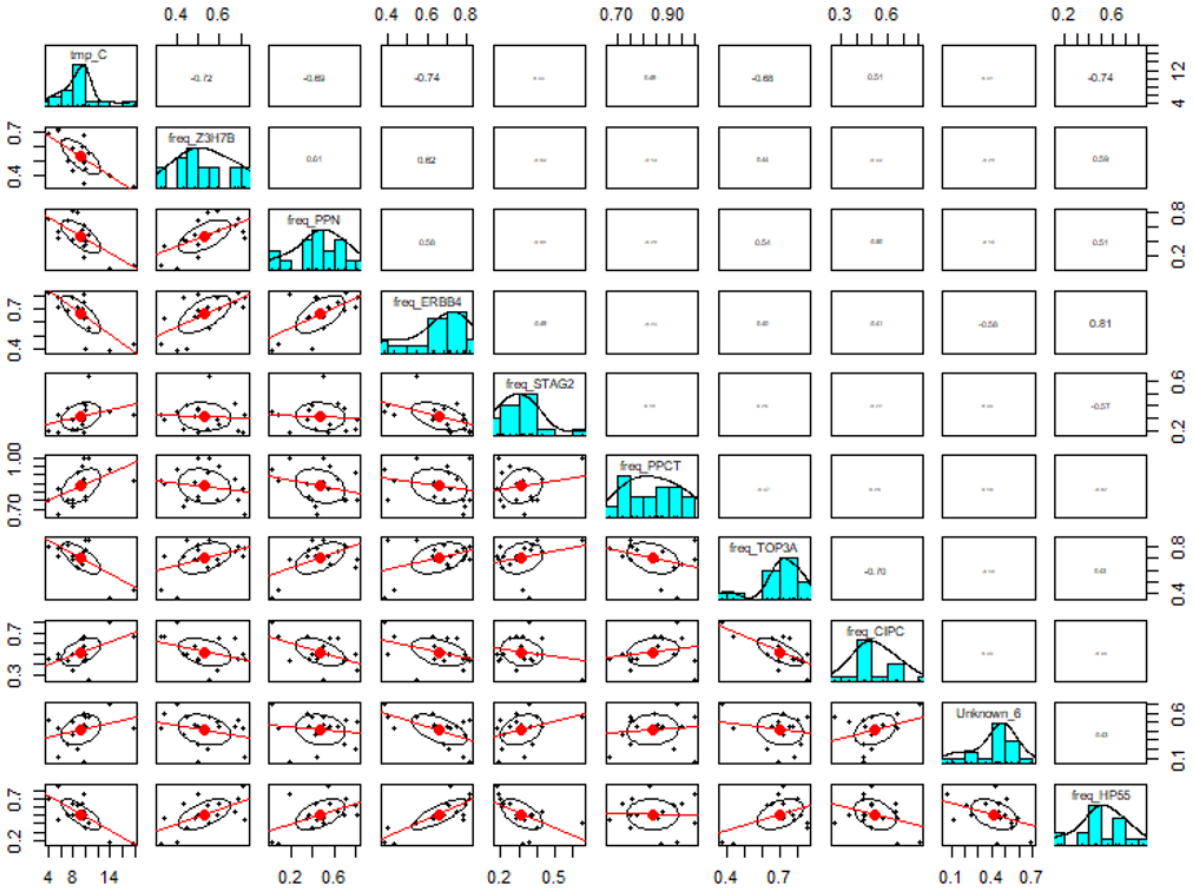

Figure S 11. Scatter plots showing relationship between the allele frequencies (y axes) of the last nine synonymous SNP loci with AWT (x axis, first column). On the diagonal are histograms of the allele frequencies. Above diagnol, scaled correlation coefficient (*r*).

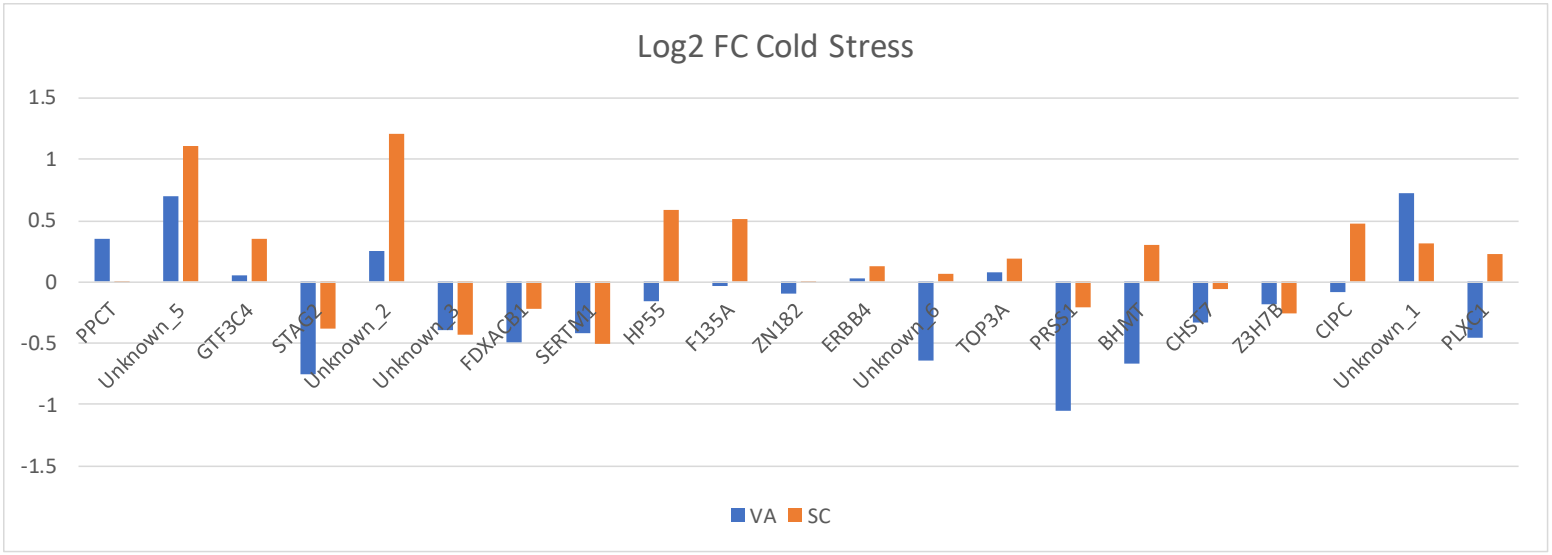

Figure S 12. Log2 fold change of the transcripts (Chapter 2) containing the 21 outlier SNP loci in response to cold stress. VA = Corrotoman River, VA; SC = James Island, SC.

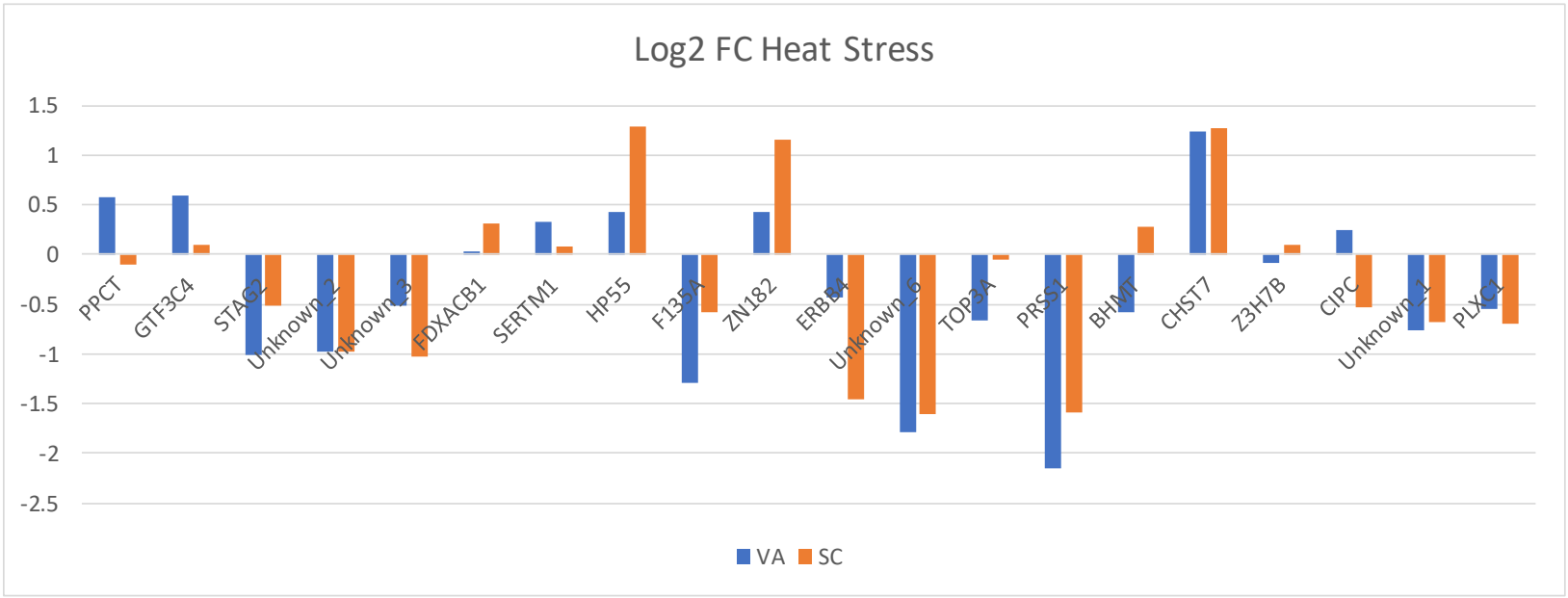

Figure S 13. Log2 fold change of the transcripts (Chapter 2) containing the 20 outlier SNP loci in response to heat stress. VA = Corrotoman River, VA; SC = James Island, SC.

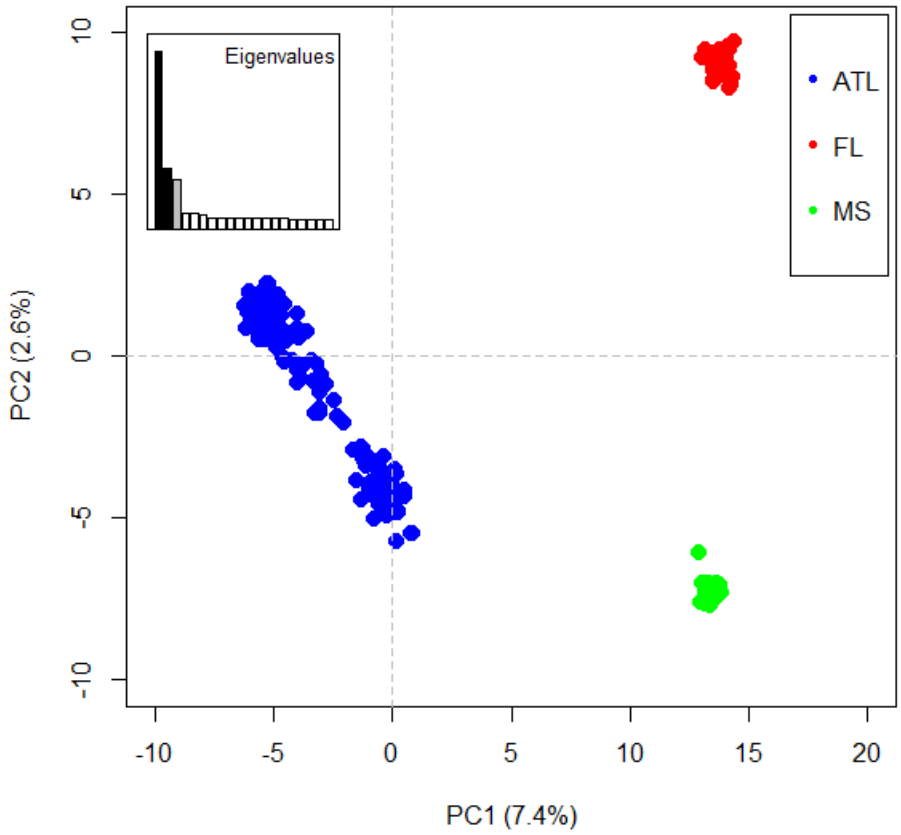

Figure S 14. Principal Component analysis (PCA), PC1 vs. PC2, using the 14,961 putatively neutral loci. ATL = U.S. East Coast, FL = Florida, MS = Mississippi.

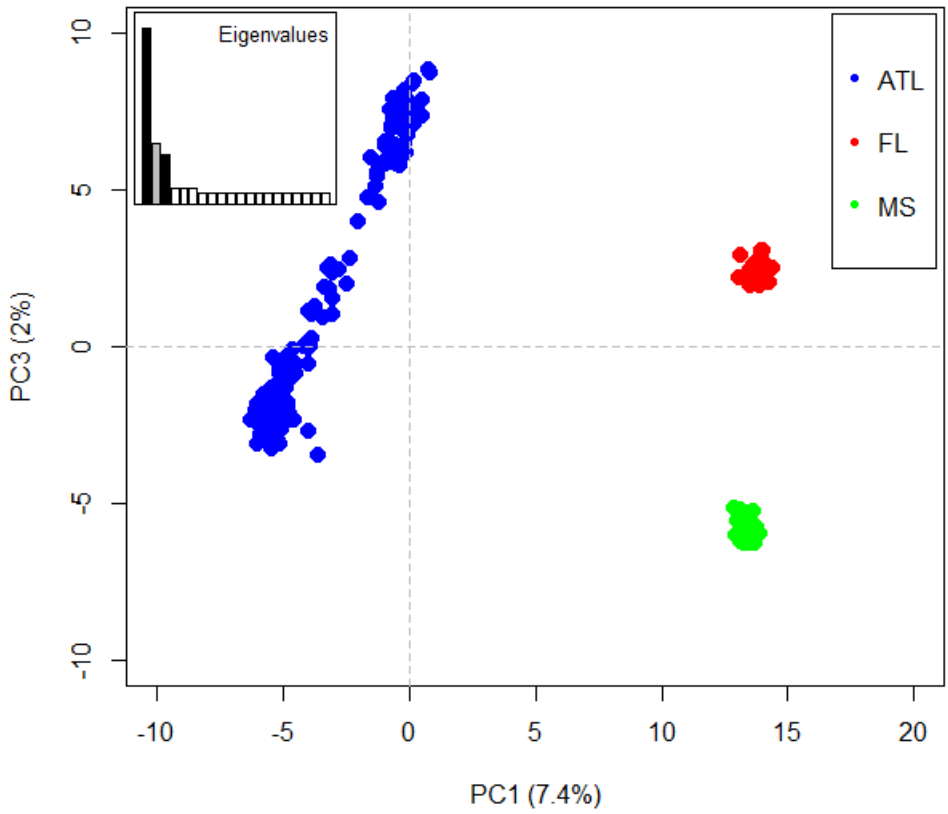

Figure S 15. Principal Component analysis (PCA), PC1 vs. PC3, using the 14,961 putatively neutral loci. ATL = U.S. East Coast, FL = Florida, MS = Mississippi.

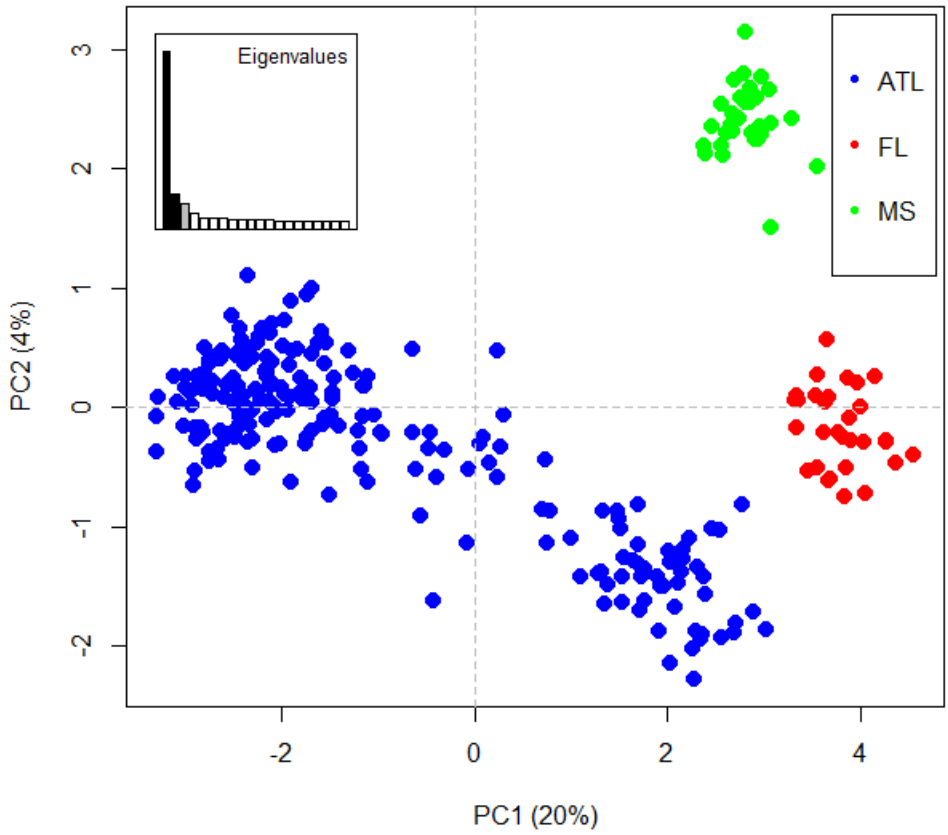

Figure S 16. Principal Component analysis (PCA), PC1 vs. PC2, using the 226 putatively adaptive loci. ATL = U.S. East Coast, FL = Florida, MS = Mississippi.

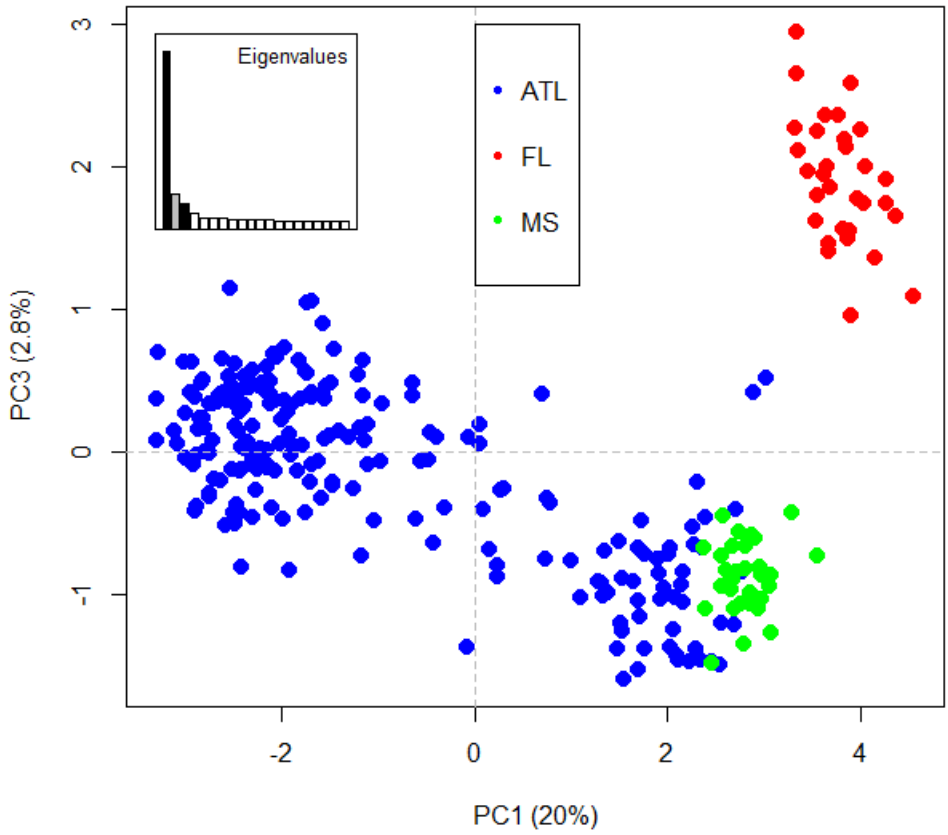

Figure S 17. Principal Component analysis (PCA), PC1 vs. PC3, using the 226 putatively adaptive loci. ATL = U.S. East Coast, FL = Florida, MS = Mississippi.

4 Conclusion

This dissertation focused on searching for signatures of natural selection in spotted seatrout at multiple levels of biological organization (Figure 18). Using an integrated approach, from comparison of whole-organism metabolic rates between spotted seatrout sampled from different temperature regimes, to the cellular mechanisms underlying differential gene expression in response to acute temperature stresses, to a genome-level evaluation of adaptive genetic variation based on samples collected across the distributional range of the species.

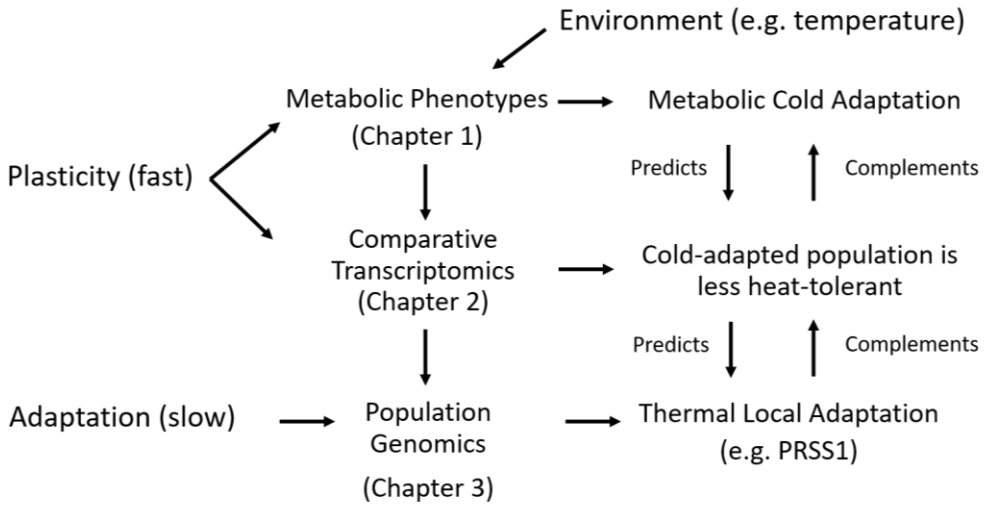

Figure 18. Conceptual diagram of how the three Chapters are related to each other.

Perhaps the most salient contribution of this dissertation is that there were significant intraspecific differences at all levels of biological organization examined. At the whole-organism level (Chapter 1), a higher standard metabolic rate and greater metabolic plasticity was observed in spotted seatrout collected from Chesapeake Bay as compared to those sampled from Charleston, South Carolina. This finding is, consistent with the prediction that fish from Chesapeake Bay are cold-adapted as a result of the

pressure of natural selection from more severe and frequent winter kills in the region. The larger aerobic scope in fish from Chesapeake Bay provides a mechanistic explanation for the observation of a faster growth rate in these fish as compared to their southern counterparts (Smith et al. 2008; Clark et al. 2013). Although there was different metabolic plasticity between spotted seatrout from distinct populations, the molecular basis of such physiological differences was still unknown and was thus further investigated using RNA-seq in Chapter 2.

At the transcriptomic level, patterns of differential gene expression also differed. The cold-adapted northern population showed a lower transcriptional response to cold stress, while the warm-adapted southern population showed a lower transcriptional response to heat stress. Functional annotation revealed molecular pathways that were both shared and unique between the two groups of spotted seatrout, suggesting that differential gene expression is contributing to differences in thermal tolerance. The first high-quality liver transcriptome was assembled for spotted seatrout, which serves as a useful genetic resource for future studies. Chapter 2 complements Chapter 1 by showing that the cold-adapted northern population is not as heat-tolerant as the southern population.

The question of whether the differences in the transcriptomic signatures could be attributed to adaptive or neutral genetic variation was further investigated in a separate population genomics study. In Chapter 3, the discovery of putatively adaptive genetic variation associated with winter water temperature and the successful annotation of a subset of the loci which have been implicated in thermal adaptation and stress responses

strongly suggest local adaptation in spotted seatrout. Previous genetic studies of spotted seatrout on the U.S. East Coast used microsatellite markers, which are presumably neutral. While these markers were effective in characterizing population structure, they were not suitable for studying local adaptation due to low genome coverage. This dissertation is the first study using genome-wide SNP markers to identify adaptive genetic variation in spotted seatrout.

An understanding of the roles of plasticity and local adaptation in shaping the current distribution of spotted seatrout provides a basis for predicting the resilience of these fish to climate change. The data from Chapter 1 and Chapter 2 strongly supports the hypothesis that the northward range expansion of spotted seatrout is restricted by the species' cold tolerance limit. This raises the question of whether plasticity and adaptation could ameliorate the negative impacts of climate change. Although the high level of metabolic plasticity observed in spotted seatrout has allowed them persist in the estuarine environment, which has large daily and seasonal temperature fluctuations, plasticity is not without limits. I have shown that spotted seatrout at its current northern range limit are more vulnerable to acute heat stress than their counterparts from further south. This should be of concern to fishery managers since the Chesapeake Bay water temperature has been warming faster than air temperature and more extreme heat waves are predicted in future summers. The high oxygen demand of fish from the northern population could also mean high post-release mortality in summer (Redpath et al. 2010). Meanwhile, there is adaptive potential among spotted seatrout on the US east coast. Despite the low level of gene flow between the northern and southern populations, the putative adaptive genetic variation is spatially distributed in both populations. In other words, the northern

population possesses the alleles that are predominantly found in the southern population and vice versa. The relatively fast maturation of spotted seatrout should also contribute to evolutionary adaptation potential.

Taken together, this dissertation supports the notion that local adaptation and differential gene expression both play a role in the population-level divergence in physiological and life history traits of spotted seatrout along the US east coast. Estuaries are one of the ecosystems most vulnerable to climate change, and the understanding of mechanisms underlying phenotypic plasticity and local adaptation of spotted seatrout provide a baseline for monitoring and predicting future population dynamics and distribution of spotted seatrout under climate change.

4.1 Future Directions

Metabolic rate, like many other physiological traits, has a complex and polygenic genetic basis. This is evidenced by the large number of differentially expressed genes in Chapter 2 and outlier loci in Chapter 3. Firm establishment of a causal link between a single locus to a fitness-related trait, however, requires more rigorous scrutiny such as transgenic techniques and multi-generational common garden experiments. The emerging CRISPR/Cas9 gene-editing tool is also starting to be applied to natural populations to advance the understanding of ecologically relevant genetic variation (Bono et al. 2015). Differentially expressed genes and outlier loci identified in this dissertation provide a basis for such work.

When a high-quality genome assembly for spotted seatrout becomes available, the RNA-seq and DArTseq data can be revisited to gain new insights such as the location of adaptive genetic variation and differentially expressed genes. For example, are outlier loci scattered across the genome, or are there "genomic islands" where outlier loci cluster? How common are structural variations (e.g., insertion, deletion, inversion, transposable elements) in the genome, compared to SNPs (Berg et al. 2017)? A phased genome (chromosome-specific) will enable the study of haplotype blocks, which have been well-known in the adaptation of human populations (Jacobs et al. 2016).

There is now growing evidence that heritable variation in ecologically relevant traits can be generated through a variety of epigenetic mechanisms (e.g., DNA methylation, histone modification, etc.), even in the absence of genetic change (Salmon et al. 2008; Massicotte et al. 2011; Morán et al. 2013). Epigenetic modifications are expected to occur at a much faster rate than genetic mutations and passed on to future generations, potentially causing populations that are subjected to different selective regimes to diverge phenotypically (Trucchi et al. 2016). A high level of genome-wide epigenetic divergence between individuals occupying distinct habitats is therefore predicted (Bossdorf et al. 2008). Bisulfite-converted restriction site associated DNA sequencing (bsRADseq) can be applied to spotted seatrout to quantify divergence in genome-wide methylation patterns in many individual samples (Trucchi et al. 2016).

Shallow estuaries are vulnerable to the effects of climate change. In addition to rising temperature and greater variability, other stressors such as decreasing pH and hypoxia will simultaneously challenge the survival of spotted seatrout in the estuarine environment. Adaptation will need to take place in order to keep pace with an ever-

changing environment. Genes that respond to temperature stress are also involved in coping with other stressors, given a conserved cellular stress response (Connon et al. 2018). Loci identified in this dissertation may prove to be useful for genetic monitoring of the stress levels of spotted seatrout. The genetic investigations of the synergistic effects of multiple stressors is also a rewarding research program, one of which is currently poorly understood.

Finally, genetic information can be incorporated into species distribution models (SDM) to more accurately project range shifts under climate change scenarios, assess extinction risks and help guide conservation efforts. Most of these studies to date have focused on terrestrial organisms such as bats (Razgour et al. 2019), birds (Bay et al. 2018) and plants (Fitzpatrick and Keller 2015; Ikeda et al. 2017). One rare marine example combining genomics and ecological modeling for a reef-building coral suggested that standing genetic variation may allow it to adapt to a warming ocean (Bay et al. 2017). It may now be possible to integrate genomic data with ecological modeling to predict the resilience of spotted seatrout to climate change.

4.2 References

Bay, R. A., R. J. Harrigan, V. Le Underwood, H. L. Gibbs, T. B. Smith, and K. Ruegg. 2018. Genomic signals of selection predict climate-driven population declines in a migratory bird. Science 359(6371):83–86.

Bay, R. A., N. H. Rose, C. A. Logan, and S. R. Palumbi. 2017. Genomic models predict successful coral adaptation if future ocean warming rates are reduced. Science Advances 3(11):e1701413.

Berg, P. R., B. Star, C. Pampoulie, I. R. Bradbury, P. Bentzen, J. A. Hutchings, S. Jentoft, and K. S. Jakobsen. 2017. Trans-oceanic genomic divergence of Atlantic cod ecotypes is associated with large inversions. Heredity 119(6):418–428.

Bono, J. M., E. C. Olesnicky, and L. M. Matzkin. 2015. Connecting genotypes, phenotypes and fitness: harnessing the power of CRISPR/Cas9 genome editing. Molecular Ecology 24(15):3810–3822.

Bossdorf, O., C. L. Richards, and M. Pigliucci. 2008, November 16. Epigenetics for ecologists. Ecology Letters 11(2):106-115.

Clark, T. D., E. Sandblom, and F. Jutfelt. 2013. Aerobic scope measurements of fishes in an era of climate change: respirometry, relevance and recommendations. Journal of Experimental Biology 216(15):2771–2782.

Connon, R. E., K. M. Jeffries, L. M. Komoroske, A. E. Todgham, and N. A. Fangue. 2018. The utility of transcriptomics in fish conservation. Journal of Experimental Biology 221(2):UNSP jeb148833.

Fitzpatrick, M. C., and S. R. Keller. 2015. Ecological genomics meets community-level

modelling of biodiversity: Mapping the genomic landscape of current and future environmental adaptation. Ecology Letters 18(1):1–16.

Ikeda, D. H., T. L. Max, G. J. Allan, M. K. Lau, S. M. Shuster, and T. G. Whitham. 2017. Genetically informed ecological niche models improve climate change predictions. Global Change Biology 23(1):164–176.

Jacobs, G. S., T. J. Sluckin, and T. Kivisild. 2016. Refining the use of linkage disequilibrium as a robust signature of selective sweeps. Genetics 203(4):1807–1825. Genetics.

Massicotte, R., E. Whitelaw, and B. Angers. 2011. DNA methylation: A source of random variation in natural populations. Epigenetics : official journal of the DNA Methylation Society 6(4):421–427.

Morán, P., F. Marco-Rius, M. Megías, L. Covelo-Soto, and A. Pérez-Figueroa. 2013. Environmental induced methylation changes associated with seawater adaptation in brown trout. Aquaculture 392–395:77–83.

Razgour, O., B. Forester, J. B. Taggart, M. Bekaert, J. Juste, C. Ibáñez, S. J. Puechmaille, R. Novella-Fernandez, A. Alberdi, and S. Manel. 2019. Considering adaptive genetic variation in climate change vulnerability assessment reduces species range loss projections. Proceedings of the National Academy of Sciences 116(21):10418–10423.

Redpath, T. D., S. J. Cooke, C. D. Suski, R. Arlinghaus, P. Couture, D. H. Wahl, and D. P. Philipp. 2010. The metabolic and biochemical basis of vulnerability to recreational angling after three generations of angling-induced selection in a teleost

fish. Canadian Journal of Fisheries and Aquatic Sciences 67(12):1983–1992.

Salmon, A., J. Clotault, E. Jenczewski, V. Chable, and M. J. Manzanares-Dauleux. 2008. Brassica oleracea displays a high level of DNA methylation polymorphism. Plant Science 174(1):61–70.

Smith, N. G., C. M. Jones, and J. Van Montfrans. 2008. Spatial and temporal variability of juvenile spotted seatrout *Cynoscion nebulosus* growth in Chesapeake Bay. Journal of Fish Biology 73(3):597–607.

Trucchi, E., A. B. Mazzarella, G. D. Gilfillan, M. T. Lorenzo, P. Schönswetter, and O. Paun. 2016. BsRADseq: Screening DNA methylation in natural populations of non-model species. Molecular Ecology 25(8):1697–1713.

VITA

Jingwei Song

Born in Shanghai, China on April 10, 1992. Graduated from Shanghai Yan'an High School in 2011. Earned a Bachelor of Arts in Biology and German, from Wabash College, Indiana in 2015. Entered the master's program at the Virginia Institute of Marine Science, College of William & Mary in 2015 and bypassed into the doctoral program in 2018.